UNIVERSITY OF MINNESOTA

This is to certify that I have examined this copy of a doctoral thesis by

Ruediger Held

and have found that it is complete and satisfactory in all respects,
and that any and all revisions required by the final
examining committee have been made.

Prof. Philip I. Cohen

Name of Faculty Adviser

Signature of Faculty Adviser

Date

GRADUATE SCHOOL

GROWTH KINETICS OF GaN GROWN BY MOLECULAR BEAM EPITAXY USING Ga AND AMMONIA

A THESIS
SUBMITTED TO THE FACULTY OF THE GRADUATE SCHOOL
OF THE UNIVERSITY OF MINNESOTA
BY

Ruediger Held

IN PARTIAL FULFILLMENT OF THE REQUIREMENTS
FOR THE DEGREE OF
DOCTOR OF PHILOSOPHY

Prof. Philip I. Cohen, Adviser

March 1999

ACKNOWLEDGEMENTS

I would like to thank my graduate adviser Prof. Philip I. Cohen for guiding me through the project, Prof. Amir M. Dabiran for always being available with helpful advice, as well as my lab-partners Devin E. Crawford, Andrew M. Johnston, Sean M. Seutter, Brian E. Ishaug, and Alexander Parkomowsky for their contributions to the project.

Further, I would like to acknowledge Prof. Sylvester Porowski and Izabella Grzegory from the High Pressure Research Center of the Polish Academy of Sciences for providing the bulk GaN crystals used in part of this work, and Greg Nowak for doing the sample preparation and AFM analysis of the bulk samples.

This work was partially supported by the Air Force Office of Scientific Research (AFOSR), the Office of Naval Research (ONR), the National Science Foundation (NSF), the Department of Chemical Engineering and Materials Science of the University of Minnesota, and the Department of Electrical and Computer Engineering of the University of Minnesota.

to my parents

for their support

ABSTRACT

Both c-plane surfaces of bulk GaN crystals were examined using reflection high-energy electron diffraction (RHEED). Differences in the RHEED pattern, time development of the RHEED intensity, and surface reconstructions were observed. On GaN(000$\underline{1}$), or GaN-B, the Ga rich reconstructions reported by Smith and coworkers were observed. On GaN(0001), or GaN-A, a (2×2) reconstruction was observed. RHEED measurements of the specular intensity vs time showed that two different surface terminations could be maintained on the B surface, one of which is a stable, gallided surface, while the other is a nitrided surface, which is unstable in vacuum. If the nitrided surface is heated in vacuum it changes to the gallided surface in several minutes at 800^{o}C. Only one termination was detected on the A surface. The results are complemented by desorption mass spectroscopy (DMS) measurements, and the resulting surfaces were then investigated using atomic force microscopy (AFM) and Scanning Tunneling Microscopy (STM). Two surface terminations were distinguished on the B surface, and a unique annealing process under NH_3 will be documented. Preliminary investigation of the A surface revealed decorated step edges. The results were compared to films grown on sapphire with different nucleation layers, which can be grown to yield either polarity. Focusing on the GaN-B polarity, the surface reactivity and growth kinetics are investigated as a function of growth parameters using DMS. Growth proceeds either by island nucleation or by step flow, depending on the steady state surface coverage of Ga. Three Ga adsorption sites are found on the surface, one chemisorption and two physisorption sites. One of the physisorption sites corresponds to an extrinsic precursor state, while the other corresponds to an intrinsic precursor state with a very short residence time. An abrupt growth mode transition is found as a function of growth parameters between island nucleation and step flow, which is directly related to the coverage of chemisorbed Ga at steady state. A quantitative model is developed for this GaN-B surface which explains the transitional Ga uptake, steady state growth, as well as the abrupt transition between growth modes.

TABLE OF CONTENTS

1. MOTIVATION

GaN is a direct, wide band gap semiconductor making it attractive for blue LED's and lasers, as well as high temperature and power devices.[1] Since the mid 80's major efforts have been underway to produce high quality material using a variety of growth methods.[2,3] The growth has proven difficult. Among the multiple challenges in growing high quality material by molecular beam epitaxy (MBE) is the control of growth kinetics, which require a good understanding of the processes taking place on the GaN surface. In order to study growth kinetics the accurate determination of growth conditions is essential, including crystal polarity, fluxes, and surface temperature. Knowing these parameters permits investigation of their effect on surface termination, growth rate, and growth mode.

For the growth of GaN by MBE using NH_3, the kinetics are complicated by (1) the temperature dependence of the dissociation and incorporation of NH_3 and (2) the temperature and compositional dependence of the residence times of the reactants on the GaN surface. This means that without knowledge of the microscopic surface processes it is not clear how to set optimum growth parameters. Since the flux and temperature dependencies of the Ga, N, and H surface coverages are not well known, the species that limit the growth can not be easily identified. To monitor these growth processes, structural and compositional changes at the surface were measured with reflection high energy electron diffraction (RHEED), and changes in the species leaving the surface with desorption mass spectroscopy (DMS). These two techniques complement each other in determining microscopic processes.

A number of issues related to growth kinetics of GaN must be addressed. Historically, the n-type conductivity commonly exhibited by GaN was attributed to N vacancies.[4] This problem was thought to arise from a kinetic barrier to N incorporation during growth.

Results by Lee et. al [5] as well as Jones et. al [6] indicated that the GaN growth rate is strongly temperature dependent, exhibiting a maximum between 750^{o}C and 800^{o}C. The high temperature decrease in growth rate was attributed to Ga desorption at elevated substrate temperature [5,6] as well as to the decomposition of GaN [7]. The common belief at low substrate temperatures was that reduced N incorporation efficiency limits the growth rate. [5]

In this thesis a quantitative model will be developed to describe MBE growth on the GaN-B polarity. Experimental issues are covered in chapter 2: The MBE apparatus, sample preparation, DMS, and RHEED. Chapter 3 is devoted to a summary of results obtained in collaboration with Devin E. Crawford and Andrew M. Johnston. These results will serve as the foundation for subsequent chapters. In chapter 4, using bulk GaN crystals, data is presented that permits identification of crystal polarity using RHEED, DMS, or AFM. This work was performed in collaboration with Grzegorz Nowak who prepared the epi-ready crystals and performed AFM after growth, and lead to the development of two growth initiation procedures to obtain unipolar films of either polarity on Al_2O_3. The use of larger Al_2O_3 substrate permitted a more detailed investigation of the GaN-B polarity in Chapter 5 by DMS. Those results lead to a rate equation model of growth, which represents the core of this thesis. Finally, chapter 6 covers qualitative findings on the development of GaN-B surface morphology, and chapter 7 contains more detailed work on GaN decomposition.

2. INSTRUMENTATION

2.1 MBE System

Most growth experiments were carried out in a cryopumped Varian GEN II MBE system which is shown schematically in Figure 1. Since NH_3 decomposes Viton, all such components were replaced by Kalrez compounds. A desorption mass spectrometer (DMS) mounted in one of the ports enabled detection of the type and intensity of desorbed species from the sample surface. RHEED data were obtained from a conventional RHEED system. Elemental Ga was provided by a Knudsen cell. The NH_3 flux was held constant during growth using a capacitance manometer in conjunction with a closed loop PID controller and solenoid control valve to maintain constant pressure in the NH_3 gas line behind a manually regulated precision leak valve. A Bayard-Alpert ionization gauge located on the back of the sample manipulator was used to determine the incident beam equivalent pressure (BEP) by rotating the sample manipulator. Absolute calibration of the Ga and Al fluxes was achieved by monitoring RHEED intensity oscillations during growth of GaAs(001) and AlAs(001) in separate experiments.

The sapphire substrate was heated directly by radiation from a high temperature resistive heater made from graphite loops deposited between pyrolytic boron nitride. A thermocouple touched the back of the heater, introducing an offset between the sample surface and thermocouple reading. This offset varied between 50 to 150^o, depending upon the growth temperature, as well as from run to run depending on the details of the sample mounting arrangement. This offset was compensated for by determining the surface temperature versus thermocouple reading, as described in Section 9.2.

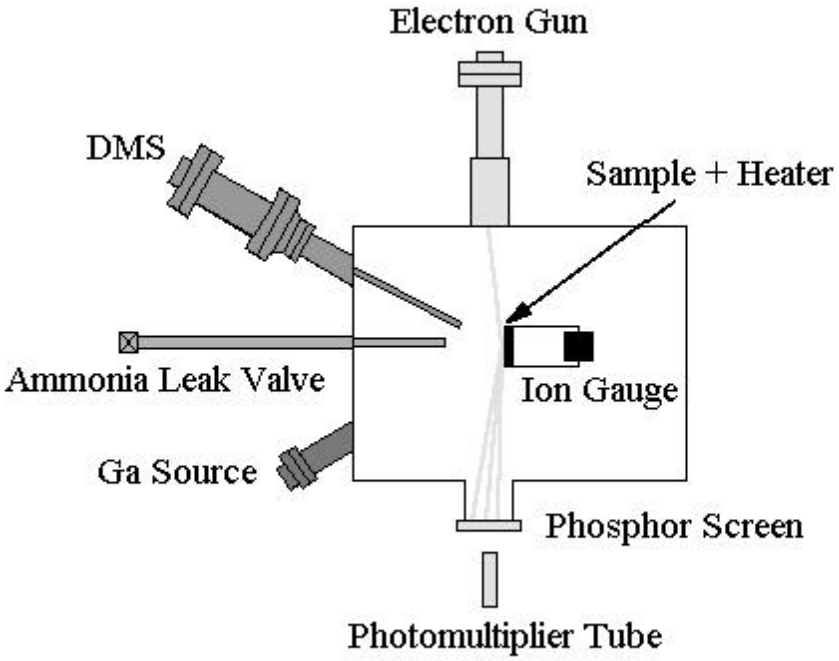

Figure 1: Schematic diagram of the Gen II MBE system used for growth.

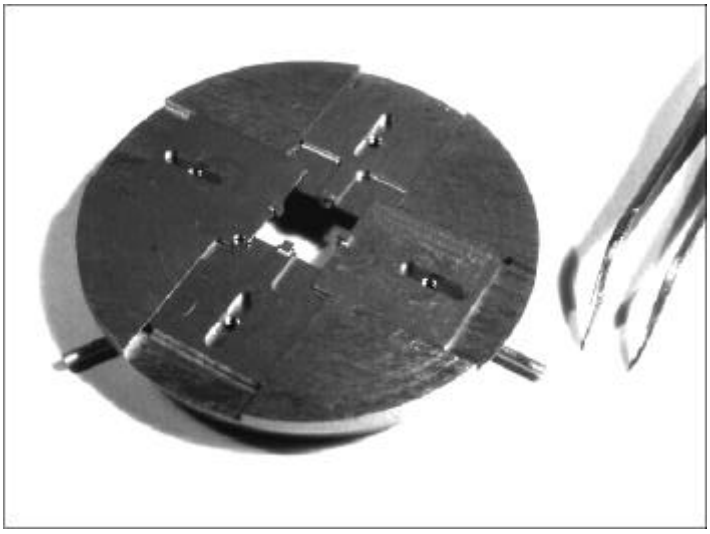

Figure 2: Sample holder to accommodate samples stress free of any shape and size, from 3x3 mm to 1/2x1/2". This is accomplished by 4 notched interleaving sliders mounted into a standard Varian GEN II sample block.

Mounting arrangements involving In or Ga-Sn bonding were found to be unreliable due to evaporation at the high substrate temperatures used in AlN and GaN growth, resulting in cold spots and eventual loss of the sample. This is due to their height vapor pressures, which limits their use to about 675^{o}C for In and to about 725^{o}C for Ga-Sn. Clips that applied even slight pressure induced unwanted stress onto the sample and caused sapphire to crack during thermal cycling. Instead mounts were used which hold the samples loosely without stress. For 1 inch diameter substrates, this was accomplished by using a retainer ring which screws onto a Mo block. The Mo block has a hole in the center, slightly less than 1 inch, exposing the back of the substrate directly to the heater. Figure 2 shows the type of sample holder used for square substrates, which has the ability to accommodate any shape and size sample from 3×3 mm to 0.5×0.5 inch via notched interleaving sliders.

2.2 Film Preparation

Single-crystal bulk GaN platelets were used for some of the measurements, with the opposing c-plane faces corresponding to the two possible polarities. A typical platelet is shown shown in Figure 3. These substrates, approximately 5×5 mm in size, were grown in Ga solution at high nitrogen pressures[8]. One of the polar faces can be chemo-mechanically polished[9] utilizing KOH, resulting in an atomically smooth surface with an RMS roughness on the order of half a lattice constant, where *c*=5.2 Å. A typical surface after polishing is shown in Figure 4. No suitable chemical method has been found yet to polish the opposite face to comparable quality, so instead only a fine mechanical polish was applied [9]. The resulting surfaces were quite rough, with polishing groove several hundred Ångstrom deep. Note that polishing could produce a slight misorientation from the c-plane. These bulk samples were cleaned by boiling them first in acetone and then in methanol at 65^{o}C before mounting them on a Mo sample holder. Two mounting methods were used: The samples were either coated on their back side with 2000 Å of Ti followed by Mo and then mounted without stress by mechanical means (see chapter 2.1), or by bonding to a sapphire wafer using a GaSn eutectic.

For measurements on c-plane Al_2O_3 both 1 inch diameter and 10x10 mm square substrates were used. The substrates were cleaned for 5 min in acetone and methanol, followed by a 5 min etch in 1:1 H_3PO_4:H_2SO_4. Each step was performed at 65^{o}C, followed by a final deionized water rinse and rapid drying with high purity N_2. Atomic force microscopy (AFM), as shown in Figure 5, confirmed atomically smooth substrates featuring atomic steps. As for the bulk crystals, a 2000 Å Ti followed by Mo coating was applied to the back of the substrates by e-beam evaporation in a separate chamber to increase the heat absorbed by radiation and to assist in even heat distribution.

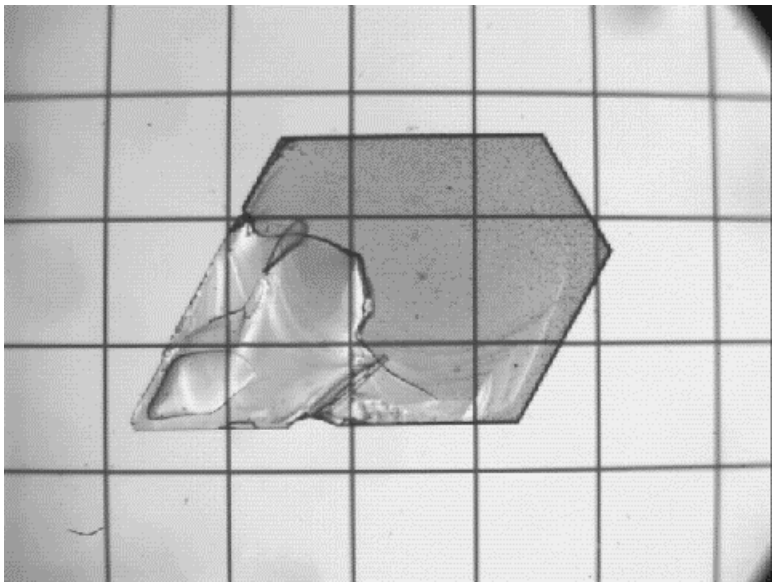

Figure 3: Typical Bulk GaN Crystal. The grid is 1mm.

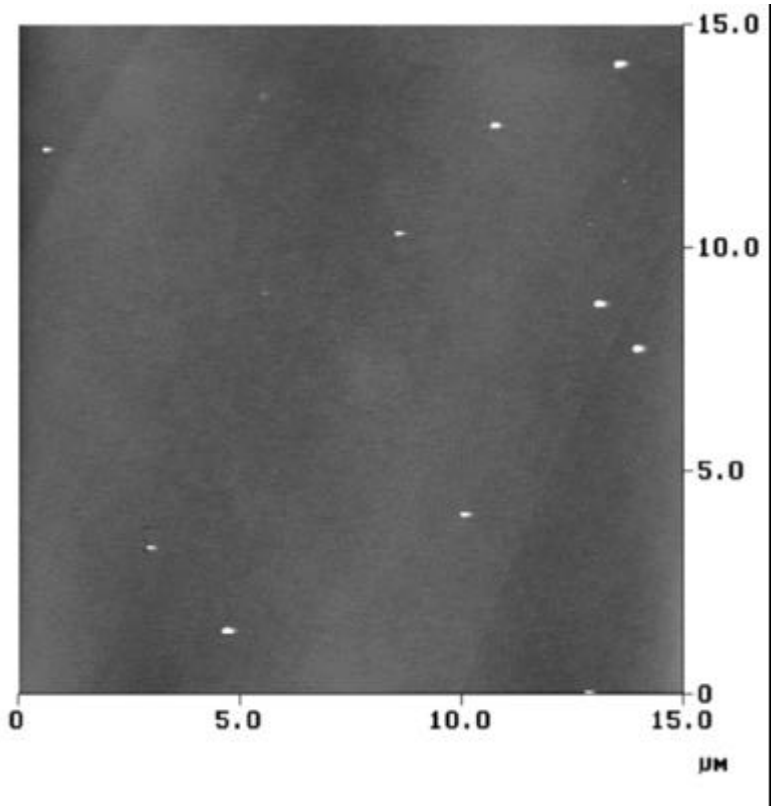

Figure 4: AFM image of bulk GaN(0001) surface after polishing.

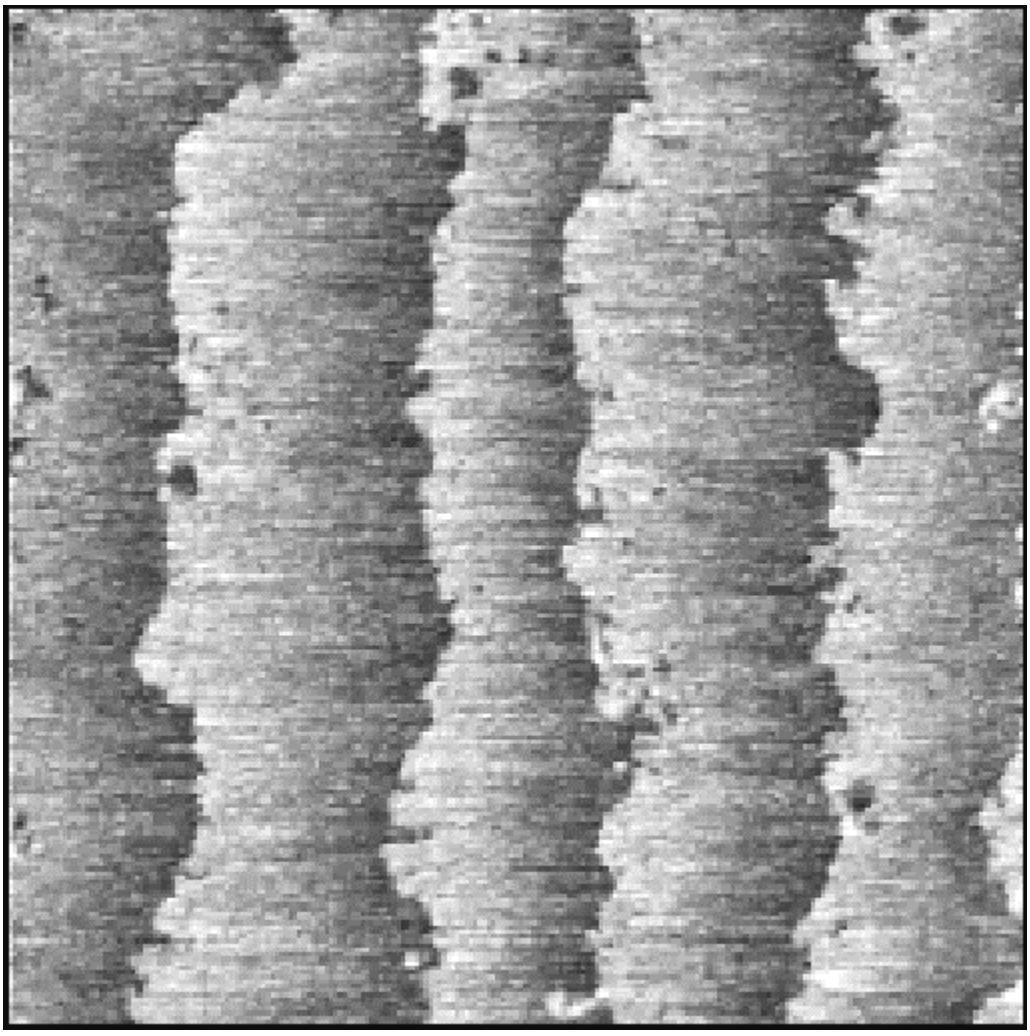

Figure 5:A 500x500 nm AFM image of an atomically smooth Al_2O_3 substrate after being cleaned in acetone and methanol, followed by an etch in 1:1 H_3PO_4:H_2SO_4. Each step was performed at 65^oC for 5 min, followed by a final deionized water rinse and rapid drying with high purity N_2. The steps are about 1000 Angstrom in width.

2.3 Desorption Mass Spectroscopy (DMS)

DMS permits the detection of the type and intensity of desorbed species from a sample surface in real time. Figure 6 shows an illustration of the DMS setup used in this study. The apparatus was similar to the one used by Tsao et al. [10] to study GaAs growth kinetics, and by several other workers [6,,11,12,13] for GaN growth. In this thesis, known fluxes of Ga and NH_3 are applied to the substrate, which react to form GaN. Any byproducts of this reaction, as well as desorbing unreacted precursors, can be detected by the DMS.

The core of the DMS is a quadrupole massspectrometer, manufactured by Stanford Research Systems, model SRS 200. The solid angle seen by the DMS is limited by collimators to subtend only a 6 mm region on the center of the sample. This collimation reduced the effect of a temperature gradient across the sample as well as the background contribution of surrounding cooler surfaces.

In order to increase the signal to noise ratio, the DMS was differentially pumped by using a liquid nitrogen cryoshroud around the ionizer. Improvements of better than one order of magnitude in signal to noise ratio were obtained. The remaining noise was identified as shot noise, since it increased as the square root of two with signal amplitude.

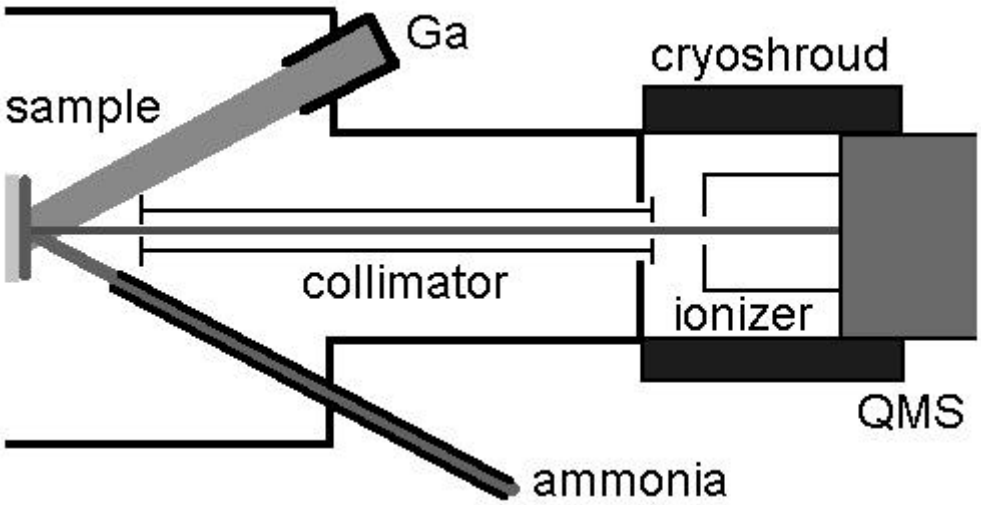

Figure 6: DMS

2.4 Reflection High-Energy Electron Diffraction (RHEED)

Reflection High-Energy Electron Diffraction (RHEED) is a technique for analyzing surfaces, and is especially well suited for *in situ* observations in MBE systems. RHEED is closely related to electron microscopy, but instead of passing an electron beam through a thin film, the electron beam impinges on the surface at a grazing angle of around 3^{o}. The electron beam is Bragg diffracted by the surface, and the diffracted beams are then observed on a phosphorus screen. RHEED is a very powerful method for surface studies since the electron beam penetrates only about 2 or 3 monolayers deep into the crystal lattice. In this section a very brief description of RHEED is given. The basics of reciprocal space and RHEED are covered by Kittel[14], and a vast source of is the collection of papers given at a NATO Advanced Research Workshop on RHEED[15].

Since only the surface is probed by RHEED the reciprocal lattice will consists of rods in the direction normal to the surface probed, instead of discrete spots as in electron microscopy. Figure 7 shows those rods. The incoming wave vector is labeled $\mathbf{K}_i$, while the diffracted beam is labeled $\mathbf{K}_f$. Constructive interference occurs where $\mathbf{K}_f$, defining the Ewald sphere, intersects with the reciprocal lattice rods. If a phosphorus screen is placed in front of the sample, diffraction spots will appear at positions on the screen which are given by extending the $\mathbf{K}_f$'s to the screen that satisfy the Bragg condition.

Ideally the reciprocal lattice rods are very thin, but due to surface irregularities those rods have a finite width, as shown in the figure. This relaxation of the diffraction condition can be described by an angle Δq_f, which causes the ideal dots on the screen to become streaks. Note that rough surfaces (3-D) cause the beam to pass through facets on the sample surface, resulting in a spotty diffraction pattern instead of the streaks, similar to a Transmission Electron Microscope (TEM) pattern.

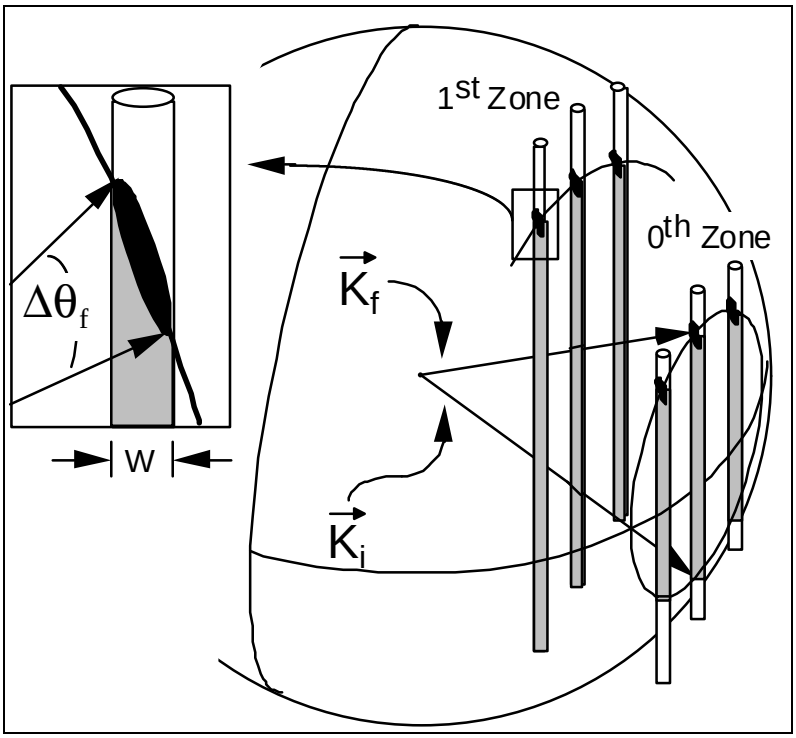

Figure 7: RHEED Pattern[16]

A surface is called unreconstructed if only integral streaks appear on the screen, as given from the bulk crystal lattice. Reconstructions usually occur in multiples of the lattice periodicity, which appear as streak between the integral streaks.

Sometimes oscillations of the streak intensity can be observed during growth, corresponding to the growth rate. This behavior is an indicator of growth by island nucleation, as shown in Figure 8. The basic cause for these oscillations is that an uncompleted layer causes some distractive interference. This causes the RHEED beam to be weaker compared to a completed layer without interference. During growth the surface oscillates between an uncompleted and a completed top layer, causing the RHEED intensity to oscillate as well. On the other hand, the absence of RHEED intensity oscillations indicates growth by step flow. During step flow growth steps propagate across the surface, which looks the same to the incoming electron beam at all times.

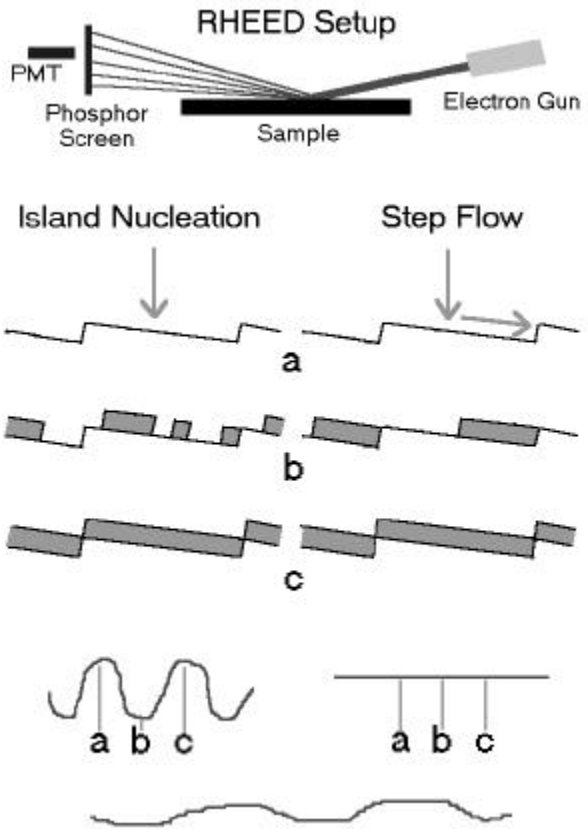

Figure 8: RHEED Oscillation Theory

Mixed growth modes are possible as well, during which part of the growth occurs by step flow and part by island nucleation. In this case the period of the RHEED intensity oscillations will be longer than expected from the actual growth rate.

In this thesis a 10 keV electron gun was employed for RHEED measurements of the specular intensity without energy filtering. Measurements were made with the electron beam directed along the GaN <11$\underline{2}$0> azimuth. The diffracted intensity of the specular beam was measured using a phosphor screen and a photo multiplier tube.

3. N VS Ga LIMITED GROWTH ON GaN-B

3.1 Introduction

In this chapter the growth kinetics on hexagonal films identified as GaN(000$\underline{1}$) (see chapter 4) will be discussed, and two distinct regimes of growth are shown [17,18]. These regimes show different surface morphologies and growth dynamics, primarily due to the surface coverages of Ga and nitrogen, along with hydrogen [11,19]. The main result is that the diffusion length of adsorbed Ga is much smaller under conditions in which the Ga flux limits the rate of growth. However, it is not yet apparent which growth mode is optimal for doping or for growth on strain free surfaces.

Next results of diffraction and mass spectroscopic measurements are presented, which show two growth regimes with different surface dynamics. These growth regimes are then explored in subsequent sections: the details of the diffraction measurements, the nature of the surface processes, and the limits of growth under excess Ga and at high substrate temperatures. From these measurements a simple kinetic model and framework is developed that describes the overall growth.

3.2 Experimental

Before introduction into the growth chamber the sapphire substrates were prepared as described in section 2.2. Prior to growth the substrates were outgassed for several hours at 300^{o}C in the preparation chamber of the MBE system, followed by 1 hour at 500^{o}C in the growth chamber. The NH_3 leak valve was set to produce a BEP of 1.0×10^{-5} Torr. Then the substrate temperature was ramped at 100^{o}/min from 500^{o}C to 1000^{o}C for a 15 min surface nitridation. AFM showed that the surface remained atomically smooth after this Al_2O_3 nitridation.

Experiments were performed by using two types of nucleation layer, AlN and GaN. The 250 Ångstrom AlN nucleation layer was grown at 1000^{o}C using an Al flux of 1.2×10^{14} cm^{-2}s^{-1} (equivalent to 0.10 ML/s AlN). RHEED showed a transmission pattern during and after AlN growth. The Ga shutter was then opened to provide a flux of 1.1×10^{15} cm^{-2}s^{-1} (or 1.0 ML/s GaN) and the sample temperature was ramped down to 800^{o}C at 100^{o}/min. The Al shutter was closed during the ramp below 900^{o}C.

The GaN nucleation layer was grown by repeating a sequence consisting of condensing Ga on the substrate surface at 700^{o}C and subsequent annealing at 800^{o}C under NH_3 ten times. This was achieved by ramping the substrate temperature to 700^{o}C, in the presence of an NH_3 BEP of 1.0×10^{-5} Torr. The Ga shutter was then opened at 1.1×10^{15} cm^{-2}s^{-1} (or 1.0 ML/s GaN) and the substrate kept at 700^{o}C for about 1 min, during which time the RHEED pattern completely disappeared. The Ga shutter was then closed and the sample ramped to 800^{o}C where it was kept for about 2 min until a RHEED pattern reappeared. This procedure was repeated 10 times, and a transmission RHEED pattern was observed after completion of this nucleation procedure.

Both types of nucleation layer were followed by a 2500 Ångstrom GaN buffer layer, deposited at 800^{o}C with a Ga flux of 1.1×10^{15} $cm^{-2}s^{-1}$ (or 1.0 ML/s GaN) and an NH_3 BEP of 1.0×10^{-5} Torr. After completion of the buffer layer, RHEED showed a streaky pattern. A (1×1) pattern was observed in the case of using GaN nucleation, while a very weak (2×2) reconstruction was typically observed using AlN nucleation. For this study, films grown with an AlN nucleation layer were found to be predominantly GaN(000$\underline{1}$) oriented featuring inversion domains, while the GaN initiation layer resulted in unipolar GaN(000$\underline{1}$) surfaces (see section 4).

3.3 Growth Regimes

3.3.1 Overview

In this chapter the different growth kinetics and growth morphologies obtained as a function of deposition parameters are described. It is emphasized, however, that the results depend on which of the two basal plane surfaces, either the (0001) or (000$\underline{1}$), is used for growth. These have different polarities and bonding configurations. A growth surface could also have inversion domains and be a mix of the two polarities. The usual III-V convention is used here, that the [0001] direction is from a Ga to a N atom. Hence, if a GaN(000$\underline{1}$) surface were terminated with a layer of N atoms according to the bulk Wurtzite structure, each N atom would be bonded to three Ga atoms in the underlying layer below. In this section only growth on GaN(000$\underline{1}$) is discussed. It will be shown that for this polarity the termination can be modified by adsorption and that the main growth regimes correspond to conditions of either excess N or excess Ga.

The two main surface morphologies observed in the MBE growth of GaN(000$\underline{1}$) on sapphire are illustrated by RHEED and AFM data in Figure 9. Both films were grown under similar conditions but with very different Ga fluxes. Both GaN films are 0.8 um thick and were grown using an AlN nucleation layer, which typically produces some inversion domains (see section 4). Growth rates were 0.5 μm/h with an NH_3 BEP of 1.0×10^{-5} Torr at a substrate temperature of 800^{o}C. Figure 9a and c show RHEED and AFM data for a Ga flux of 1.1×10^{15} $cm^{-2}s^{-1}$ (or 1.0 ML/s GaN) while Figure 9b and d show data for a sample grown with a Ga flux of 6×10^{14} $cm^{-2}s^{-1}$ (or 0.5 ML/s GaN). AFM reveals that the film grown with a higher Ga flux is locally smoother, featuring atomic steps with 50 nm terraces, than the one grown with a lower Ga flux. Similar to what is shown by the AFM data, the RHEED pattern shows a well defined specular beam with

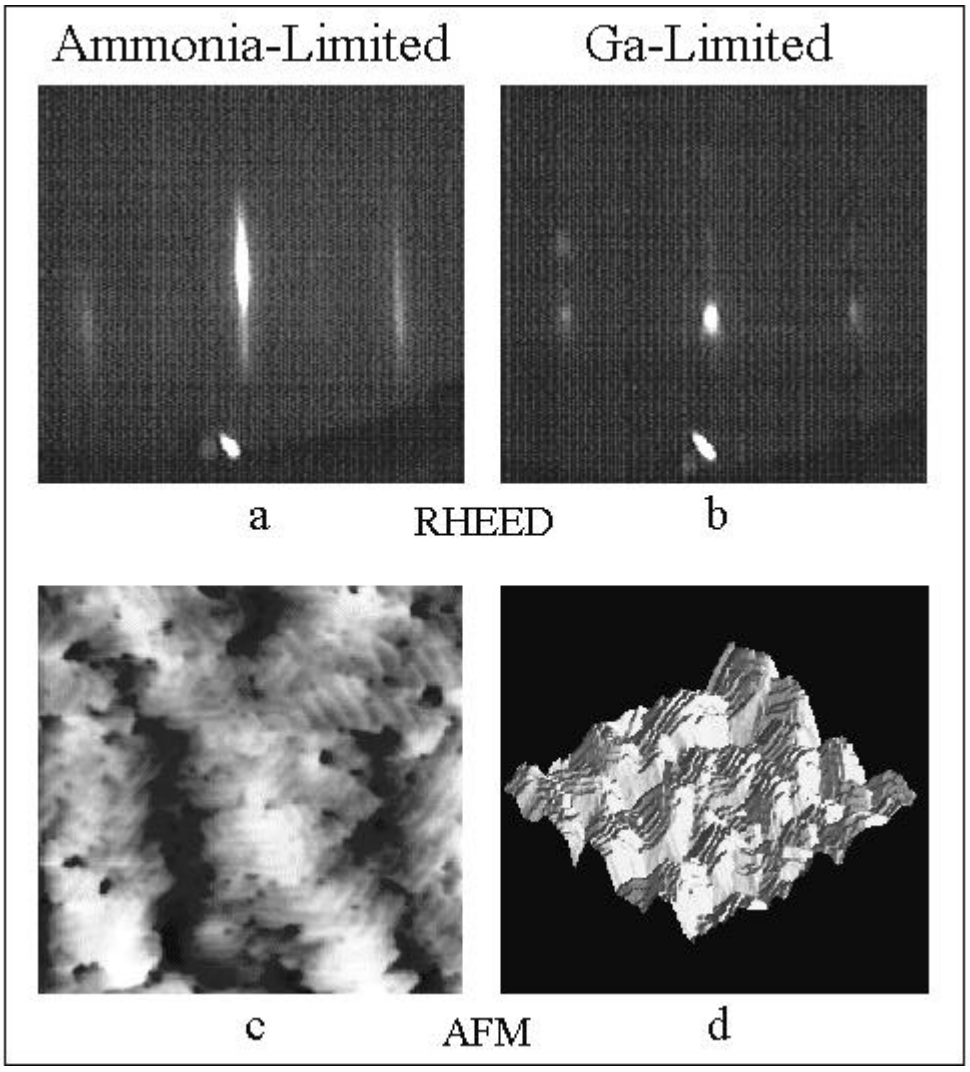

Figure 9: RHEED patterns with the incident beam along the <11̲20> azimuth and AFM images for both NH_3 and Ga-limited growth. The AFM scans cover an area of 2x2mm with a z-range of 50 Ångstrom and 1000 Ångstrom, respectively. NH_3-limited growth gives rise to a streaky RHEED pattern (a) and AFM shows atomic steps on islands (c). Ga-limited growth results in a RHEED pattern with a strong transmission component (b) and AFM indicates that this is due to facets (d). Note that for high Ga:NH_3 ratios pinholes with diameters of approximately 1000 Ångstrom are observed.

long streaks, indicative of two-dimensional layers with random atomic steps. The surface exhibited a very weak (2×2) reconstruction. By contrast, the film grown at a lower Ga flux is much rougher and faceted. Consistent with these AFM results, the RHEED pattern shows transmission-like features that do not move as the incident electron angle is

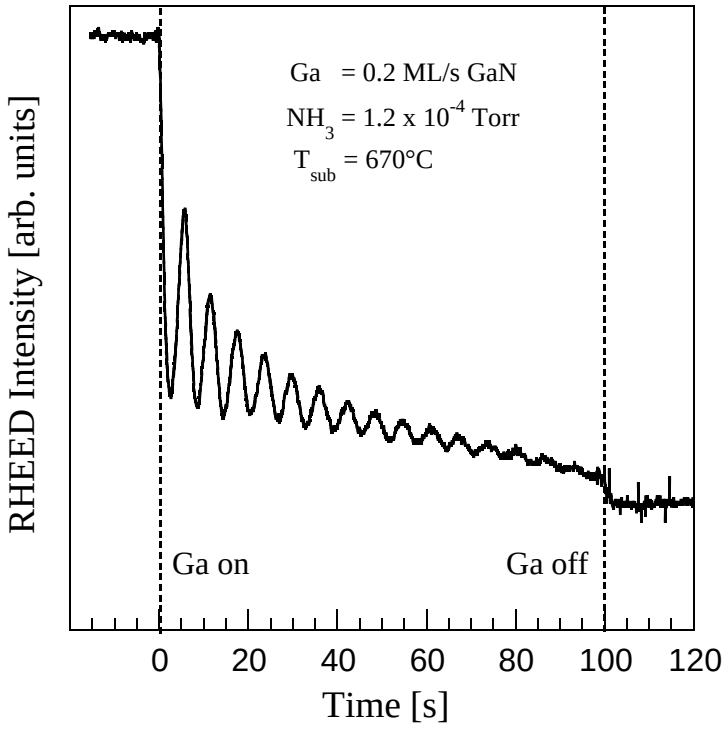

Figure 10: GaN monolayer (c/2) RHEED intensity oscillations observed by first growing in the NH_3-limited regime until the RHEED pattern was streaky. Then the Ga shutter was closed, the NH_3 flux increased to provide Ga-limited conditions, and the substrate temperature lowered from 800°C to 670°C. Upon opening of the Ga shutter RHEED intensity oscillations were observable, recorded along the <11̲20> azimuth. Prolonged growth resulted in a 3-D RHEED pattern. The film is best recovered by growth in the NH_3-limited regime.

changed. Similar results are obtained on films with single-domain GaN, grown with GaN nucleation layers, and on bulk GaN(000$\underline{1}$), also free of inversion domains. These two morphologies are seen in the following subsections to correspond to distinct growth regimes.

The growth dynamics are also very different under these two Ga:NH_3 flux ratios. Two examples of the evolution of the surface structure, as measured by the specular RHEED intensity versus time, are shown in Figure 10 and Figure 11. In Figure 10 the intensity of

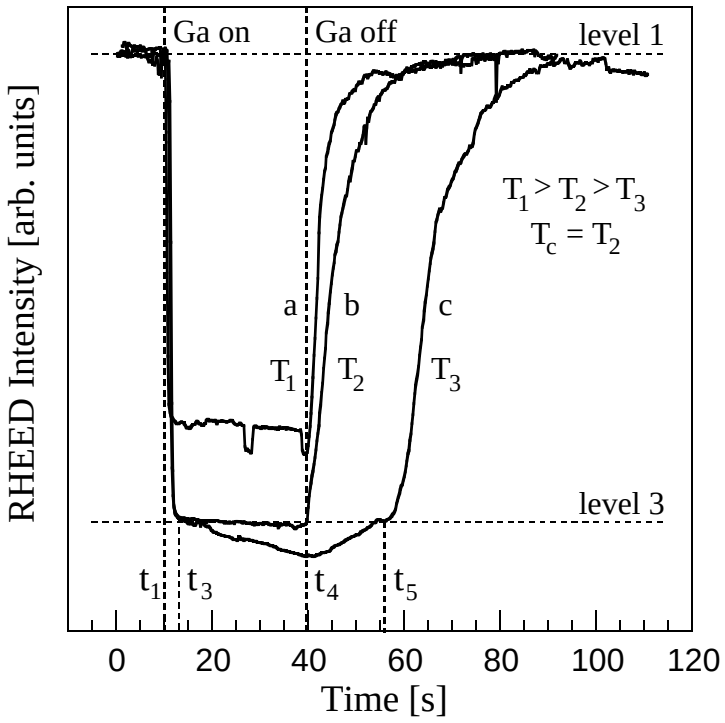

Figure 11: Fig. 6: Intensity variation of the specular RHEED beam along the <1120>azimuth during opening and closing of the Ga shutter in an NH_3 flux for (a) above, (b) at, and (c) below the condensation temperature. Curve (a) corresponds to a partial layer of weakly adsorbed Ga and partial nitridation, curve (b) to a complete layer of weakly adsorbed Ga, and curve (c) to Ga condensation.

the specular RHEED beam vs time is plotted for a sample held at 670^{o}C for a low Ga:NH_3 flux ratio, while Figure 11 shows a similar plot for a sample held at 780^{o}C at a high Ga:NH_3 flux ratio. These are distinctly different behaviors, with one showing island nucleation and the other suggesting step flow. The rate limiting reactions will be explored with DMS as well as the composition and reactivity of the surfaces corresponding to these growth conditions. It will show that island nucleation observed in these RHEED data correspond to Ga limited growth while step flow corresponds to NH_3 limited growth.

3.3.2 Growth Regimes

To understand these distinct types of surface morphologies and growth kinetics, DMS was used to determine the rate limiting reactions. The main advantage of this technique is that measurements are made on the same sample under controllable growth conditions. The basic assumptions is made that the incident Ga either desorbs or contributes to GaN formation, and that no Ga inclusions or droplets are formed. Then, the difference between the incident and the desorbing Ga flux, as measured by DMS, is the growth rate. This method (see appendix 9.1) [17] does not require measurement of the sample area. It only requires a comparison of the desorbing Ga flux with and without an NH3 flux. In conjunction with a calibrated Ga source, absolute growth rates are obtained. Figure 12a shows a measurement of the desorbing Ga flux with and without NH_3; the method of extracting growth rates from this data is discussed in more detail in Section 9.1. This method works best when the desorbed Ga signal is large. With this method, the absolute growth rates vs incident NH_3 and Ga flux as well as substrate temperature can be measured.

If the desorbed Ga flux is small, the desorbed H_2 signal is used instead. Figure 12b shows that H_2 is released during growth using NH_3. This figure is a plot of the H_2 signal vs time with the sample under constant NH_3 flux, while opening and closing the Ga shutter. Under the assumption that this increased H_2 desorption is attributed to the forward reaction

$$2Ga + 2NH_3 \rightarrow 2GaN + 3H_2 \qquad (3\text{-}1)$$

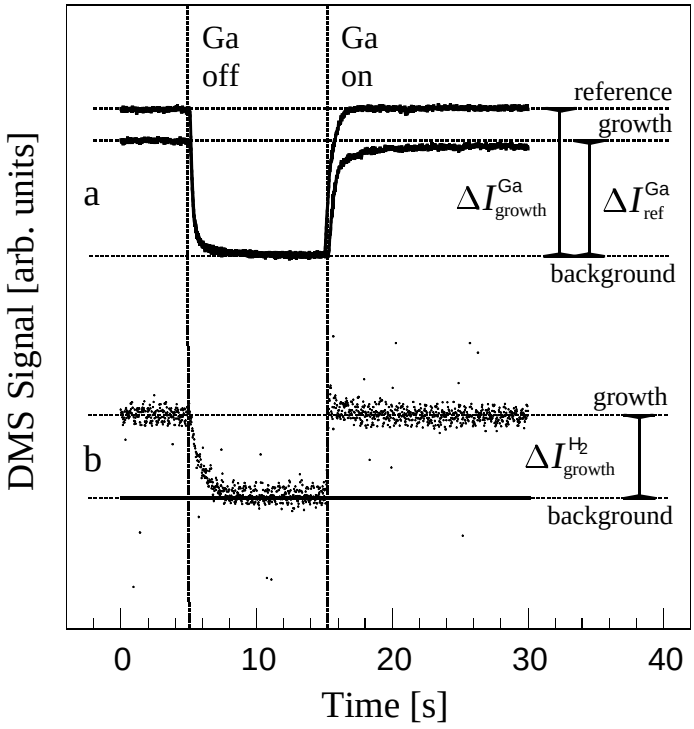

Figure 12: Typical uncollimated Ga and H_2 DMS signal during closing and opening of the Ga shutter. The growth and reference signal is obtained by measuring the rapid change in signal after closing the Ga shutter to avoid contributions of the slowly varying background signal from other cooler parts of the system. Growth rates are obtained from the Ga signals by calculating the incorporation fraction and multiplying by the known incident flux. The H_2 signal was found to be proportional to the growth rate. Note that the growth rate is obtained by closing the Ga shutter instead of opening to ensure steady state after 15 min of growth.

we can obtain relative growth rates. Measurement of the H_2 DMS signal is especially useful when the Ga signal is below the detection limit of the DMS. The H_2 signal intensity is larger because lower mass ions have a larger transmission through the mass spectrometer. A disadvantage of this technique is that absolute growth rates cannot be determined as easily. Nonetheless in combination with measurement of the Ga signal, growth rates can be determined over a wide range of conditions. These DMS measurements that identify the rate-limiting fluxes are particularly important since RHEED is not able to measure growth rates under conditions of step-flow growth.

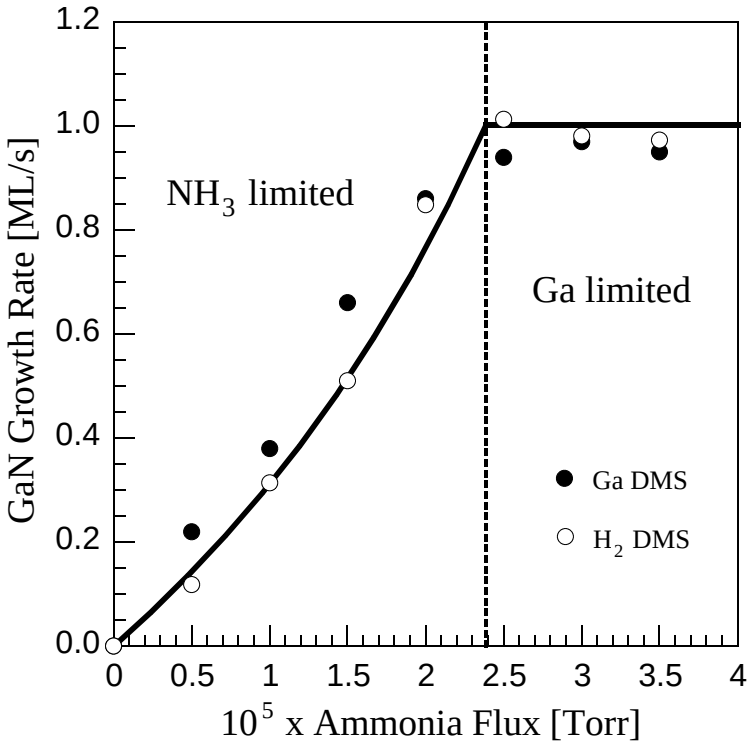

Figure 13: GaN growth rate as a function of NH_3 flux at constant Ga flux of 1.0 ML/s (GaN) and surface temperature of 785°C, using both the Ga and H_2 signal. Both growth regimes can be identified, NH_3-limited and Ga-limited. In the NH_3-limited regime the growth rate is an approximately linear function of the NH_3 flux, while in the Ga-limited regime near unity Ga incorporation is obtained. Note the good agreement between using Ga and H_2 DMS.

Applying the above DMS method, Figure 13 shows the GaN growth rate vs NH_3 flux at a fixed Ga flux and substrate temperature. These data represent a series of *in situ* measurements on the same sample, with 15 min of growth between data points under conditions of the point to be measured. The H_2 signal is proportional to the Ga data, indicating that using the H_2 signal is a valid method of obtaining relative growth rates. Growth rates calculated from the Ga signal agreed well with stylus and RBS measurements. From this figure a number of observations can be made: At low NH_3 fluxes the growth rate is approximately a linear function of the NH_3 flux, suggesting that a fixed fraction of the available NH_3 contributes to GaN formation. The deviation from linearity will be discussed later in terms of a proposed growth model. At high NH_3 fluxes

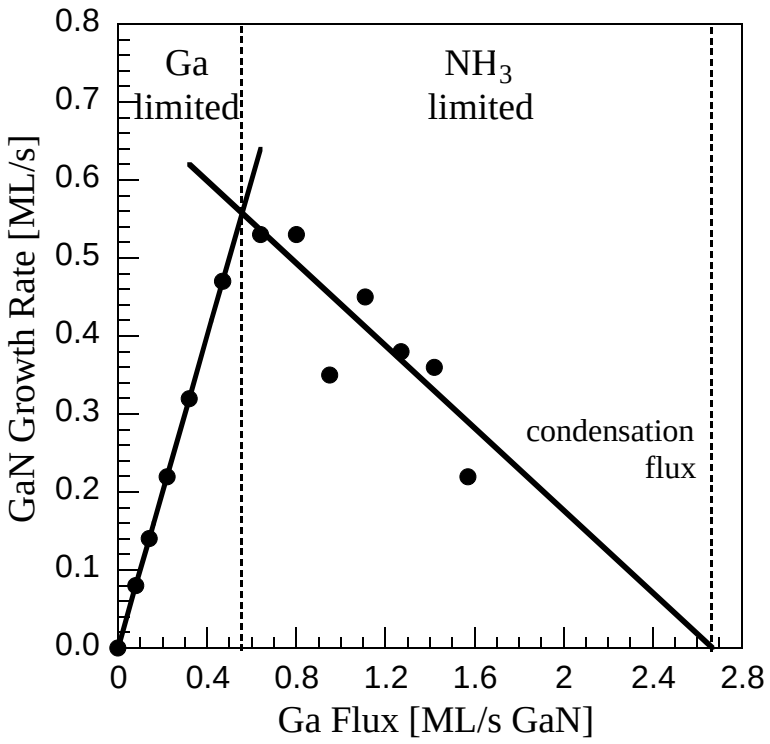

Figure 14: GaN growth rate as a function of Ga flux at constant NH_3 flux of $1.0x10^{-5}$ Torr and surface temperature of 785°C, using Ga DMS. Two growth regimes can be identified, Ga-limited and NH_3-limited. Near unity incorporation of Ga is obtained during Ga-limited growth. During NH_3-limited growth the growth rate reduces as a function of Ga flux, approaching zero at the flux required for condensation at this temperature. This reduction is attributed to weakly adsorbed Ga blocking active Ga terminated GaN sites.

no Ga desorption is measured. Hence the growth rate is a constant with unity Ga incorporation, within an uncertainty of less than 15%. The crossover between those two regimes is relatively abrupt, allowing the identification of at least two growth regimes: when there is excess Ga, the growth rate is limited by the NH_3 flux; when there is excess NH_3, the rate is limited by the Ga flux.

The crossover can also be seen by measuring the growth rate as a function of Ga flux, at a fixed NH_3 flux and substrate temperature. The results are shown in Figure 14. From this figure the following conclusions can be made about the MBE growth of GaN(000$\underline{1}$): At

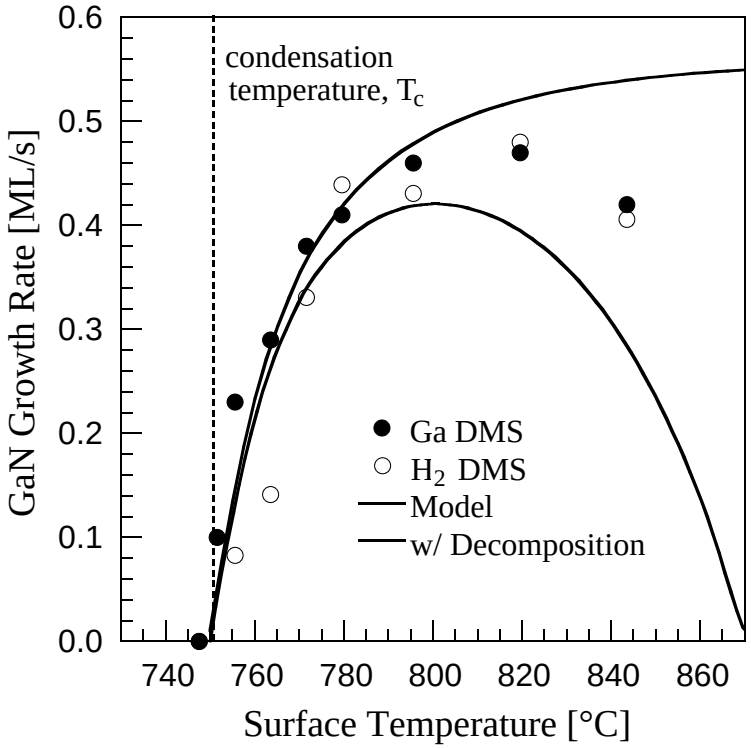

Figure 15: GaN growth rate as a function of surface temperature at constant Ga flux of 1.0 ML/s (GaN) and NH_3 flux of $1.0x10^{-5}$ Torr, using both the Ga and H_2 signal. The growth rate reduces towards the condensation temperature, attributed to weakly adsorbed Ga blocking active Ga terminated GaN sites. The high temperature growth rate reduction is due to GaN decomposition competing with growth.

low Ga fluxes the growth is Ga limited, as was observed above. At higher Ga fluxes a desorbed Ga signal was measured, indicating that not all Ga was incorporated and that there is insufficient NH_3. At these fluxes growth is thus NH_3 limited. Further, the growth rate decreased with increasing Ga flux, going towards zero. In Section 3.5.1 it will be shown that the flux at which the growth ceased corresponds to the condensation condition for this substrate temperature. This can also be seen in Figure 15, where the growth rate is plotted as a function of substrate temperature in the NH_3-limited regime.

3.3.3 Ga-Limited Growth

In the Ga-limited growth regime RHEED intensity oscillations were observed that indicate epitaxy proceeds via the nucleation and growth of two-dimensional islands. An example of a measurement was shown in Figure 10. The strongest oscillations were recorded below 700^{o}C, but can seen at temperatures as high as 850^{o}C. Though, intensity oscillations have been reported previously [20,21], these are, to our knowledge, the strongest observed to date. The period of these intensity oscillations, however, corresponds only approximately to monolayer (*c*/2) growth.

Further, these intensity oscillations are not characteristic of a narrow growth front. Instead, continued growth eventually led to a transmission RHEED pattern. And, except perhaps at very high temperatures, the intensity does not recover upon closing the Ga shutter. In the case of other III-V semiconductor growth, such as GaAs(100), growth interruption at the growth temperature is sufficient to prepare a surface sufficiently smooth to subsequently observe intensity oscillations. But here, in order to repeat a series of intensity oscillations, an anneal to as high as 800^{o}C was necessary. Alternatively a smoothing procedure involving growth in the NH_3-limited regime was helpful. Growth in the NH_3-limited regime, as described below, usually resulted in subsequently stronger oscillations than just annealing.

The process for smoothening by overgrowth starts by depositing approximately 100 Angstrom of GaN in the NH_3-limited regime. Typical conditions are a substrate temperature of 800^{o}C, a Ga flux of 1.1×10^{15} $cm^{-2}s^{-1}$ (or 1.0 ML/s GaN), and an NH_3 BEP of 1.0×10^{-5} Torr. After this smoothening step strong oscillations could again be observed. It should be noted that these strong oscillations were only observed when using a GaN nucleation layer, while in the case of an AlN nucleation layer oscillations were not observed or at best were exceedingly weak.

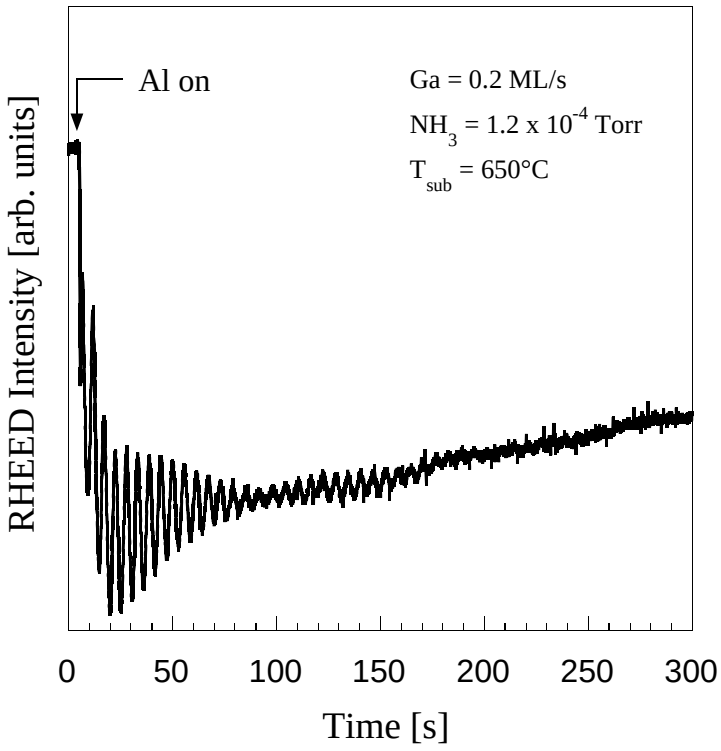

Figure 16: AlN RHEED intensity oscillations were observed by preparing a GaN surface in the NH_3-limited regime similar as for GaN oscillations. The AlN surfacecould not be smoothened sufficiently to obtain AlN oscillation from an initial AlN surface. These AlN oscillations were the first ones reported.

We also obtained damped AlN RHEED intensity oscillations by growing on GaN, as shown in Figure 16, using similar conditions and surface preparation procedures as for GaN on GaN. These oscillations correlate roughly to monolayer growth with unity Al incorporation. The GaN film was prepared by the previously described overgrowth method in the NH_3-limited regime. Then the substrate temperature was lowered to 670^{o}C and the Al shutter opened at a flux of approximately 0.2 ML/s. The main requirement was preparation of a sufficiently smooth surface and growth under high NH_3 flux.

GaN RHEED intensity oscillations cannot be used directly to measure growth rate, as shown in Figure 16. Here the frequency from data like those measured in Figure 10 are plotted as a function of Ga flux at two different NH_3 fluxes. Contrary to previous

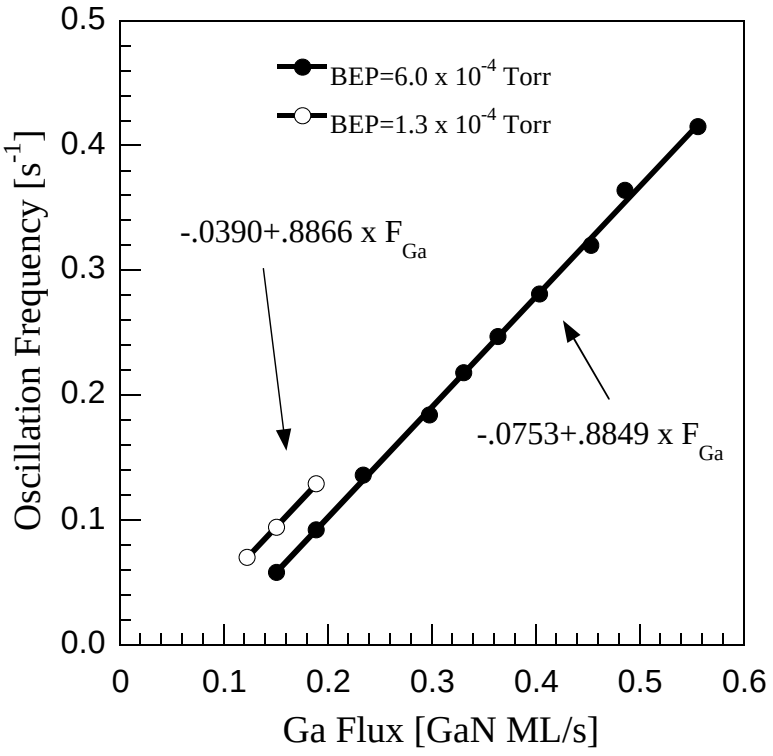

Figure 17: GaN RHEED intensity oscillations at the low temperature limit show a linear increase in oscillation frequency as a function of Ga flux. The frequency does not quite correspond to monolayer growth. The slope is roughly 0.9, and an offset is observed. This offset increases with increasing NH_3 flux.

suggestions [21,20], the period of these oscillations does not correspond exactly to monolayer (half a conventional unit cell) layer deposition. Note that the Ga flux was calibrated from GaAs intensity oscillations measured in the same growth chamber. The slope of the curve is about 0.9 for the fluxes investigated, and there is an offset of up to 0.08 ML/s at zero Ga flux. This offset depends on the NH_3 flux, increasing with increasing NH_3 flux.

The temperature dependence of the oscillations at different Ga fluxes is shown in Figure 18. For these three fluxes no oscillations were observed outside the temperature range covered, and the strongest and longest lasting oscillations were observed at the lowest temperature of each curve. Below this temperature, continued growth did not result in a

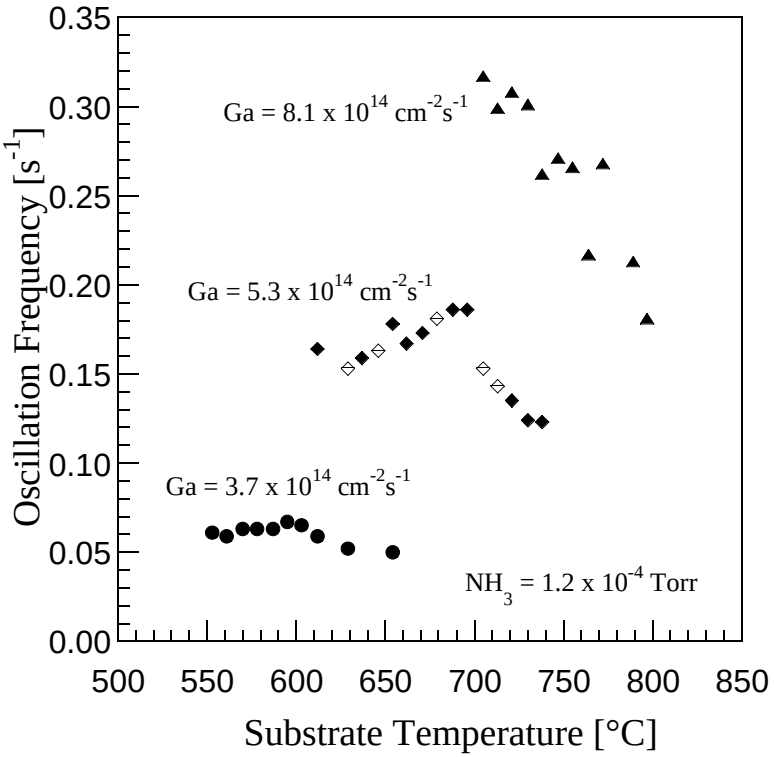

Figure 18: GaN RHEED intensity oscillation frequency as a function of sample temperature for different Ga fluxes. The decrease in oscillation frequency at higher temperatures is attributed to a transition from island nucleation to step flow growth. The activcation energy of this process was found to be 1.2 eV.

transmission RHEED pattern, but a pattern that indicated amorphous growth, representing the low temperature limit of single crystal GaN growth in the Ga-limited regime. At high substrate temperatures the oscillation frequency decreases, and the activation energy of this decrease was found to be 1.2 eV. Other samples with miscuts ranging from 0 to + 0.3^{o} off the c-axis, including stress-free bulk GaN, gave similar results. This reduction is not due to Ga desorbing from the GaN surface, as verified by DMS earlier under similar conditions. It is proposed that this reduction in RHEED oscillation frequency is due to Ga atoms diffusing to step edges, participating in step flow growth, and therefore not contributing to the oscillations.

Above about 850^{o}C, with excess NH_3, intensity oscillations were not observed. At these temperatures, the streaks in the initial RHEED pattern from a smooth surface transform into a 3D transmission pattern of spots, and the corresponding RHEED intensity shows a slow decrease. This transition to 3D was somewhat slower as the NH_3 flux was reduced. This is much different from the case of NH_3-limited growth, showing a rapid initial decrease upon opening of the Ga shutter, as presented earlier in Figure 11. The behavior at high temperature in the Ga limited regime is likely due to the increase in the sublimation of GaN along with the reduction in the rate at which Ga incorporates into islands.

3.3.4 NH3-Limited Growth

By contrast, for high Ga:NH_3 flux ratios, no intensity oscillations are observed, indicating that there is no cyclic change in surface roughness. This could still be a layer-by-layer mode. For example, the surface diffusion of Ga could be large resulting in the step flow on the surface, as in the case of GaAs MBE when Ga stabilized. However, using these high Ga:NH_3 flux ratios, there is still a significant change in the diffracted intensity.

The key RHEED intensity behavior is shown in Figure 11, where the specular RHEED intensity is plotted from a GaN surface during and after Ga exposure at three different substrate temperatures. The Ga shutter is opened at time t_1 and later closed at t_4. The incident Ga and NH_3 fluxes were the same for all three curves. The starting RHEED intensity depends only on whether there has been sufficient initial NH_3 exposure. About 100 Langmuirs were used to completely nitride the surface as discussed in Section 3.4 (Note that 1 Langmuir equals equals an exposure sufficient to adsorb 1 ML with unity incorporation.). This nitridation is relatively independent of typical growth temperatures. Three distinct behaviors are observed: Curve (a), measured at T_s=800^{o}C, shows between t_1 and t_3 an initial rapid decrease to a value that is relatively constant, and then at time t_4 a

rapid recovery. Curve (b), measured at a temperature 5^{o}C lower, shows a similar but larger decrease to a constant value, as well as a rapid recovery. And curve (c), reduced by an additional 5^{o}C, shows a similar initial behavior but then a slower steady decrease, followed by a two stage recovery having a slow and fast component. For the high and medium temperature case, the magnitude of this decrease is a function of growth parameters, less at higher substrate temperatures, higher NH_3 fluxes, and lower Ga fluxes. For the low temperature case, the magnitude of the initial rapid decrease is independent of temperature. However the subsequent slower decrease becomes steeper with lower temperatures. After closing the Ga shutter the time required for the first stage of the two stage recovery increases with lower temperatures.

The transition between curve (b) and (c) is very abrupt -- a temperature change of a few degrees is sufficient for its observation. It was found that this transition is independent of NH3 flux in the excess Ga regime (under excess NH_3 it is completely absent). The transition between curve (b) and (c) will be interpreted to correspond to the temperature, T_c, at which Ga condenses on the GaN surface. In Section 3.6.1 the RHEED data will be compared with DMS measurements, connecting the transition with the amount of adsorbed Ga.

3.4 Surface Processes

3.4.1 Surface Termination

Once again it is emphasized that surface termination is different than crystal polarity. Surface termination refers to the structure at the surface of a film which could be either GaN(0001) or GaN(000$\underline{1}$)polarity. If the structure can be maintained without an incident flux at a given substrate temperature, it will be termed stable. It was found that two stable surface terminations could be maintained and manipulated on GaN(000$\underline{1}$). DMS and RHEED were used to control and monitor these terminations.

First, a surface was prepared by exposure of a GaN(000$\underline{1}$) film to an NH_3 flux in the absence of Ga. After a 100 Langmuir exposure, the specular RHEED intensity had reached a maximum value. This nitrided surface is a stable termination since it does not change after the NH_3 flux is removed and serves as the starting surface for the measurements in Figure 19.

Preparation of a GaN(000$\underline{1}$) surface with a Ga termination is illustrated in Figure 19. A substrate temperature above that for Ga condensation was chosen (cf. Section 3.5.1). A nitrided surface was then exposed to a Ga flux in the absence of NH_3 while monitoring the specular diffracted intensity as well as the desorbing Ga. After opening the shutter at t_1, the RHEED intensity decreased to a steady state value at t_3, after going through a change in slope at t_2. The time to reach this steady state depended on the Ga flux. Since this is a steady state condition, the Ga desorption flux is equal to the incident flux. The Ga shutter was then closed at t_4, at which time the RHEED intensity increased until it reached at t_6 an intensity marked level 2, and the DMS signal simultaneously decreased to

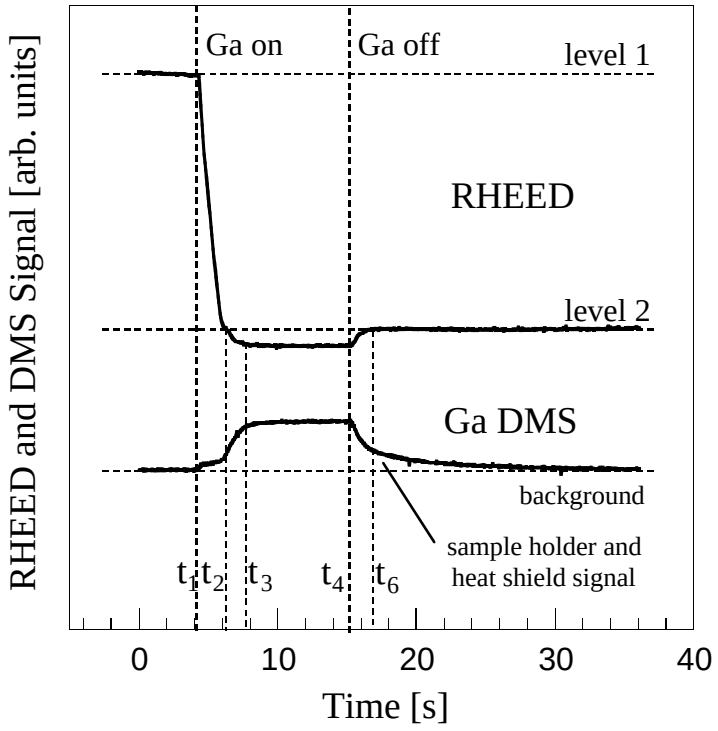

Figure 19: RHEED and uncollimated Ga DMS signal without NH_3 flux above the condensation temperature. Level 1 indicates a nitrided starting surface, while a stable level 2 is reached after Ga exposure, indicating a Ga terminated surface. Note that during Ga exposure the intensity level reaches steady state below level 2 suggesting fractional coverage of weakly adsorbed Ga.

a background. The final RHEED intensity was independent of the steady state Ga coverage that was achieved during deposition, when the RHEED intensity was below level 2. The DMS shows Ga desorbing, beyond t_4, which must be weakly bound compared to any Ga remaining at t_6. This last surface is stable in the absence of a Ga or NH_3 flux. Our interpretation of this data is that this surface consists of a strongly bound Ga termination layer on GaN(000$\underline{1}$).

If the surface is subsequently reacted with NH3 , the behavior seen in Figure 11 would again be obtained and the RHEED intensity rises to the nitrided value of level 1. These observations indicate that there are at least two stable surface terminations possible on

GaN(000$\underline{1}$) -- one is reached after the GaN surface is exposed to an NH_3 flux in the absence of Ga (level 1), and the other is obtained after Ga exposure, followed by an anneal in the absence of both NH_3 and Ga (level 2).

Knowing how to prepare these two surface terminations on GaN(000$\underline{1}$), the reconstructions reported by Smith et al. [22] were looked for (see section 4.3). Smith used a hydrogen free, RF plasma as a nitrogen source. It was found that in order to obtain the same reconstructions, the Ga termination had to be prepared first. Then the sample temperature was lowered to 400^{o}C. After deposition of additional Ga, the substrate temperature was lowered to below 300^{o}C and all of the reconstructions reported by Smith were observed, depending on the coverage of weakly bound Ga deposited. This suggests that H plays no role in the symmetry of partial Ga coverages on the Ga terminated, GaN(000$\underline{1}$) surface.

3.4.2 Surface Reactivity

We now investigate the reactivity of Ga on a previously nitrided surface, which will give us a better understanding of the growth process in the NH_3 limited regime.

The transient response of the specular RHEED intensity as well as the response of the desorbed Ga and H_2 fluxes to a step-function of incident Ga on the GaN surface are shown in Figure 20. These data were measured after growth had been stopped and the surface was nitrided. Then the background NH_3 pressure was reduced to 10^{-9} Torr while maintaining a constant substrate temperature of 760^{o}C.

A number of important features are observed in Figure 20 after opening the Ga shutter at a substrate temperature above Ga condensation. The initial shoulder in the curve corresponds to an initially low Ga desorption flux. This indicates that Ga adsorbs in a

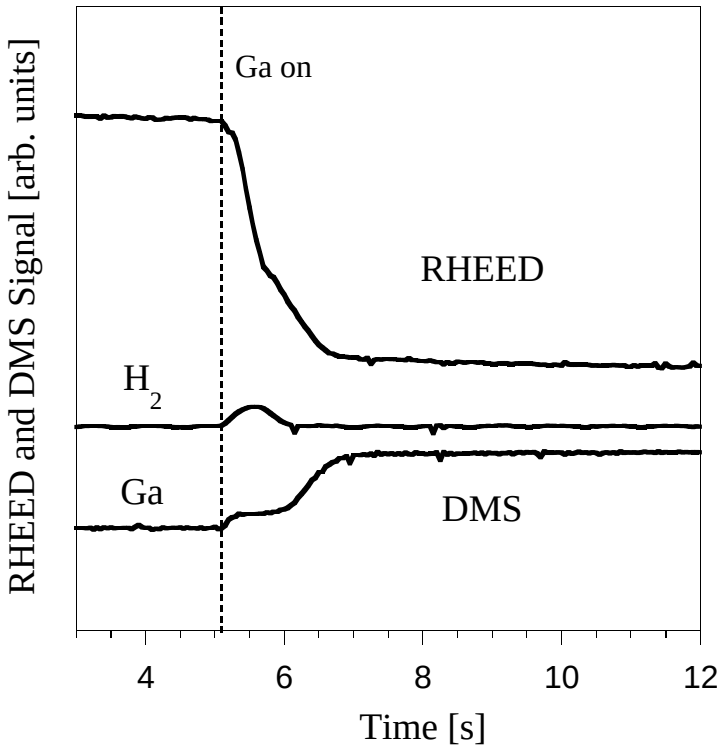

Figure 20: The transient response of the Ga and H_2 desorption to a step-function of incident Ga is shown in the absence of incident NH_3. The response of the specular RHEED intensity observed along the <11̲20> azimuth is also shown. $F_{Ga} = 1.6x10^{15}$ $cm^{-2}s^{-1}$, $T_{sub} = 760^oC$).

strongly bound site until the available sites are saturated. A H_2 pulse is seen as well that is a by-product of this adsorption process, indicating that this surface contains H [11]. After deposition of roughly one monolayer, the Ga desorption increases and the H_2 desorption decreases, indicating the presence of a second, weakly bound state. These results are consistent with the data showing two adsorption sites presented in Section 3.4.1. After the initial Ga pulse, the Ga shutter is closed and the weakly bound Ga is allowed to desorb from the surface. Subsequent exposure to incident Ga results in only the higher Ga desorption flux, with no detectable change in the H_2 desorption. This indicates that the hydrogen left in the nitridation process has been depleted. The hydrogen released required approximately one ML of incident Ga, deduced from the area under the desorbed Ga curve. Further, no additional Ga is adsorbed into the strongly bound sites, confirming that

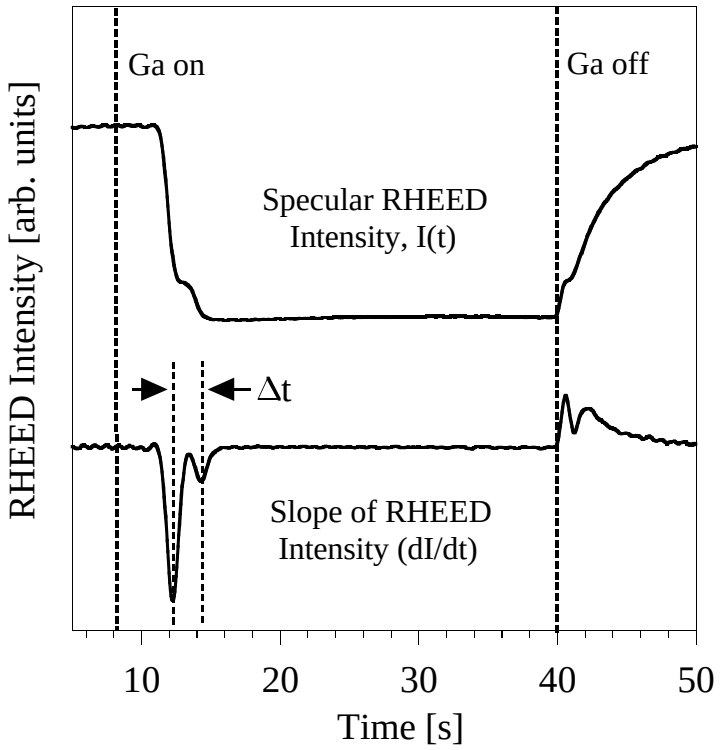

Figure 21: Specular RHEED intensity and its first derivative. Differentiation of the signal allows quantitative analysis of the transient signal. Experimental conditions for the data shown here are T_{sub} = 780^{o}C, NH_3 BEP=1.1x10^{-5} Torr. F_{Ga} = 1.45ML/s.

those sites are stable with time in the absence of any fluxes. Again, a surface could be prepared that would adsorb Ga in the strongly bound sites by exposing the sample to NH_3.

To quantify the Ga adsorption, the RHEED intensity was measured and its derivative plotted for different growth conditions. Figure 21 shows a measurement which was performed under NH_3 exposure while opening the Ga shutter. The derivative clearly reveals that two slope maxima occur during the initial transient RHEED decrease. Quantitative information can be extracted from this RHEED intensity variation by definition of a time interval, Δt, as indicated in Figure 21. It was found that the time dependence of the transient Ga and H_2 desorption track variations in the RHEED

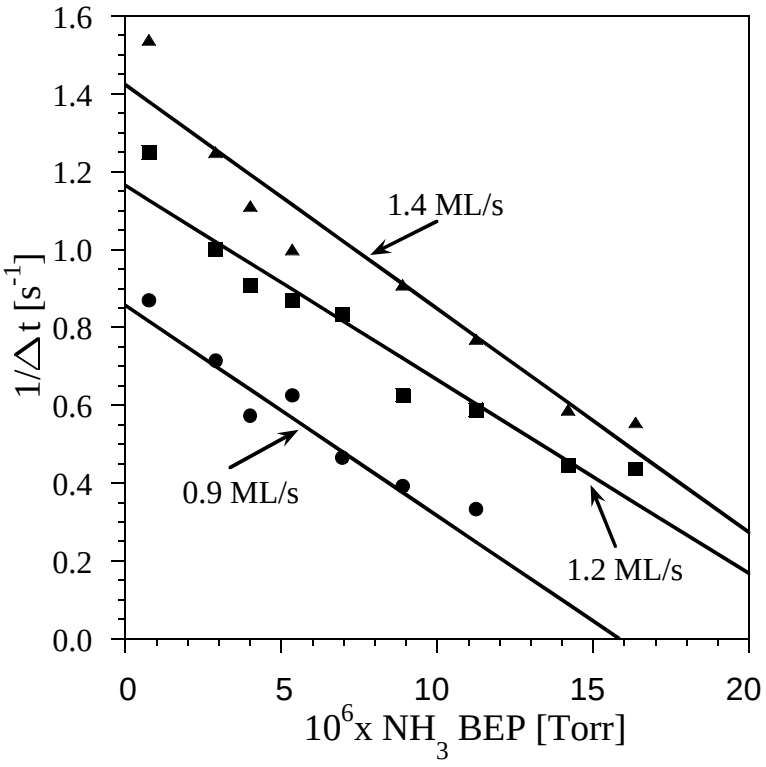

*Figure 22: Dependence of the surface transformation rate, 1/D*t, *on incident NH_3 BEP. Substrate temperature is 780°C. The linear curve fits shown in the figure were obtained using the least-squares method.*

intensity, exhibiting a change in slope. Based on this observation, it is concluded that Δt gives an estimate of the time required for saturation of the strongly bound Ga sites.

The dependence of Δt on both NH_3 and Ga flux is shown in Figure 22, which shows $1/\Delta t$ versus NH_3 BEP for three different Ga fluxes. It can be seen that $1/\Delta t$ increases for increasing Ga flux, but that it decreases as the incident NH_3 flux is increased. It is noted that the intercept on the $1/\Delta t$ axis is nearly equal to the incident Ga flux for all three curves, again suggesting that 1 ML of Ga can be adsorbed in strongly bound sites on a nitrided surface. The decrease in $1/\Delta t$ with increasing NH_3 pressure indicates that the physical process responsible for these transients is slowed by increasing the amount of incident NH_3.

A simple first order estimate of the time required for a termination change from a nitrided to a surface with strongly bound Ga sites can account for this behavior. In this model the Ga diffusion length is assumed to be large so every incident Ga atom will react with the nitrided surface. It is desired to estimate the time required for the entire surface to become Ga terminated. The small desorption of Ga from the strongly bound sites observed in Fig. 15 is neglected. The time derivative of the N-H surface coverage, q_N, is given by the difference between the incident fluxes

$$\frac{dq_N}{dt} = F_{Ga} - kP_{NH_3} \qquad (3\text{-}2)$$

where F_{Ga} is the incident Ga flux in ML/s, and kP_{NH3} is the active N flux in ML/s as supplied by the NH_3, with k being the system dependent conversion factor between measured NH_3 BEP and active N flux. Solving the above equation subject to the initial condition $q_N = 1$ at $t = 0$:

$$q_N = 1 - (kP_{NH_3} - F_{Ga})t \qquad (3\text{-}3)$$

It can be seen that $q_N = 0$ when $t = 1/(F_{Ga} - kP_{NH3})$, which is the time required to change all of the surface sites from N(H) terminated to Ga terminated. Consistent with this simple picture of the surface kinetics is the observation that the linear curve fits shown in Figure 22 intercept with the $1/\Delta t$ axis close to the incident Ga flux, as expected from the equation.

3.4.3 Transient Behavior

In this section the transient DMS response to a pulse of Ga under conditions of excess N and excess Ga is investigated. Figure 23 and Figure 24 show the desorbing H2 and Ga fluxes resulting from exposure of the GaN surface to a 15 second pulse of Ga while the NH_3 BEP is held constant. For the data shown in Figure 23, representing the Ga-limited regime, the Ga flux was 4.2×10^{14} $cm^{-2}s^{-1}$. In Figure 24, representing the NH_3-limited regime, it was increased to 1.4×10^{15} $cm^{-2}s^{-1}$. All other growth parameters were the same for both plots. In Figure 24 it can be seen that initiation of growth causes a transient pulse of H_2 to desorb from the surface, whereas in Figure 23 the desorbed H_2 flux reaches its maximum value at steady-state. A similar H_2 pulse is observed after closing the Ga shutter in the NH_3-limited regime, also seen in Figure 24.

The data in Figure 24 point to a crucial aspect of growth under conditions of excess Ga. If the H_2 signal is taken to be proportional to the GaN growth rate, these data indicate that the growth rate is enhanced in this NH_3-limited regime just after opening and closing the Ga shutter. It was shown in Section 3.4.1 and Section 3.4.2 that Ga adsorbs in two adsorption sites, strongly bound and weakly bound. After closing the Ga shutter the weakly adsorbed Ga either desorbs or is consumed by active N sites. Similarly, just after initiating the Ga flux, Ga first adsorbs into strongly bound sites, and then into weakly bound sites. The enhancement occurs during those times when the coverage of weakly adsorbed Ga is lower than that at steady state during growth. This behavior suggests that the presence of weakly bound Ga reduces the growth rate. In other words, this suggests that when excess Ga atoms are in the lattice sites deduced by Smith [22], the growth rate is reduced from its maximum value. This will be included in a first order in Section 3.6.2.

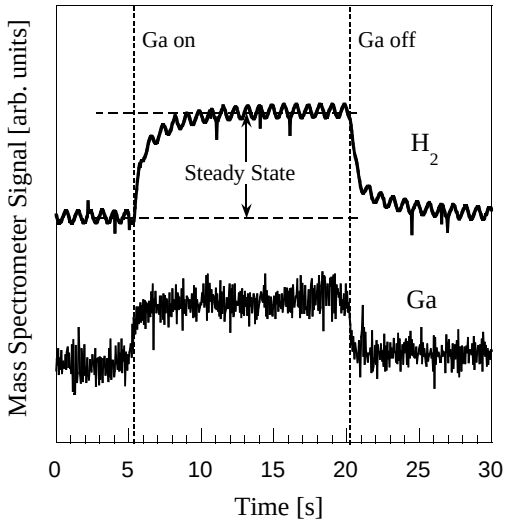

Figure 23: Changes in the H_2 and Ga desorption are caused by exposing a smooth GaN sample to a 15 second pulse of incident Ga under excess NH_3 conditions. Tsub = 820°C, NH_3 BEP = $7x10^{-6}$ Torr, F_{Ga} = $4.2x10^{14}$ $cm^{-2}s^{-1}$. The high frequency H_2 signal oscillations arise from fluctuations in H_2 background pressure caused by temperature cycling of the cryopumps.

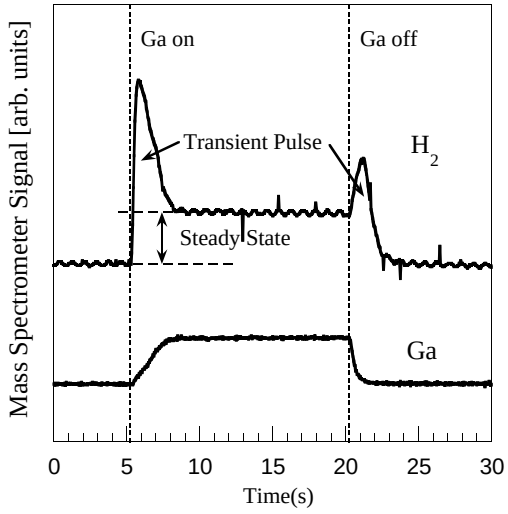

Figure 24: Changes in the H_2 and Ga desorption are caused by exposing a smooth GaN sample to a 15 second pulse of incident Ga under excess Ga conditions. Tsub = 820°C, NH_3 BEP = $7x10^{-6}$ Torr, F_{Ga} =$1.4x10^{15}$ $cm^{-2}s^{-1}$. The H_2 signal oscillations arise from fluctuations in H_2 background pressure caused by temperature cycling of the cryopumps. Note the pulse in the H_2 signal after opening and closing the Ga shutter.

3.5 Limits of Growth

3.5.1 Ga Condensation

One of the important limits of GaN growth is the weak adsorption of Ga on the GaN surface. This is relevant at low substrate temperature or high Ga flux. The adsorption behavior can be seen in Figure 25, which shows the desorption behavior of Ga as a function of substrate temperature. Desorption is shown both with an NH_3 flux as well as without an NH_3 flux in the excess Ga regime. The substrate temperature was calibrated beforehand under the assumption that the condensation behavior is well described by liquid Ga vapor pressure data. This method of measurement is consistent with temperature measurements described elsewhere (see section 9.2). The key point of the figure is that there is a temperature at which the desorbed Ga flux changes abruptly. This behavior is seen with and without an NH_3 flux and is independent of the magnitude of the NH_3 flux in the excess Ga regime. The temperature only depends on the incident Ga flux. Just above this temperature the NH_3 reduces the Ga desorption, indicating that there is growth of GaN. Just below this temperature, Ga desorption is the same with and without an NH_3 flux, indicating that there is no growth.[23] This abrupt transition temperature is very reproducible and is part of the model discussed in Section 3.6.2.

This same adsorption behavior in this excess Ga regime was also seen in the RHEED data of Figure 11, where the transition between curve (b) and (c) was interpreted to correspond to the temperature, T_c, at which Ga condenses. This behavior was not observed in the Ga-limited regime. Instead, RHEED intensity oscillations, as shown in Figure 10, were recorded at low temperatures, their frequency indicating near unity Ga incorporation. These results indicate that the GaN growth kinetics in those two regimes differ

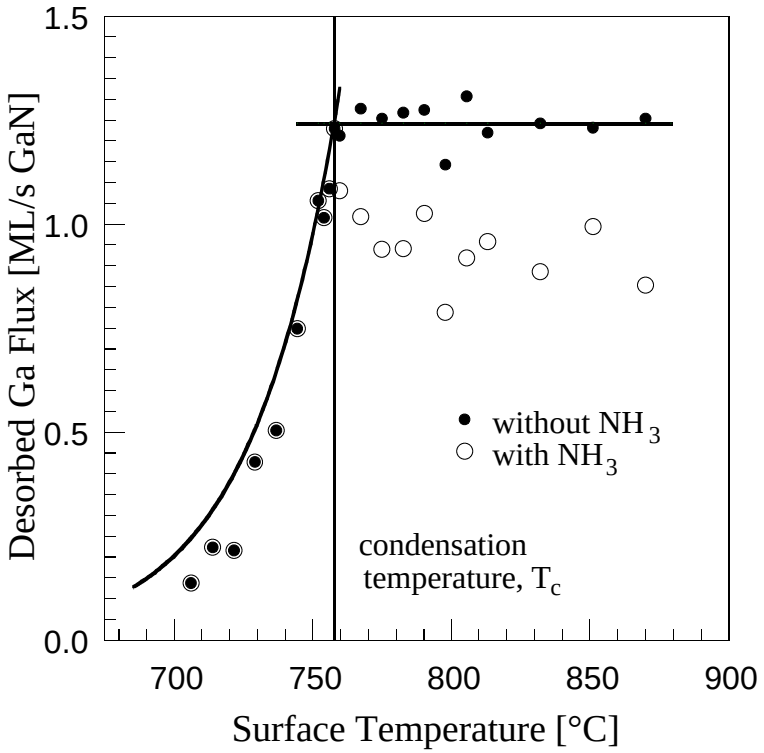

Figure 25: Condensation temperature determination using collimated Ga DMS with and without NH_3 for an incident Ga flux of 1.25 ML/s GaN. Without NH_3 the DMS signal remains constant above the condensation temperature, while with NH_3 the signal is reduced due to GaN formation. The condensation temperature is found as illustrated by observing the temperature at which the signal drops exponentially. No growth is observed below the condensation temperature. The solid curve at temperatures below Tc is calculated from Ga vapor pressure data, closely followed by the experimental data. (The data presented in this figure should not be used for growth rate determination since steady state was not obtained.)

significantly. The abrupt transition temperature, between growth and no growth, is identified as the temperature at which multilayers of Ga begin to condense on the surface.

To correlate RHEED and DMS measurements in terms of Ga condensation and surface termination, Figure 26 compares measurements of the desorbed Ga to the corresponding RHEED intensity vs time, at a temperature below T_c at which Ga condenses on the surface. To improve the signal to noise ratio no collimation was used for this set of DMS measurements and therefore the DMS averages over the entire surface of the 1 inch

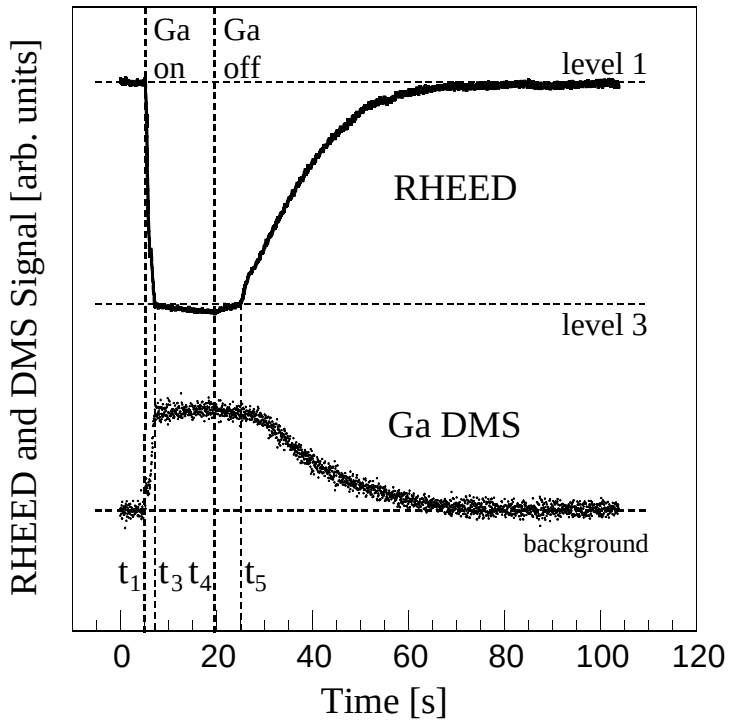

Figure 26: RHEED and uncollimated Ga DMS signal during Ga accumulation below the condensation temperature. After the Ga shutter is closed at t_4 Ga desorption remains constant until part of the GaN surface is exposed at t_5. At the same time, the RHEED intensity increases slowly up to t_5 where a large change in slope takes place. The slow decrease of the DMS signal after t_5 is partly due to the temperature gradient across the sample, resulting in unsynchronized completion of Ga desorption from the surface.

sample. The RHEED measurement, on the other hand, is more localized, and by moving the beam across the surface it was determined that there was an approximately 30^{o} temperature gradient across the sample surface. After opening the Ga shutter at t_1, the decrease in the RHEED intensity parallels an increase in the Ga DMS signal to a steady state value at t_3. There is a slight decrease in the RHEED intensity after t_3 due to increased attenuation of the signal originating from ordered regions. By contrast, the Ga DMS signal is constant after t_3. This is consistent if the desorption energies from successive layers are approximately equal. The magnitude of this desorbed Ga is independent of temperature above T_c and then decreases below T_c due to condensation.

The recovery behavior of the two signals after the Ga source is shuttered are also correlated to an extent -- the DMS indicates that the increase in the diffracted intensity can be associated with a decrease in the amount of adsorbed Ga and not just to a coalescence of surface adatoms that reduces the step density. The correlation is not exact, however. After the Ga source is shuttered at t_4 the RHEED intensity increases slightly until, at t_5, there is a rapid increase. The DMS signal remains constant during this time and then decreases to a background. Difference in recovery rates would be expected if regions on the sample surface at lower temperature, where there is a larger amount of condensed Ga to desorb, also contribute to the DMS signal. Thus the condensation is seen in both the RHEED and DMS data, though regions sampled can be quite different.

3.5.2 GaN Decomposition

GaN decomposition must be considered both during NH_3-limited and Ga-limited growth at high substrate temperatures in order to be able to predict growth rates. In the following section data on the decomposition of GaN will be reviewed, which represents the fundamental limit to its growth at high temperatures. Determination of the GaN decomposition rate was carried out after growth of about 1μm of GaN, and after the base pressure of the system was reduced to the mid 10^{-9} Torr range. Residual gas analysis indicated that the gas remaining in the system was predominantly NH_3 .

Determination of the GaN decomposition rate was accomplished by monitoring both Ga and molecular nitrogen signals while varying the substrate temperature. The Ga signal coming from the GaN sample, as detected by the DMS, was calibrated previously in terms of absolute flux. This was achieved by exposing the GaN sample with a known Ga flux above the condensation temperature, at which the incident flux equals the desorbing flux.

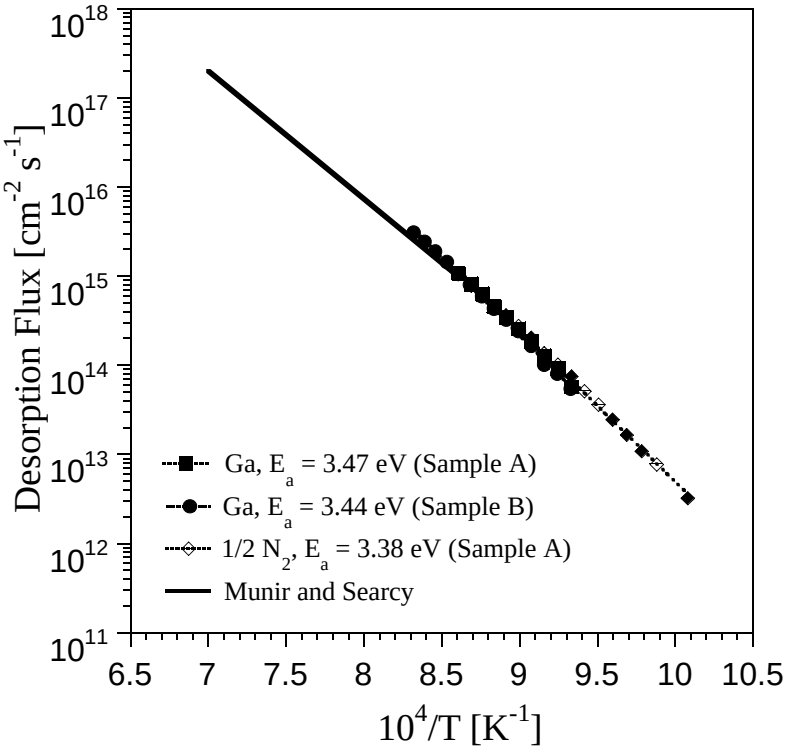

Figure 27: The rate of GaN decomposition compared with values previously reported by Munir and Searcy. The data presented here extends the experimental curve to lower temperatures. The current measured on the mass spectrometer while monitoring desorption of molecular nitrogen was multiplied by a constant factor such that the signals are equal in the middle of the range of measured values. The close agreement between the activation energies of the 1/2 N_2 curve and the Ga curve indicate that decomposition is congruent.

The incident flux was known from the measurement of RHEED intensity oscillations during growth of GaAs(001) in a separate experiment.

Quantification of the N_2 flux desorbing from the substrate was not possible by direct means. However, a useful comparison between N_2 and Ga signals can be obtained assuming that sublimation is congruent. In this case, the N_2 flux leaving the substrate is related to the Ga flux leaving the substrate via the relation

$$F_{N_2} = \frac{1}{2} F_{Ga} \qquad (3\text{-}4)$$

Hence, to within a scale factor that depends on the sensitivity of the mass spectrometer, the two signals should equal. Fig. 22 shows a plot of 1/2 FN_2 and F_{Ga} versus substrate temperature resulting from GaN decomposition. The scale factor used to obtain the absolute N_2 flux is based on the assumption of congruent sublimation. The assumption is justified by the fact that the slope of the twoCurves are the same to within the experimental error. It is noted that the data presented here are consistent with previous measurements [24], and also that these results extend the temperature range of available experimental data. The activation energy of GaN decomposition was therefore verified to be 3.4 eV in the experimental range covered. It was found that the GaN decomposition rate reduces in the presence of Ga, consistent with the law of mass action (see section 7). The exact dependence of GaN decomposition in the two growth regimes, as a function of both Ga and NH_3 fluxes, still has to be investigated and the results are expected to follow the law of mass action. The main point is that at growth temperatures above 800^oC the growth rate can be reduced significantly due to GaN decomposition, which cannot be neglected in an overall growth model.

3.6 Discussion

3.6.1 Ga Adsorption

The experiments presented in Section 3.4 have identified two Ga adsorption sites on GaN(000$\underline{1}$) which can be inferred from both RHEED and DMS data. Strongly adsorbed Ga was identified which does not desorb in the temperature range investigated, as well as weakly adsorbed Ga, on top of the strongly adsorbed Ga sites, which desorbs according to Ga vapor pressure data in the absence of any incident fluxes. The weakly adsorbed Ga is necessary to give the low temperature reconstructions observed by Smith et al. [30]. Our results are consistent with the findings of Jones et. al.[6] and Lee et. al.[25] who both proposed that Ga exists in two adsorption sites during growth. At typical growth temperatures, this Ga terminated GaN(000$\underline{1}$) surface is stable in the absence of Ga and NH_3.

The DMS and RHEED data presented in Section 3.4 can be understood by considering the adsorption of Ga onto an otherwise inert surface in the absence of NH_3. Examine two limits: First, at sufficiently high temperature, an incident Ga flux will produce a steady state Ga coverage that depends on the incident Ga flux and the Ga residence time. In this steady state, the total amount of adsorbed Ga is constant so that the incident flux must equal the desorbing flux. Second, if the substrate temperature is decreased sufficiently, there will be a temperature below which Ga condenses on the surface forming multilayers and/or droplets. Below this temperature the system is not in steady state since the incident flux exceeds the desorbing flux, and Ga is adsorbed continuously. The transition from steady state to condensation is sharp and can be determined by measuring the temperature at which the desorbed Ga flux begins to decrease. For a given incident Ga flux, this

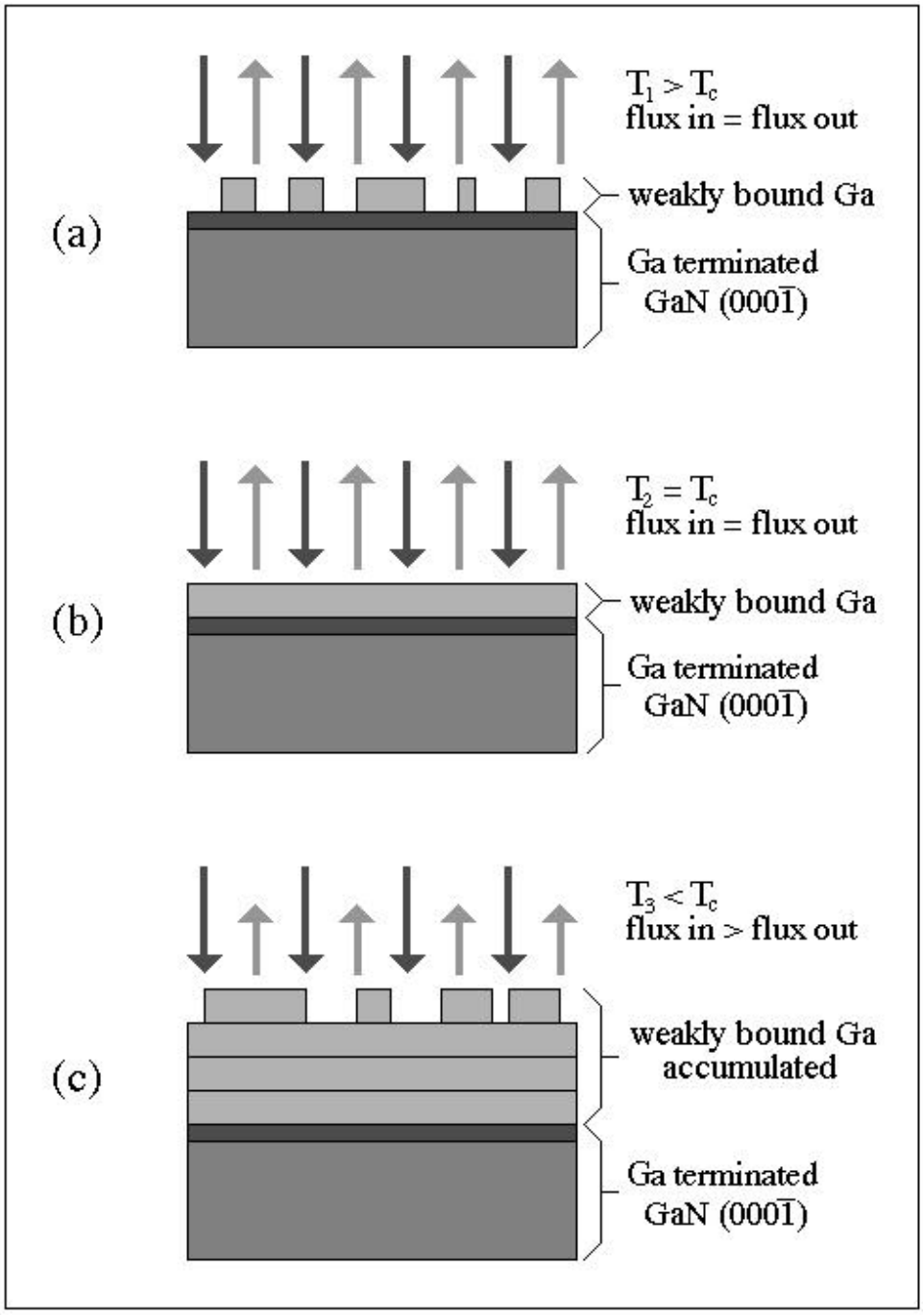

Figure 28: Behavior of incident Ga on a rigidly attached (strongly bound) Ga termination layer as a function of temperature in the absence of NH_3 Above the condensation temperature (a) steady state partial Ga coverage is obtained, and the incident flux equals the desorbing flux. Complete steady state Ga coverage is obtained at a critical temperature (b) below which Ga condensation takes place. Note that the incident flux still equals the desorbing flux. Below this critical temperature (c), Ga multilayer accumulation takes place and the incident flux exceeds the desorbing flux.

transition corresponds to a unique surface temperature well described by equilibrium vapor pressure data.

The picture that emerges is illustrated in Figure 28 where weakly bound Ga adsorbed on Ga terminated GaN(000$\underline{1}$) is shown. In this situation, if there were no NH_3 or Ga flux present, the weakly bound Ga desorbs, leaving the strongly bound Ga to make up the Ga terminated GaN(000$\underline{1}$) surface. If now an NH_3 flux is provided, the strongly bound Ga of the Ga terminated surface would react resulting in a nitrided surface. If then a Ga flux is provided to this nitrided surface, in the absence of NH_3, the Ga would react with the nitrided surface causing hydrogen to desorb. After the nitrogen is consumed by strongly binding Ga, a surface coverage of weakly bound Ga will built up. If the substrate temperature is above the condensation temperature the weakly bound Ga, likely less than a monolayer, will reach steady state, as shown in Figure 28a. If the substrate temperature is below the condensation temperature for that incident Ga flux, Ga multilayers and/or droplets will form, illustrated in Figure 28c. The crossover between steady state coverage of weakly adsorbed Ga and condensation is shown in Figure 28b. Once the Ga flux is stopped, any weakly bound Ga will again desorb to eventually expose the strongly bound Ga terminated surface.

During growth the steady state coverage of weakly adsorbed Ga is maintained by the incident Ga minus the desorbing Ga and Ga forming GaN. A model will be presented in Sec. IV B in which the strongly bound Ga contributes to growth, whereas the weakly bound Ga acts to inhibit growth by blocking these strongly bound Ga sites. The effect of weakly adsorbed Ga on growth rate can only be observed in the NH_3-limited regime, while in the Ga-limited regime near unity incorporation of Ga is obtained, as discussed later in Section 3.6.3.

3.6.2 NH3-Limited Growth

As showed earlier in Figure 14, at constant substrate temperature above Ga condensation and at constant NH_3 flux, the growth rate increases linearly with increasing Ga flux, but then decreases as the Ga flux exceeds a certain value. The reduced growth rate at high Ga fluxes can be accounted for by consideration of the following simple kinetic model. As a start a number of assumptions are made about the atomistic behavior of adsorbed Ga which will be justified by agreement with measured data. First, Ga in the weakly adsorbed state is considered. The fractional area of the surface covered by weakly bound Ga is s_{Ga}. The second assumption is that Ga desorption occurs only from this weakly bound site, which results in a Ga desorption term that is proportional to s_{Ga}. It is assumed that for complete coverage ($\sigma_{Ga} = 1$) the desorption flux is equal to the evaporation rate of Ga from liquid Ga, $F_o(T_{sub})$, and therefore approximate the Ga desorption rate as s_{Ga} $F_o(T_{sub})$. The model does not require that Ga completely wet the GaN surface, since the shadowing effect of droplets could account for the observed behavior as well. In the limit of complete wetting, s_{Ga} is the surface coverage of weakly adsorbed Ga.

We assume that NH_3 reacts only with strongly bound Ga, and that the excess Ga in the weakly bound site reduces the growth rate by blocking the underlying reactive Ga sites. Further motivation for such a growth mechanism can be found in the work of Liu and Stevenson[26], who found that the coexistence of Ga and GaN enhanced the decomposition of NH_3 relative to Ga alone.

We let the growth rate be proportional to the fraction of strongly bound Ga sites that are exposed to the incident NH_3 , $(1 - s_{Ga})$. DMS measurements of the H_2 flux showed that the NH_3 reactivity does not depend on substrate temperature over the range (700^oC-820^oC), and we therefore let the active N flux, F_N, be independent of substrate

temperature. We wish to determine the steady-state growth rate when the incident Ga flux exceeds the active N flux, $F_{Ga} > F_N$. The time derivative of the Ga coverage is given by

$$\frac{1}{A}\frac{dN_{Ga}}{dt} = F_{Ga} - F_N(1 - s_{Ga}) - s_{Ga}F_o(T) \qquad (3\text{-}5)$$

where the growth rate is $F_N(1 - s_{Ga})$, and N_{Ga} is the number of weakly bound Ga atoms on the substrate surface of area A. Solving the equation for s_{Ga} at steady-state gives the growth rate

$$G = F_N(1 - s_{Ga}) = F_N \frac{F_{Ga} - F_o(T)}{F_N - F_o(T)} \qquad (3\text{-}6)$$

The result of this model is shown as a solid line in Figure 14. As stated earlier, we estimate the desorption term $F_o(T_{sub})$ from the equilibrium vapor pressure of Ga over liquid Ga.[27] We see from Figure 14 that the growth rate as extracted from the Ga data is in reasonable agreement with the steady-state solution *G*. The only fitting parameter used was F_N, which is equated to the known Ga flux for which the growth rate is maximum. The main point to be extracted from this discussion is that weakly adsorbed Ga reduces the formation rate of GaN. The model predicts further that the growth ceases completely when $F_{Ga} = F_o(T_{sub})$, where $s_{Ga} = 1$. This is completely consistent with the results of Section 3.5.1, where it was found that the onset of Ga condensation is independent of NH_3 flux in the NH_3-limited regime. Eq. (3-6) was also applied to Figure 13 predicting a deviation from a linear increase in growth rate as a function of NH_3 flux in the NH_3-limited regime. This deviation from linearity decreases with increasing substrate temperature due to a reduction in the coverage of weakly adsorbed Ga.

This result shows that we can use substrate temperature to control the coverage of weakly adsorbed Ga. For example we can increase the growth rate by increasing the substrate temperature, in effect reducing the steady state surface coverage of weakly adsorbed Ga. This is seen in Figure 15 where the GaN growth rate is plotted as a function of substrate temperature at a fixed Ga and NH_3 flux. The result is counter to the notion that decreased Ga residence times at higher temperature lead to decreased growth rates [13] as discussed below. The drop in growth rate at high temperatures will be attributed to GaN decomposition competing with growth. This conclusion is motivated by comparing the data to the proposed growth rate model, Eq. (3-6). Two solid curves are shown in Figure 15, the top one showing the growth rate as given by Eq. (3-6), while the bottom one is given by Eq. (3-6) minus the GaN decomposition rate in the absence of any fluxes. The measured data fall between those two curves, suggesting that GaN decomposition is responsible for the growth rate reduction. Further, during growth, GaN decomposition is suppressed compared to the decomposition measured in the absence of any fluxes.

A similar drop in growth rate was observed by Guha et al[13] at a much lower substrate temperature, and they attributed this reduction to the decrease in residence time of the incident Ga on the GaN surface. However, their data were apparently taken in the Ga-limited regime, but close to the NH_3-limited regime, at a Ga flux of 0.6 ML/s and an active N flux of 0.8 ML/s. The substrate temperature ranged from 720^{o}C to 840^{o}C, and the growth rate decreased from 0.5 ML/s at 720^{o}C to zero at approximately 760^{o}C. Those results are in sharp contrast to ours which were obtained at what should have been very similar growth conditions. Figure 14 indicates that at a Ga flux of 0.6 ML/s and an active N flux of only 0.5 ML/s, at a substrate temperature of 785^{o}C, all of the available Ga incorporates within the measurement error of less than 0.1 ML/s. Even though our data were taken at a substrate temperature 25^o higher, as well as at a lower active N flux, they disagree significantly with Guha's results. Possible differences include errors in substrate temperature determination as well as differences in growth kinetics between NH_3 and RF nitrogen sources.

3.6.3 Ga-Limited Growth

The period of the RHEED oscillations shown in Figure 17 were longer than the growth rates measured by DMS. Further, though the measured periods were linear with the Ga flux, the slope was not unity. This is surprising since it is contrary to experience with most other materials under comparable conditions. Two limiting cases should be considered, either that the RHEED intensity oscillations correspond to the growth rate but with less than unity Ga incorporation, or the frequency does not correspond to the growth rate indicating that not all Ga atoms contribute to island nucleation.

Assuming that the RHEED intensity oscillations indicate the true growth rate, we are losing some of the incident Ga either by desorption, scattering, or accumulation. In the case of desorption we expect that by increasing the NH_3 flux we can increase the probability of incident Ga to combine with Nitrogen sites, effectively increasing the slope of the curve. On the other hand, the mean free path of the Ga atoms between the source and the sample shortens at the high NH_3 pressures used, which should result in a decrease in slope. In either case the constant offset observed is not expected. When increasing the NH_3 flux this offset increased, but the slope of the curve did not change as we might expect. No evidence of Ga accumulation was observed either to explain the behavior.

If we consider the case that the RHEED intensity oscillations do not indicate the true growth rate, we conclude that we are losing some Ga that does not take part in island nucleation. Possibilities might be the migration of Ga atoms to step edges participating in step flow, or the migration to defects on the GaN surface. It becomes evident that a more detailed study is needed to resolve the issue, keeping in mind that several processes combined might be responsible for the observed behavior.

Finally it should be mentioned that part of the differences obtained between films grown under NH_3 limited conditions and those under Ga limited conditions might be due to the presence of inversion domains. For example, Romano and Myers[28] have recently examined growth on mixed polarity films, using plasma sources for N, and showed that one polarity grows faster than the other under excess N conditions, and that more balanced growth rates are obtained under excess Ga. This resulted in smoother films under excess Ga compared to excess N. It was found however, that even by growing on bulk unipolar GaN(000$\underline{1}$) surfaces, films showed the 2D and 3D growth regimes. Further, these latter films could be annealed at 800^{o}C, as indicated by a reduction in the intensity of the 3-D transmission RHEED features. This suggests that changes in surface diffusion play a dominant role.

3.6.4 Overall Framework

Figure 29 summarizes the findings reported in this paper. The figure shows three main (solid) lines: the incident Ga flux, labeled F_{Ga}, the equilibrium Ga desorption flux, $F_o(T)$, and the flux of Ga corresponding to the decomposition of GaN. In the figure the incident Ga flux is chosen to be 1.1×10^{15} $cm^{-2}s^{-1}$ (1.0 ML/s of GaN). The substrate temperature and the magnitude of the nitrogen flux supplied by the NH_3 , F_N, determine the growth mode.

For example, if F_N and a substrate temperature corresponding to point (a) were chosen, then the growth would be Ga limited (excess NH_3) and the growth would be 3D. At somewhat higher NH_3 fluxes, RHEED intensity oscillations would be observed on initially smooth surfaces. Similarly, at point (b, the growth would be Ga-limited and 3D, though at these substrate temperatures, the decomposition of GaN becomes significant and reduces

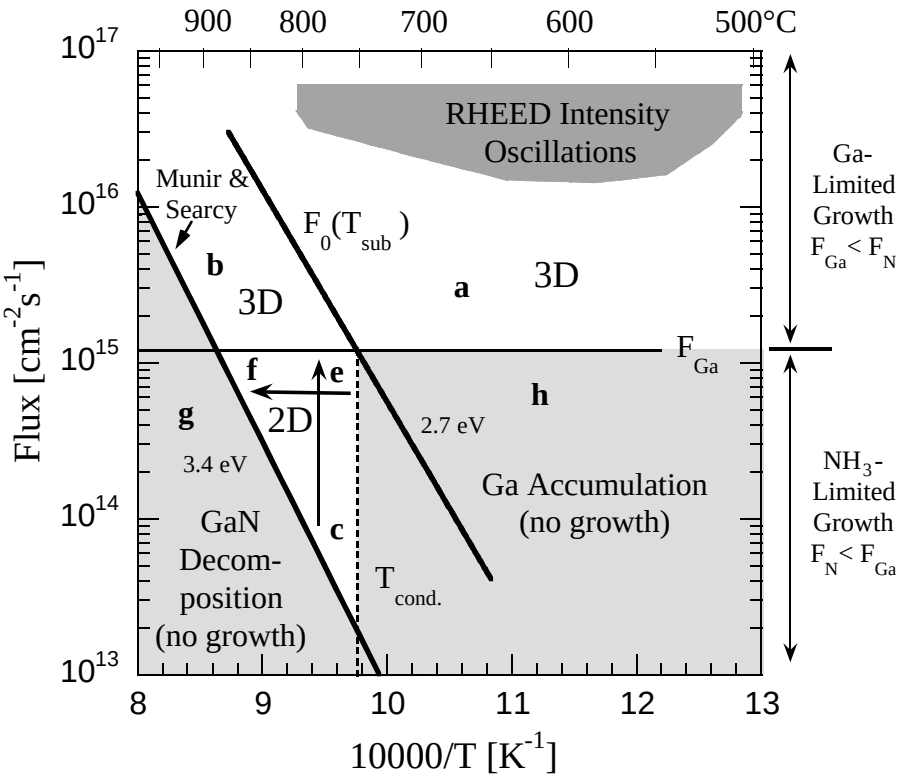

Figure 29: Fig. 24: GaN growth map showing the different growth regimes and limits for a fixed Ga flux. Growth is limited by GaN decomposition at high temperatures and Ga accumulation in the NH_3-limited regime at low temperatures. 3-D growth occurs in the Ga-limited regime, while layer-by-layer growth takes place in the NH_3-limited regime between the GaN decomposition and Ga accumulation limits. Strong GaN RHEED intensity oscillations are observed by first growing in the NH_3-limited regime until a streaky RHEED pattern is obtained, followed by growth in the Ga-limited regime.

the growth rate. In this Ga-limited mode RHEED intensity oscillations are observed, and the observed decrease in oscillation frequency indicates that Ga diffusion can be increased by raising the substrate temperature.

Alternatively, if F_N is less than F_{Ga} then the growth is NH_3-limited (excess Ga) and is described by the data below the horizontal solid line corresponding to the incident Ga flux. The key temperature value corresponds to the intersection of $F = F_o(T)$ and $F = F_{Ga}$. This is the condensation temperature, Tc, and is indicated by the vertical dashed line

since it is unchanged for all lower NH_3 fluxes at this incident F_{Ga}. For any NH_3 flux in the shaded region to the right of T_c, for example at point (h), Ga will condense on the surface since the incident Ga flux, F_{Ga}, is greater than the flux that would desorb from liquid Ga. There is no GaN growth in this regime. Our results do not show a reduction in desorbed Ga flux in this region when NH_3 is introduced.

In the 2D regime, at temperatures higher than T_c and under excess Ga, growth is possible since multilayers of Ga that would otherwise block growth do not form. In this regime, surface diffusion is evidently high and RHEED oscillations are not observed. It is assumed that this corresponds to step-flow growth. The arrows in this region summarize the results of much of the data presented in Section 3.3 and the model of Section 3.6.2. Under these conditions the GaN(000$\underline{1}$) surface is terminated by a layer of strongly bound Ga that reacts with NH_3. However, additional weakly adsorbed Ga blocks growth and reduces the growth rate. The change in growth rate vs NH_3 flux, shown in Figure 13, corresponds to the arrow from (c)-(e). Along this line the main effect is that the growth rate is limited by the arrival of nitrogen and so increases approximately linearly with NH_3 flux. However it does not increase linearly with unity slope since initially there is some fraction of a ML of weakly adsorbed Ga on the surface that blocks growth. As the NH_3 flux is increased, the coverage of weakly adsorbed Ga is reduced and hence the fraction of the NH_3 that can be incorporated increases. Similarly, the arrow from point (e) to (f) is illustrated by the data in Fig. 10. At point (e) there is a fraction of a ML of weakly adsorbed Ga on the surface that blocks reaction with the strongly adsorbed Ga. As the substrate temperature is increased, at a fixed Ga and NH_3 flux, the coverage of weakly adsorbed Ga decreases and the growth rate increases. As point (f) is reached, the decomposition of GaN becomes important and there is a reduction in growth rate. If the substrate temperature were increased past the decomposition line to point (g), there would be no net growth and the decomposition of GaN would dominate.

3.7 Conclusion

GaN(000$\underline{1}$) was grown by MBE on sapphire using a Ga Knudsen cell and an NH_3 leak valve, and the growth was investigated by DMS and RHEED. It was shown that DMS and RHEED could be used to observe and control surface termination, Ga coverage, and surface temperature. GaN growth and decomposition rates were obtained by DMS. It was shown that hydrogen is present on the surface during growth on GaN(000$\underline{1}$) and that its desorption rate is proportional to the growth rate. Two distinct growth regimes were identified: Growth under excess NH_3 (Ga-limited growth) and growth under excess Ga (NH_3-limited growth). Under conditions of excess NH_3, damped oscillations in the specular RHEED intensity were observed. The magnitude of these oscillations depended on sample history and was larger at lower temperatures and higher NH_3 fluxes. Contrary to previous suggestions, the period of these oscillations does not correspond exactly to integral layer deposition and are not characteristic of a narrow growth front. Further, as the substrate temperature was increased the growth mode changed from island nucleation to step flow with an activation energy of 1.2 eV. When the Ga flux was interrupted, the intensity did not recover without a smoothing step and the growth became 3-D. Under conditions of excess Ga, surfaces were much smoother, but RHEED intensity oscillations were not observed, indicating a step-flow growth mode. In this regime, it was shown that increasing the Ga flux caused the growth rate to decrease. This reduction was explained by a model that states that weakly adsorbed Ga blocks reactive Ga, which are strongly bound. At low temperatures condensation of Ga limited the growth in the excess Ga regime. It was shown that increasing the substrate temperature reduced the coverage of weakly adsorbed Ga and increased the growth rate. At higher temperatures, growth was limited by GaN decomposition.

4. SURFACE STRUCTURE AND COMPOSITION

4.1 Introduction

Since wurtzite GaN is not centrosymmetric there are two distinct {0001} planes. These planes, GaN(0001) and GaN(000$\underline{1}$), will have different structure, composition, and chemistry. These differences could impact growth kinetics and possibly the doping characteristics of GaN. Studying these differences on GaN films grown on sapphire present two main difficulties: first, dislocations could dominate observations of growth, and second, it is often difficult to obtain single domain material of either polarity. To avoid high dislocation densities and inversion domains, growth on the two {0001} surfaces of bulk GaN single crystals was examined. The two polarities will be distinguished using their reconstructions and their response to adsorption of Ga and nitrogen will be examined. Initial investigations of the resulting structures are presented.

Different polarity assignments were reviewed by Hellman et al.[29]. We follow the convention that the [0001] direction is a vector from a Ga atom to a N atom in the bulk Wurtzite lattice. Then in a model in which the unreconstructed bulk surface is terminated with the fewest dangling bonds, the GaN(0001) surface (or GaN-A) would have a Ga face and the GaN(000$\underline{1}$) surface (or GaN-B) would have a nitrogen face. Of course these surfaces reconstruct, most likely according to the currently accepted models[30].
In this paper reflection high energy electron diffraction (RHEED) observations of unipolar films grown on bulk GaN{0001} will be reported, and compared to results of GaN grown on sapphire. Atomic force microscopy (AFM), scanning tunneling microscopy (STM), and desorption mass spectroscopy (DMS) were used to relate the RHEED data to the structure and composition of the surface.

4.2 Experimental

Bulk GaN platelets were prepared as described in section 2.2 before introduction into the growth chamber. Prior to the experiments the samples were outgassed for several hours at 300^{o}C and 1 hour at 500^{o}C in a Varian Gen II molecular beam epitaxy (MBE) chamber. The base pressure of the growth chamber, with cryoshrouds cold, was 3×10^{-9} Torr. The samples were then ramped to a temperature of 800^{o}C under an ammonia beam equivalent pressure (BEP) of 1.0×10^{-5} Torr, with the ammonia background pressure being 1.6×10^{-7} Torr. For the RHEED experiments, an approximately 3000 Å buffer layer was grown under slightly excess Ga conditions (see chapter 3.2) by using a Ga flux of 1.0 ML/s (equivalent to a flux of 1.1×10^{15} cm^{-2}s^{-1}). All of the chemo-mechanically polished samples used for AFM measurements were grown at a lower substrate temperature of around 700^{o}C, and a Ga flux of 0.1 ML/s. Those conditions resulted in the lowest hillock density, therefore improving our ability to resolve features between hillocks by AFM (see chapter 6).

GaN films were also grown on sapphire for comparison, both with GaN and AlN nucleation layers. The detailed procedures for etching, cleaning, and sample mounting are covered in section 2.2. Prior to growth the substrates were outgassed for several hours at 300^{o}C in the preparation chamber of the MBE system, followed by 1 hour at 500^{o}C in the growth chamber. The ammonia leak valve was set to produce a BEP of 1.0×10^{-5} Torr. Then the substrate temperature was ramped at 100^{o}/min from 500^{o}C to 1000^{o}C for surface nitridation.

Experiments were performed by using two types of nucleation layer, AlN and GaN. In case of the GaN nucleation layer the sapphire was nitrided for 15 minutes, whereas 3 or 15 minutes was used for the AlN nucleation layer, as discussed later. The 250 Å AlN nucleation layer was grown at 1000^{o}C using an Al flux of 0.10 ML/s (equivalent to

1.2×10^{14} $cm^{-2}s^{-1}$). RHEED showed transmission features in the pattern during and after AlN growth. The Ga shutter was then opened to provide a flux of 1.0 ML/s and the sample temperature was ramped down to 800°C at 100°/min. The Al shutter was closed during the ramp below 900°C.

The GaN nucleation layer was grown by repeating a sequence consisting of condensing Ga on the substrate surface at 700°C and subsequent annealing at 800°C under ammonia ten times. This was achieved by ramping the substrate temperature to 700°C, in the presence of an ammonia BEP of 1.0×10^{-5} Torr. The Ga shutter was then opened at 1.0 ML/s and the substrate kept at 700°C for about 1 min, during which time the RHEED pattern completely disappeared. The Ga shutter was then closed and the sample ramped to 800°C where it was kept for about 2 min until a RHEED pattern reappeared. This procedure was repeated 10 times. Streaks were observed in the diffraction pattern after completion of this nucleation procedure.

Both types of nucleation layer were followed by a 2500 Å GaN buffer layer, deposited at 800°C with a Ga flux of 1.0 ML/s and an ammonia BEP of 1.0×10^{-5} Torr. After completion of the buffer layer, RHEED showed a streaks without a transmission component. A (1×1) pattern was observed in the case of using GaN nucleation, while a weak (2×2) reconstruction was typically observed using AlN nucleation.

4.3 Results

After growth of the buffer layer on the bulk crystals, as described above, the Ga flux was turned off and the RHEED patterns shown in Figure 30 were observed. For these measurements the electron beam was along the <11$\underline{2}$0> direction and the ammonia flux was held constant. The chemo-mechanically polished face exhibited a (1×1) pattern while the mechanically polished face was (2×2) reconstructed [31].The streaks are elongated, even on these very smooth bulk samples, indicating the presence of atomic steps. The patterns are generally sharper than from the smoothest films of GaN that were grown on sapphire.

To determine the crystalline polarity, a procedure similar to that described by Smith et al. was followed[32]. Their method examines surface reconstructions with varying amounts of Ga on the surface. In our case, a chemo-mechanically polished surface was prepared as described above and then annealed in an ammonia flux. Ga was then deposited in the absence of ammonia at a rate of 0.1 ML/s at about 700^{o}C for 1 min. The substrate temperature was then lowered to about 400^{o}C and an additional fractional monolayer of Ga was deposited. Depending on the amount of additional Ga deposited, and upon cooling to below 300^{o}C, various reconstructions could be observed. Figure 31a and b shows the reconstructions observed on the chemo-mechanically polished face [31],along the <11$\underline{2}$0> direction. These are compared to those observed on sapphire, grown with a GaN nucleation layer, shown in Figure 31c and d.

The same procedure was followed on the mechanically polished face, but did not result in the observation of any reconstructions. In fact, the (2×2) reconstruction seen at typical growth temperatures disappears upon cooling the sample to 400^{o}C, resulting in a (1×1) RHEED pattern. The only effect of adding Ga was a weakening of the (1×1) pattern. Based on these observations [31] the GaN-B polarity will be assigned to the chemo

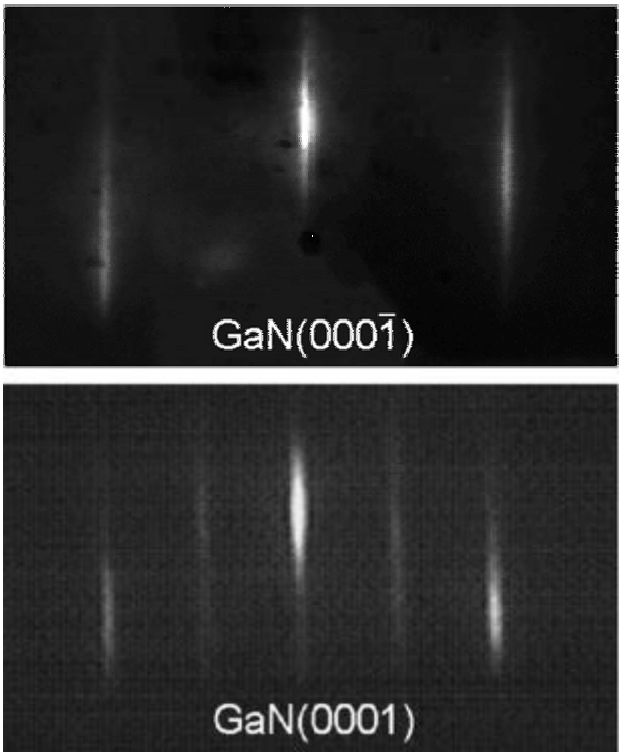

Figure 30: RHEED pattern observed on bulk GaN along the <11$\underline{2}$0> direction for both polarities, under ammonia after growth is stopped at about 800^{o}C.

mechanically polished, bulk face, which is in agreement with convergent beam diffraction (CBD) studies performed by Liliental-Weber et al. [33] and hemispherically scanned x-ray photoelectron diffraction (HSXPD) studies by Seelmann-Eggebert et al [34].

In order to extract more information on the adsorption behavior of Ga, the specular RHEED intensity was monitored on both polarities along the <11$\underline{2}$0> beam direction, shown in Figure 32. Note that these measurements were taken at a typical growth temperature around 750^{o}C, significantly above the temperature required to observe the low temperature reconstructions on GaN-B. The behavior of the specular intensity, upon opening and closing the Ga shutter, is very different on the two surfaces.

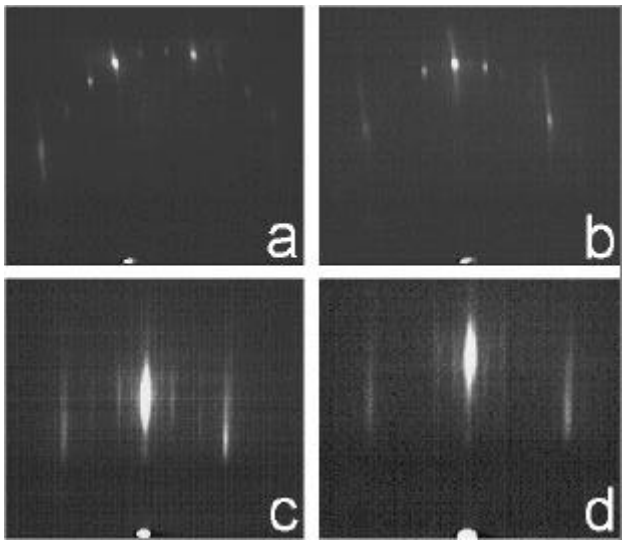

Figure 31: Low temperature surface reconstructions observed on GaN-B, first reported by Smith et al. a) (3´3) on bulk; b) (6´6) on bulk; c) (3´3) on sapphire ; d) (6´6) on sapphire; The c(6´12) reconstructions are not shown; It was found that these reconstructions are only observed on a Ga terminated (gallided) GaN-B surface.

On GaN-B , shown in Figure 32a, we start with a surface that had been annealed in ammonia ; then all fluxes were removed. Exposing the surface to a Ga flux causes the diffracted intensity to drop to a new steady state value that depends on the magnitude of the Ga flux and the substrate temperature. When the Ga flux is interrupted, a fractional monolayer of Ga desorbs, as measured by DMS (see chapter 3) [17], and the intensity rises to a slightly higher value. This last value of the diffracted intensity will remain indefinitely and is independent of temperature. In this sense this gallided surface is stable and neither a flux of N nor Ga need be supplied in order to maintain it. If an ammonia flux is then reintroduced and the surface nitrided, the diffracted intensity returns to its initial value. This nitrided surface can be maintained at this relatively low temperature without incident fluxes for some time; however, as shown later, it ultimately goes to the previous, stable, gallided surface.

In order to better understand the adsorption of Ga on both a nitrided and a gallided GaN-B surface, the transient Ga adsorption behavior with DMS from both surfaces was

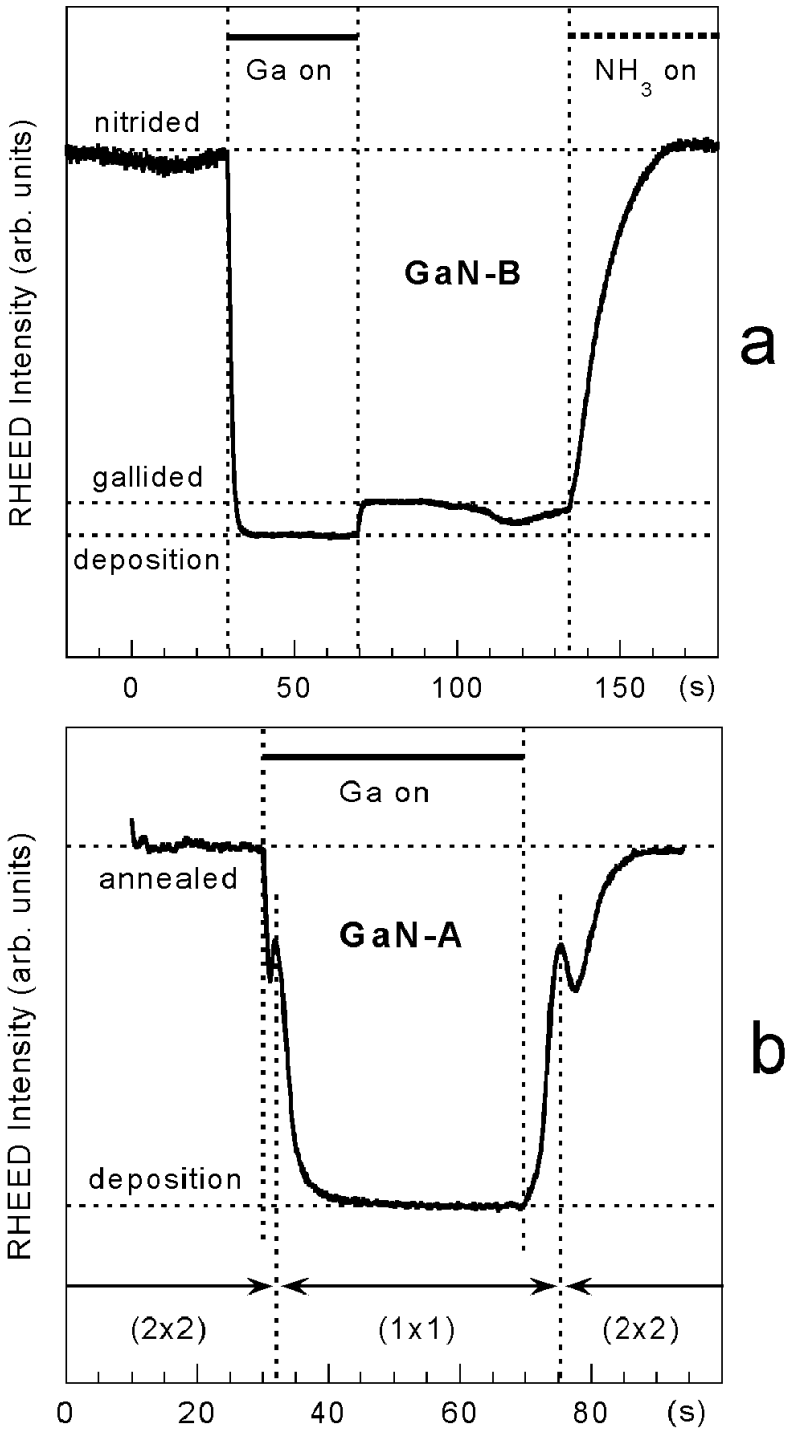

Figure 32: RHEED intensity behavior of both polarities at around 750°C. a) Two surface terminations were observed on GaN-B . b) Only one surface termination was detected on GaN-A , but a reconstruction transition between (2´2) and (1´1) is observed.

recorded, which are shown in Figure 33a as superimposed curves. The first curve was obtained from a GaN-B surface which was prepared by exposure to ammonia . Then ammonia flux was removed, and the film exposed to Ga for approximately 1 min. The transient DMS signal upon opening the Ga shutter is recorded in Figure 33a as one curve. The Ga shutter was then closed for approximately 1 min. Then reopened again, plotted as a superimposed curve in Figure 33a. Comparing both curves we see that the nitrided surface adsorbs more Ga than the gallided surface, apparent from the reduced Ga desorption on the nitrided surface in comparison to the gallided surface. We also note that the Ga adsorbed on a previously gallided surface is identical to the amount desorbed after the shutter is closed, which is not shown in the figure. It is therefore concluded that the nitrided surface adsorbs Ga strongly, and once gallided it adsorbs Ga only weakly. This says that the nature of the adsorption sites on GaN-B depends on how the surface has been prepared.

It was stated before that the nitride surface is unstable in vacuum, and that it will ultimately convert to the gallided surface. Evidence for such process is shown in Figure 33a as another superimposed curve, where the same Ga adsorption experiment was performed after annealing a previously nitrided film for a long time in vacuum. As seen from the transient response, this annealed surface behaves like the gallided surface, and does not adsorb any additional Ga like the nitrided surface. In comparison, the GaN-A surface gave similar adsorption results regardless of sample history, i.e. after exposure to Ga or ammonia only, and after vacuum annealing. A sample curve is shown in Figure 33b, which looks very similar to the curve from the gallided GaN-B surface. It is noted that all of the adsorbed Ga was desorbed again after closing the Ga shutter. This result suggests that the GaN-A surface structure is the same in vacuum after Ga or ammonia exposure, very different from the GaN-B surface.

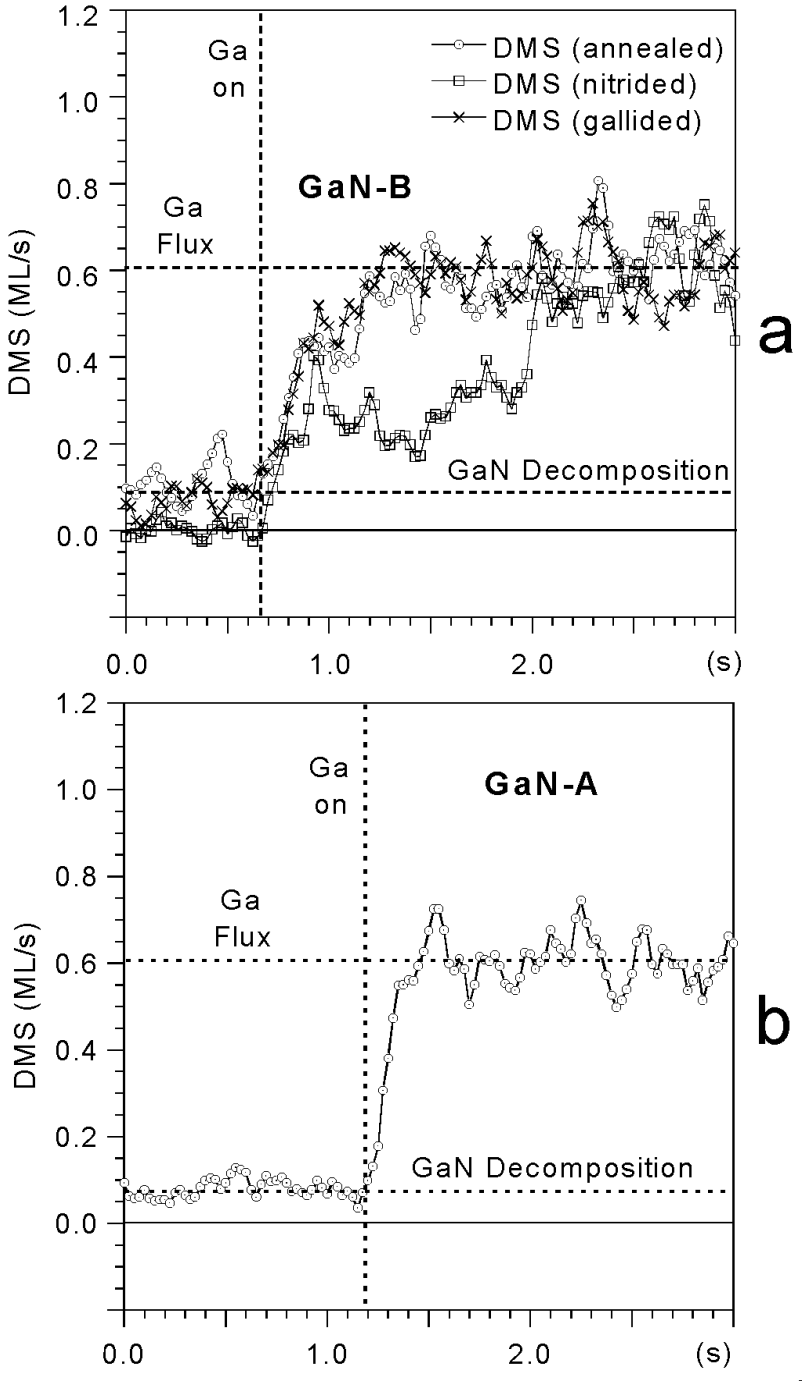

Figure 33: Transient DMS measurements of GaN grown on sapphire upon opening the Ga shutter at 0.61 ML/s at a substrate temperature of 813°C. a) superposition of three Ga adsorption measurements on a GaN-B surface which was nitrided, then gallided, and finally nitrided followed by annealing in vacuum; b) GaN-A surface which resulted in similar curves regardless of sample history;

We investigated the annealing behavior of the nitrided GaN-B surface in more detail. Both the RHEED intensity as well as the Ga DMS signal were monitored during annealing, which is plotted versus time in Figure 34. Initially the sample is kept under ammonia, and a steady state RHEED intensity is recorded during that time along with no detectable Ga signal by DMS. At t_1 the ammonia flux is turned off, and an approximately linear decrease of the RHEED signal is recorded between t_1 and t_2, accompanied by an approximately linear increase in the DMS signal. At t_2 a steady state is reached, with perhaps a slight decrease in the RHEED signal due to surface roughening. Between t_3 and t_4 the sample was exposed to a Ga flux, but there is no detectable change before and after exposure, both for RHEED and DMS. At t_5 the ammonia is turned back on, after which the RHEED intensity recovers to its original value and the DMS signal reduces again below the detection limit. The annealing process between t_1 and t_2 was found to be temperature activated. The activation energy was found to be 4.4 eV as plotted in the insert of Figure 34. If our interpretation is correct that the nitrided surface anneals to the gallided surface during decomposition in vacuum, we would expect the decomposition rate after annealing to equal the decomposition rate obtained after galliding a nitrided surface before annealing. This results, not shown, was in fact obtained. Therefore it is concluded that a nitrided surface is unstable in vacuum, annealing to a stable gallided surface via a temperature activated process with E_a = 4.4 eV. This process was found to take on the order of minutes even at temperatures as high as 800^{o}C.

By comparison, on the GaN-A polarity shown in Figure 32b, the diffracted intensity also decreases when Ga is adsorbed. But here, once the Ga flux is removed, the diffracted intensity returns to its original value. The change in intensity with time is not monotonic, which was correlated to a reconstruction change between (2×2) and (1×1). At this temperature, we cannot add any amount of Ga that will remain in the absence of a Ga flux, as discussed earlier in Figure 33b. At sufficiently high Ga fluxes the (2×2)

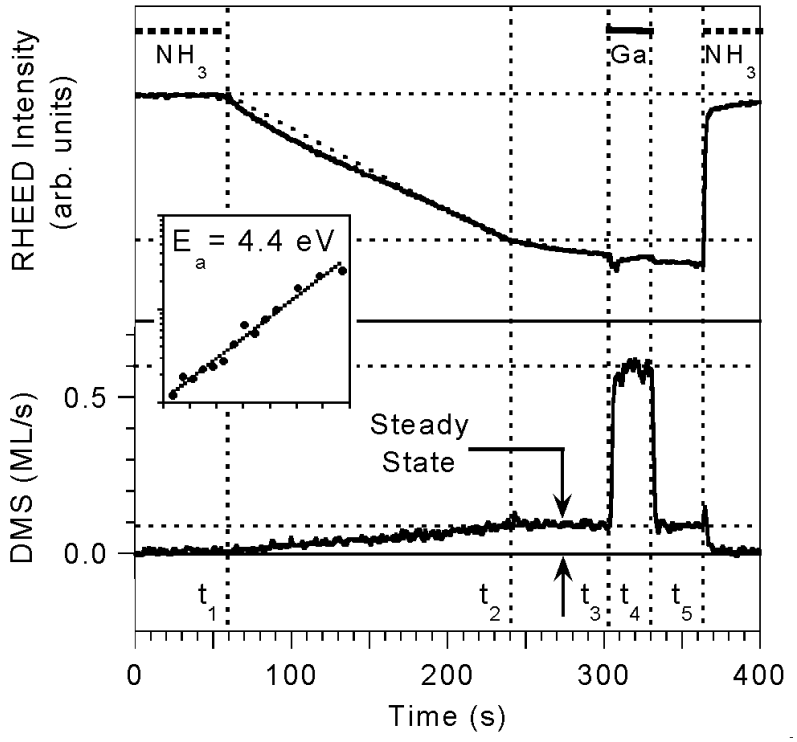

Figure 34: RHEED and DMS signal during annealing of a nitrided GaN-B surface, showing the change from a nitrided to the gallided surface (Ga Flux = 0.61 ML/s, T = 823°C). The inset is an Arrhenius plot of the time required to go from a nitrided to a gallided surface over the temperature range from 790 to 870°C. It shows an activation energy of 4.4 eV.

reconstruction changes to a (1×1) RHEED pattern. This (1×1) pattern returns back to (2×2) once the Ga shutter is closed, even in the absence of ammonia . The initial and final RHEED intensities were found to be independent of ammonia flux. Thus, in contrast to the GaN-B surface, we can not change the steady state surface coverage of Ga on the GaN-A surface. Excess Ga cannot be maintained at typical growth temperatures without an incident Ga flux. At these high growth temperatures surface processes such as desorption and diffusion are quite rapid, suggesting that the growth front and the annealed surface could be quite different.

To examine this possibility, to some extent guided by the variation in the RHEED intensity data shown in Figure 32a, the morphology of the GaN-B surface vs the rate at

which growth was interrupted was examined. GaN films were grown for 3 hours under the conditions described earlier, followed by different cooling procedures. The ammonia flux was held fixed since it could not be interrupted easily. The results of those experiments are shown in the series of AFM images in Figure 35, which all show macrosteps, but with different structures on the step terraces [35]. Specifically, Figure 35a shows a sample that was annealed after growth for several minutes under ammonia before cooling, which resulted in terraces covered with irregularly shaped islands on the order of 500 Å across and 2-5 Å in height. Note that samples typially showed a reduced island density or "denuded zones" near steps on upper terraces, similar to observations on GaAs.[36] Figure 35b shows a sample that was cooled down slowly, at a rate of roughly 100^{o}/min. Areas with similar islands are observed, but only in regions starting at a descending step edge. Apart from this island region, the rest of the surface appears to be featureless. The width of these regions was approximately equal, each roughly 350 Å. Finally, the sample shown in Figure 35c, was quenched rapidly after the Ga shutter was closed. These last data were obtained in a different MBE apparatus, with a base pressure of 1×10^{-10} Torr, but using otherwise similar growth conditions. In this last case, all terraces appear to be featureless, except for a few small steps between the macrosteps. The height of these steps was approximately half a lattice constant *c*/2. The width of the island regions originating from descending step edges depends on annealing time (or quenching rate) under ammonia, while the remainder of the surface is unchanged.

We note that the featureless terraces are also obtained when an annealed or partially quenched surface is exposed to Ga in the absence of ammonia , which shows that ammonia is required in order for the surface transformation illustrated in Figure 35 to occur. Further, gallided films were annealed in ammonia while monitoring the RHEED intensity recovery like in Figure 32, with the difference that the samples were quenched in results clearly show that the change in RHEED intensity during annealing in

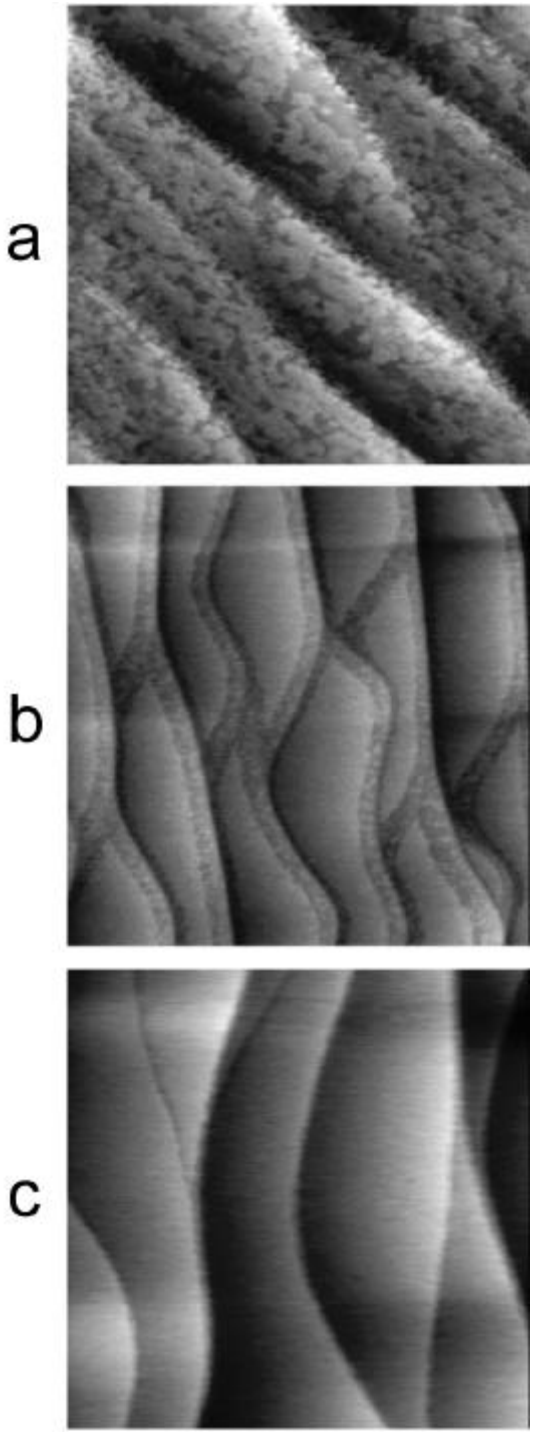

Figure 35: Three 1´1 mm AFM scans of the GaN-B surface with macrosteps cooled at different rates under ammonia after growth was interrupted at 725°C. a) annealed, then cooled; b) slowly cooled; c) quenched. Note that the same featureless surface as in c) is obtained after Ga only exposure in the absence of ammonia.

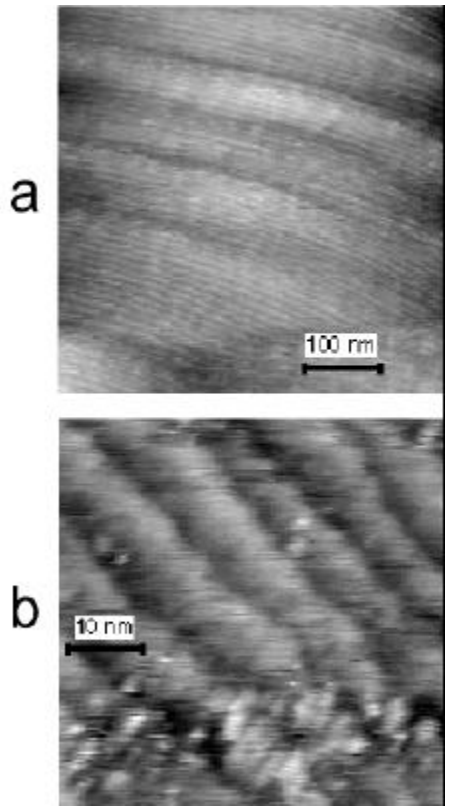

Figure 36: Monatomic Steps on a GaN-B surface. a) 500´500 nm STM scan; b) 50´50 nm STM scan.

the early stages of this recovery. Subsequent AFM scans resulted in films similar to Figure 35b, which showed partial nitridation originating from the descending step edges. These ammonia originates from the development of the island zones on the sample surface.

Monatomic steps, instead of the macrosteps of Figure 35, could sometimes be observed as shown in Figure 36. Figure 36a shows a 500×500 nm STM scan, and *c*/2 steps on the order of 200 Å. These were only barely resolvable in AFM. A zoom is shown in Figure 36b. This film was annealed in ammonia and then cooled to room temperature before STM. Steps are observed, measured to be half a lattice constant (*c*/2) in height, and

separated by approximately 100 Å. At the higher magnification in Figure 36b one can see line defects perpendicular to the step edges.

Comparing GaN films grown on sapphire to bulk GaN, it was found that films grown with our GaN initiation layer on sapphire exhibit a (1×1) RHEED pattern and low temperature reconstructions. On the other hand, GaN films grown with our AlN initiation layer on sapphire behaved differently. Films which were nitrided for 15 min typically featured a very weak (2×2) reconstruction as well as very weak low temperature reconstructions. Films nitrided for 3 min showed a much stronger (2×2) reconstruction, and the low temperature reconstructions were absent.

The time dependence of the RHEED intensity for these films is shown in Figure 37. The film with the GaN nucleation layer behaved like the chemo-mechanically polished GaN-B bulk face. The film with the AlN nucleation layer which was nitrided 3 min was similar to the mechanically polished GaN-A bulk face. The data shown in Figure 37b shows a behavior similar to that of Figure 32b, but is superimposed on top of a linearly decreasing background, suggesting surface roughening, as indicated by the dashed lines. At these temperatures there is an increase in the desorbed Ga DMS signal, suggesting that the increased roughness is due to decomposition of the highly defected GaN on sapphire. Finally, in Figure 37b one can also clearly see an intermediate maximum when there is a transition between (2×2) and (1×1) reconstructions. This transition occurs when about ½ ML of Ga is added or desorbed, as determined from the known incident flux and DMS calibration. In short, these RHEED measurements from GaN/sapphire films give nearly identical results to those of much smoother bulk surfaces. This means that in both cases the step edges and non-{0001} faces do not play a significant role in the RHEED data. Further, since the two polarities give very similar results to the single domain bulk crystals, and since the low incident angle RHEED beam samples a large stripe on the

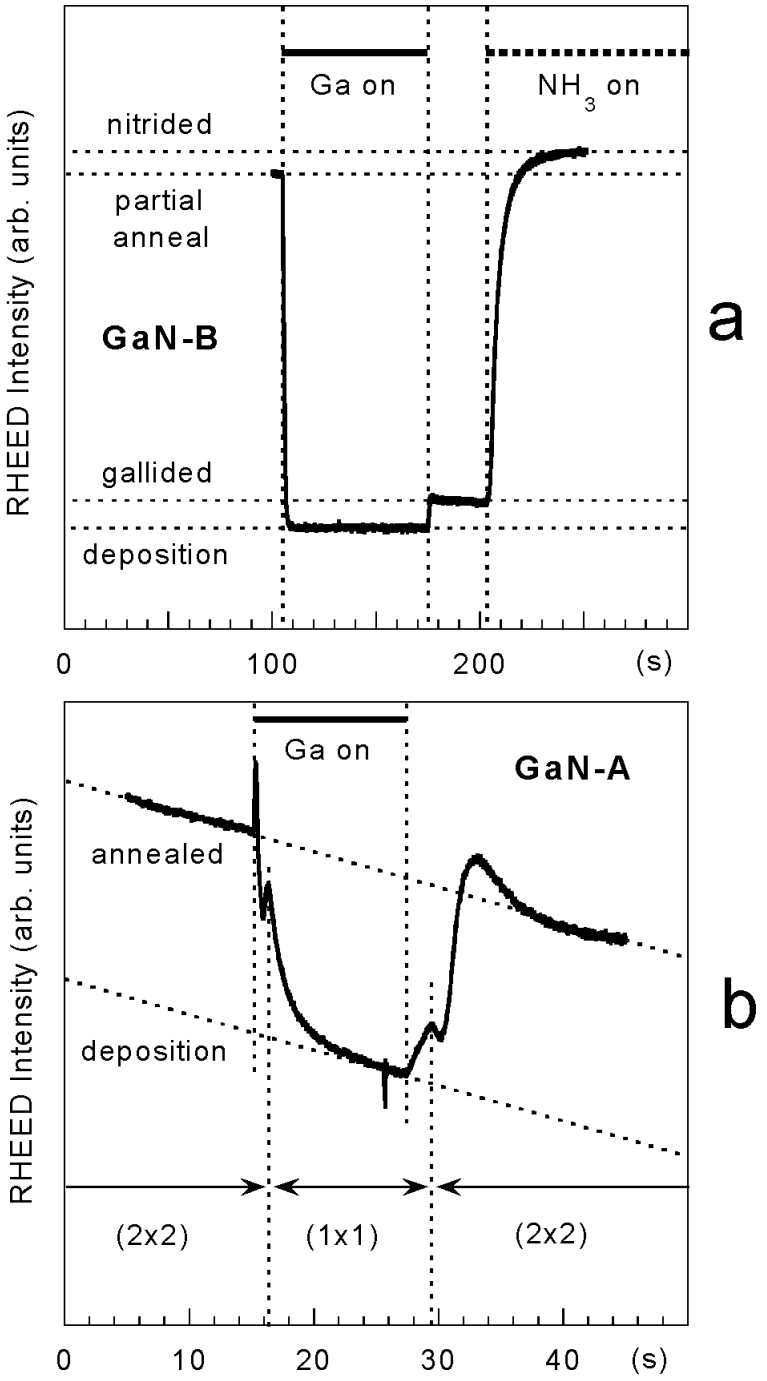

Figure 37: RHEED intensity behavior of GaN grown on sapphire at around 750°C, with: a) GaN nucleation layer (Ga flux at 0.6 ML/s); b) 3 min nitridation and AlN nucleation layer (Ga flux at 0.1 ML/s);

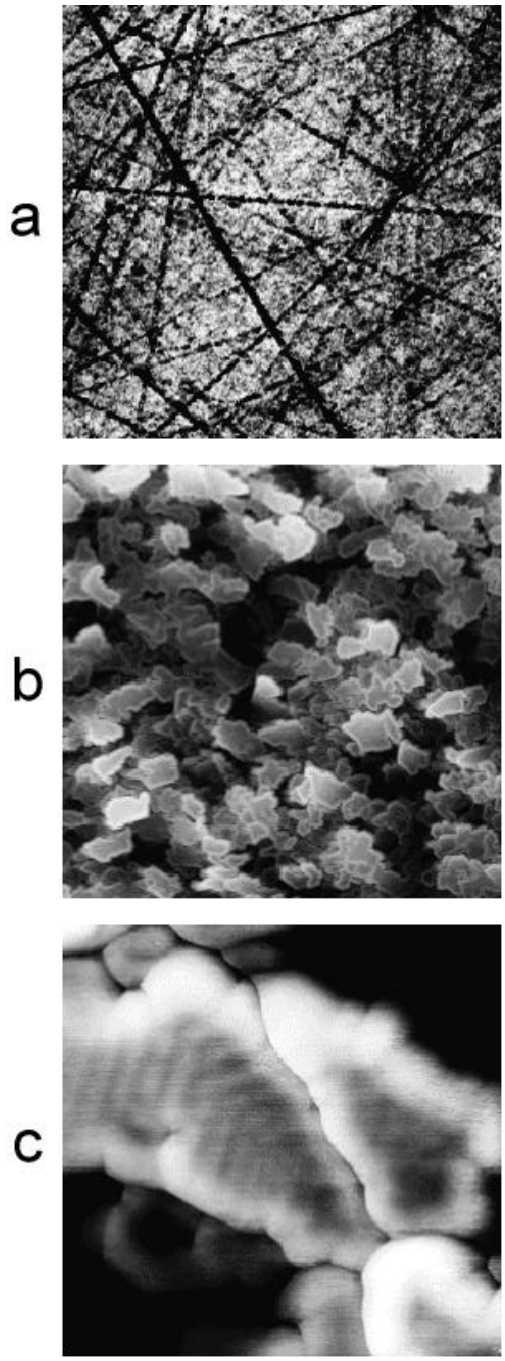

Figure 38: AFM images from a GaN-A surface after 3 hours of growth at about 800^{o}C, with a Ga flux of 1.3 ML/s and an ammonia BEP of 1´10^{-5} Torr. a) Grooves left from the mechanical polishing process (50´50 mm, z = 150 nm); b) Posts of different height with raised perimeters (5´5 mm, z = 90 nm); c) Atomic steps on top of posts with raised step edges (500´500 nm, z = 30 nm);

surface, these data suggest that in both cases, using the nucleation procedures noted, we have essentially single domain films.

The above films were etched in KOH [34,30] in order to distinguish between polarities and check whether there are indeed no inversion domains. Etching is expect to occur for defects, including GaN-B inversion domains. It was found that there was significant etching for films with a GaN nucleation layer, while no detectable etching took place for the film with the AlN nucleation layer which was nitrided for 3 min. The film that was nitrided for 15 min before depositing the AlN nucleation layer showed etched and unetched regions, indicative of defects and inversion domains. For the unetchable film the density of inversion domains was found to be less than 5%, which places a limit on the RHEED method to detect inversion domains.

Due to the surface roughness of the bulk GaN-A samples no extensive series of AFM measurements were done. Figure 38a-c are AFM images of the mechanically polished surface, at various magnifications, after 3 hours of growth at approximately 800^{o}C, a Ga flux of 1.3 ML/s, and an ammonia beam equivalent pressure of 1.0×10^{-5}. The surface is quite rough, consisting of flat topped posts, typically around 2500 Å across. Steps can be seen on top of these posts with terraces that are about 250 Å wide. Further, the step edges and post edges appear to be decorated, as evident from elevated lines at those locations. It was not possible to measure the exact height of the steps since both the steps and the decorations are on the order of only a few Å. The grooves in Figure 38a must be remnants of the polishing procedure, and to some extent the flat-topped posts follow these lines.

4.4 Discussion

It was shown that GaN-A and GaN-B differ significantly in their adsorption behavior of Ga and ammonia . In particular, data was presented that showed that GaN-B has at least two types of adsorption sites. One type exists on a nitrided surface and permits Ga to bond strongly. If a surface is exposed to a sufficient amount of Ga these strongly bonding sites are replaced by weak bonding sites. This gallided surface allows the addition of weakly bound Ga that desorbs quickly once the Ga flux is removed. In contrast to the GaN-B surface, the GaN-A surface adsorbs Ga only weakly, independent of sample history, i.e. previous exposure to Ga, ammonia, or annealing in vacuum.

During growth on the GaN-A surface both a (1×1) and (2×2) RHEED pattern could be observed. This reconstruction change was found to depend on the Ga to ammonia flux ratio. Hacke et al. [37] investigated this transition as a function of growth parameters. Since they observed the same reconstruction change, this leads to the conclusion that their films were GaN-A films. They found that the transition is temperature activated with an activation energy of about 2.76 eV. This activation energy is close to the activation energy of Ga over liquid Ga, consistent with our results that GaN-A has only one weakly adsorbing site.

Since the GaN-A surface structure is the same in vacuum, during ammonia exposure, and after ammonia or Ga exposure, the question arises how the weakly adsorbed Ga participates in the growth process. It is noted that no RHEED intensity oscillations (see chapter 3) were observed on GaN-A. Further, in Figure 33 we saw that unlike for GaN-B, no significant amounts of Ga adsorbed on GaN-A, after ammonia exposure. Ga adsorbs only if there is a coincident ammonia flux. Therefore it is concluded that growth does not occur by island nucleation on terraces, but rather by step flow.

GaN-A films which were grown under the conditions indicated in Figure 38 resulted in the RHEED pattern of Figure 30. Since there are no transmission features seen in this RHEED pattern, the diffraction must be due to the flat surfaces on top of the posts in Figure 38. These posts are typically 2500 Å in diameter and so the incident beam cannot be transmitted through them. Further, it is noted that there are steps on top of the posts that are seen to intersect with angles of 120^{o} between them. The steps on top of the posts, as well as the post edges, feature raised lines, suggesting decoration by Ga atoms due to a step-edge barrier on GaN-A .

In conjunction with the STM measurements conducted by Smith et al [30] we can draw a clear picture of the two GaN-B surfaces which provide the two different types of adsorption sites. Exposure to ammonia results in the nitrided surface structure. Although this structure is unstable in vacuum, it can be maintained for a long time depending on sample temperature, as shown earlier in Figure 34. This nitrided surface, which was prepared in Figure 35a, is characterized by islands on top of otherwise flat terraces between steps. Note that there seem to be fewer islands very close to step edges. When exposing this nitrided GaN-B surface to a Ga flux in the absence of ammonia, the surface becomes essentially featureless between steps, as presented in Figure 35c. DMS measurements showed that Ga strongly bonds onto that surface until the surface is covered by 1 ML of Ga (see chapter 5). Any additional Ga weakly bonds on top of the strongly adsorbed Ga and desorbs quickly after the Ga shutter is closed. If the substrate temperature is lowered below 300^{o}C, the reconstructions reported by Smith et al. [32] are observed, provided additional weakly adsorbing Ga (less than 1 ML) is added at a temperature low enough to prevent desorption. Note that it is essential to first gallide the surface in order to observe these reconstructions. Above 300^{o}C these reconstructions disappear, but reappear once the temperature is lowered again below 300^{o}C. Smith et al. argued that this reversible transition represents an order/disorder transition; hence at these low temperatures no significant amount of this fractional weakly bound Ga layer is desorbed, in agreement with the result that this weakly adsorbed Ga is well described by

the adsorption of Ga on liquid Ga (see chapter 3.5.1), which at this temperature is below the detection limit of our DMS.

The gallided surface is nitrided by exposure to ammonia . It was shown in the AFM scans of Figure 35 that this nitridation process proceeds from descending step edges. The nitrided surface has been shown to contain both N and H [11]. On relatively flat areas between macrosteps, the small islands of Figure 35a were observed on an otherwise smooth surface. These islands, which are big enough to be resolved laterally by AFM, appear to be irregularly shaped, different from those reported by Xie et al [38]. Those islands were triangular pointing in two different directions. When looking at the bonding arrangements of a strongly adsorbed Ga island versus a GaN island on a GaN-B surface, we notice that GaN islands have two possible sides with different bonding arrangements, while strongly adsorbing Ga according to the model of Smith et al. [32] does not. Assuming that one of the GaN Island bonding arrangements is more stable than the other, we could expect such islands to be triangular in shape. Since the islands observed are of irregular shape it is believed that they are strongly binding Ga islands. This conclusion is supported by DMS measurements in chapter 5, which show that somewhat less than a monolayer of Ga is needed to complete the monolayer of strongly binding Ga.

We presented AFM and STM results in Figure 35 and Figure 36 that showed both macrosteps and monatomic steps on GaN-B samples grown under similar conditions, and regions with both types of steps were observed even on the same sample. At this point the origin of the different types of steps is unclear. It is not known yet if the macrosteps are the final development of the step bunching observed in Figure 36. Another possibility for the formation of the macrosteps might be the nature of the nucleation process, depending on slight differences in sample preparation resulting in impurities or defects on the surface, permitting preferential growth at certain defect sites.

Samples with monatomic steps were shown in the STM image of Figure 36. After annealing in ammonia , line defects can be seen that run parallel to each other, perpendicular to the step edges. Packard et al. [39] reported a similar structure after annealing MOCVD samples in vacuum at 900^{o}C for several minutes. According to our results, this procedure would have either led to the gallided GaN-B surface, or kept a GaN-A surface unchanged, ignoring GaN decomposition. It should be noted that Smith et al. [32,30] did not observe any similar defects on their gallided GaN-B surfaces, nor on the GaN-A surface. Based on those results it was not possible to match Packard's observations with the ones reported here.

4.5 Conclusion

GaN was grown on both c-plane surfaces of bulk GaN using MBE with ammonia . Due to their unipolar nature, the availability of bulk GaN platelets permitted us to unambiguously compare the adsorption behavior of Ga and ammonia on both GaN{0001} polarities. RHEED was used to distinguish both polarities and to investigate different surface structures on those polarities, which was related to the transient Ga adsorption as measured by DMS. These surface structures were then imaged by AFM and STM. From the observed surface reconstructions, the face that could be chemo-mechanically polished was assigned to the GaN-B surface, and the face that can only be mechanically polished to the GaN-A surface. After growth on the GaN-B surface, *c*/2 steps as well as macrosteps 15-20Å high were observed. Two different GaN-B surface terminations could be prepared by exposing the surface to either Ga or ammonia only. The gallided surface was found to be the stable surface termination after annealing in vacuum. The gallided surface is essentially featureless between steps, while the nitrided surface exhibits an island structure. This island structure is initiated at the upper terrace of a step edge during annealing in ammonia. The GaN-A surface showed residual polishing damage and a post-like surface morphology with decorated step edges. Only one stable surface termination was found after growth above 700^{o}C. Since it is now possible to determine the polarity of GaN films by RHEED, these techniques were applied to GaN films grown on sapphire. Two different nucleation procedures were developed yielding unipolar films of either polarity.

5. SURFACE REACTIVITY OF GaN-B

5.1 Introduction

Growth processes of III-V compound semiconductors have mainly been studied in the past by two theoretical approaches, thermodynamics and Monte Carlo simulations. Each of these methods have their limitations in order to describe surface processes.[40] The thermodynamic approach uses a minimum set of experimental parameters, but says little about the surface. Monte Carlo simulations are well suited to describe surface processes, but need first principle parameters which can only be approximated. In order to overcome those difficulties Karpov *et al* [40] developed a kinetic growth model based on rate equations. Those equations describe the change in surface coverage of both group III and group V species. Several terms are considered: adsorption, desorption, incorporation, and decomposition. Group III and V species can combine to incorporated into the crystal, leaving behind a surface vacancy. A specie hitting the surface is assumed to be adsorbed with a certain probability described by a sticking coefficient, neglecting the possibility of different adsorption states.

It was shown earlier in chapter 3 and 4 that at least two types of Ga adsorption sites exist on the GaN surface, strongly adsorbed Ga as well as weakly adsorbed Ga on top of strongly adsorbed Ga. This weakly adsorbed Ga was found to be well described by Ga on liquid Ga, desorbing with an activation energy of 2.7 eV. Evans *et al* [41] found that Ga on GaN can exist in a much weaker state than Ga on liquid Ga, which he suggested to be physisorbed on hydrogen terminated GaN. It will be shown as part of this chapter that such second weak state in fact exists, with a very short residence time and a population inversely proportional to the coverage of strongly adsorbed Ga.

In chapter 3 a first attempts was made to describe GaN growth by a rate equation model. In this model only one coverage of weakly adsorbed Ga was considered. Weakly adsorbed Ga was added to the GaN surface by an incoming Ga flux, and removed either by desorption or incorporation into the GaN crystal. The main feature of this model was a growth inhibitation term proportional to the coverage of weakly adsorbed Ga, which caused growth to cease at the Ga condensation temperature in the excess Ga regime. One of the shortcoming of this model was that it did not apply to the excess NH_3 regime and did not consider growth at step edges.

The structure and composition of both GaN{0001} polar surfaces was examined in chapter 4, which had very different reactivities to Ga. Focusing on the GaN-B polarity, it was found that two surface terminations could be prepared on this polarity, by exposure to either a flux of Ga or NH_3 only (see also chapter 3).[17] In this chapter a rate equation model will be developed taking into account those different surface reactivities. In contrast to Karpov's model, only coverages of Ga will be considered, and related to the two surface terminations. It will be shown that the gallided surface adsorbs Ga only weakly, while the nitrided surface has strong and weak adsorption site with a very short residence time. Those results will be incorporated into the rate equation model.

5.2 Experimental

In order to investigate surface processes, desorption mass spectroscopy (DMS) can be used for measuring molecules leaving the sample surface in response to incident fluxes.[17,42,10,6] The DMS used in this thesis employs a quadrupole mass spectrometer aimed at the sample, which is collimated to restrict the sampled region to an area of about 6 mm in diameter (see chapter 2.3). Over this region temperature variations were estimated to be less than 1^{o}C, as determined from changes in the adsorption behavior measured by RHEED over a similar area (see chapter 9.2).[17] However, collimation reduced the signal relative to background and shot noise. Installation of a liquid nitrogen shroud around the ionizer reduced the NH_3 background, increasing the signal to noise ratio by more than one order of magnitude. Nonetheless, because bulk samples available were less than 6 mm in diameter, all of the DMS measurements reported here were performed on GaN films grown on sapphire. All films were prepared with a GaN buffer which was found to give the GaN-B polarity, as discussed in chapters 3 and 4.

All measurements were performed by monitoring the Ga flux that desorbed from the sample surface. This flux was calibrated by comparing a known incident flux to the Ga signal measured by the quadrupole analyzer. First, the sample temperature was set just high enough to prevent Ga condensation. At this temperature, and in the absence of an NH_3 flux, a steady state is reached in which the incident Ga flux equals the desorbed flux. The incident Ga flux was calibrated with GaAs RHEED intensity oscillations. Hence the measured analyzer signal could be set to correspond to the incident flux, without having to know either the solid angle subtended by the detector or the transmission function of the analyzer. With this method the measured DMS current was calibrated to better than 10 percent, as covered in chapter 3.[17]

5.3 Results

The adsorption behavior of Ga on GaN-B was studied by exposing the surface to an incident Ga flux while measuring the desorbing Ga flux vs time. The type of data to be analyzed is shown in Figure 39 for two different initial surface conditions. No NH_3 flux was incident on the surface in this case, and the Ga shutter sequence is indicated by two vertical dashed lines. Above the condensation temperature the desorbing Ga flux matches the incident Ga flux at steady state, as indicated by a horizontal dashed line labeled F_{Ga}; its absolute value was determined from GaAs RHEED intensity oscillations. When adding an NH_3 flux, a reduction in the steady state desorbing Ga flux is observed, which will be covered later in Figure 42. In order to understand the adsorption behavior of Ga, these data will be analyzed and fitted to a rate equation model of the adsorption kinetics. First, the data shown in Figure 39 will be considered, where there is no growth, and later the model will be extended to include an NH_3 flux as well.

The adsorption of Ga in Figure 39 is seen to depend strongly on the initial preparation of the surface, as evident from very different transient responses to an incident Ga flux. In Figure 39a, the surface was initially exposed to a Ga flux of 0.6 ML/s in the absence of NH_3. Upon initiation of the Ga flux, the Ga desorption signal rises until the desorbing flux equals the incident flux. By contrast, in Figure 39b, a surface was prepared by annealing in NH_3 at a BEP of 1×10^{-4} Torr for approximately 1 min. Then the NH_3 flux was switched off and the chamber evacuated. Upon opening the Ga shutter there is an initial signal rise to about 1/3 of the incident Ga flux, where it levels out. After a few seconds, though, the desorbing Ga flux rises again, eventually reaching steady state at a value equal to the incident Ga flux. If only one state on the surface were being filled by Ga, one would expect the desorbing flux to rise gradually without delay. Instead, the near instantaneous increase to an intermediate value (knee) suggests that a fraction of the

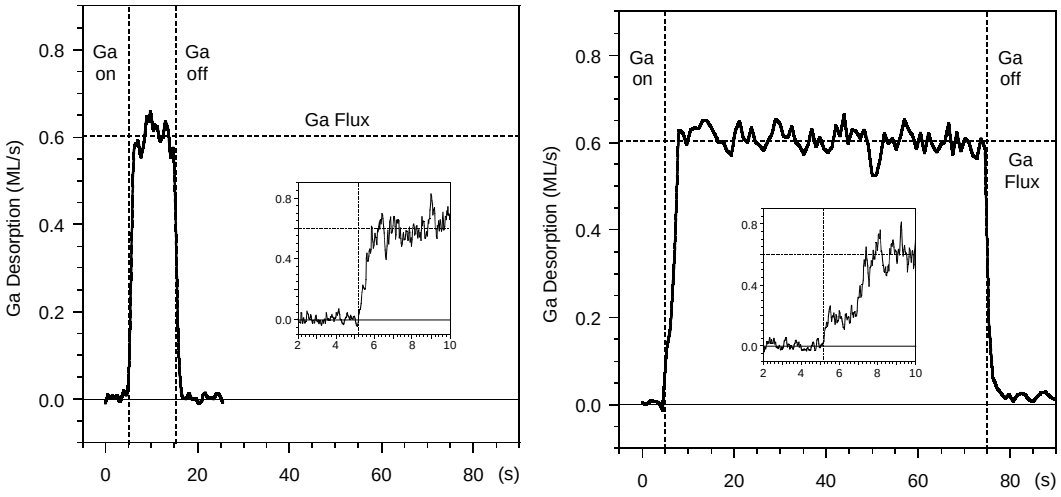

Figure 39: Measured Ga desorption vs time for a a) gallided surface and b) nitrided surface. The incident Ga flux, F_{Ga}, was 0.6 ML/s and the substrate temperature was 765^{o}C. The data was filtered for clarity, but the insets show unfiltered data for the transient response just after opening the Ga shutter.

incident flux is returned very quickly, while the remainder gradually fills a site that has a slow desorption rate. This will be discussed further in section 5.4. These measurements on both a gallided and an initially nitrided surface [17] (see chapters 3 and 4) should represent the limits of growth under high Ga/NH_3 and NH_3/Ga flux ratios, respectively.

When exposing an initially nitrided surface (Figure 39b) to a sufficient amount of Ga, some of the Ga is adsorbed resulting in the gallided surface (Figure 39a). On the gallided surface, however, there is no net adsorption. More specifically, both surfaces in Figure 39 were exposed to $F_{Ga}t_o$ layers of Ga, where F_{Ga} is the incident Ga flux and t_o the exposure time between opening and closing the Ga shutter. The net amount of Ga adsorbed is the area between the line at F_{Ga} and the desorbed Ga flux during exposure, less the area under the curve of the desorbed flux after exposure. For the gallided surface, the Ga adsorbed after opening the Ga shutter equaled the amount desorbed after closing the shutter, i.e., the difference between the two areas was within the DMS measurement error of about 0.1

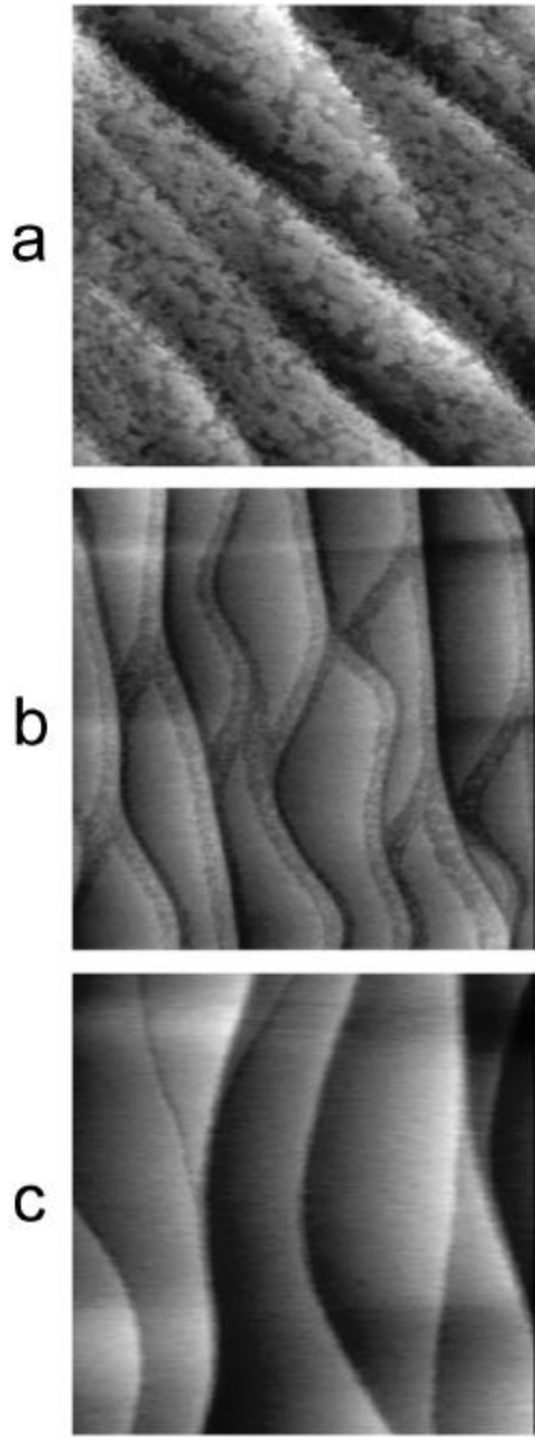

Figure 40: Three 1´1 mm AFM scans of the GaN-B surface with macrosteps cooled at different rates under NH_3 after growth was interrupted at 725°C. a) annealed, then cooled; b) slowly cooled; c) quenched. (from chapter 4)

ML. By contrast, the nitrided surface retained a net amount, usually on the order of 0.5 to 1.0 ML. As discussed further in section 5.4, the exact amount depended on sample history, since a nitrided surface slowly converts to the gallided surface upon heating in vacuum (see chapters 3 and 9.3).

The morphology of both gallided and nitrided GaN-B surfaces was examined by atomic force microscopy on bulk samples. Growth on these surfaces was described previously in chapter 4 and showed a range of features, depending on the growth parameters. On samples that exhibited macrosteps with large terraces, two distinct morphologies were obtained, which are shown in Figure 40. Figure 40a shows a sample that was annealed after growth for several minutes under NH_3 and then cooled, which resulted in terraces covered with irregularly shaped islands on the order of 500 Å [43] across and 2-5 Å in height. Figure 40b shows a sample that was cooled down slowly, at a rate of roughly 100^o per min. Areas with similar islands are observed, but only in regions starting at a descending step edge. Apart from this island region, the rest of the surface is featureless, with an RMS roughness of less than 0.5 Å.[44] The width of these regions was approximately equal, each roughly 350 Å. Finally, the sample shown in Figure 40c, was quenched rapidly after the Ga shutter was closed. These last data were obtained in a different MBE apparatus, but using otherwise similar growth conditions. In this last case, all terraces appear to be featureless, except for a few small steps between the macrosteps. The height of these steps was approximately half a lattice constant, $c/2$. Therefore, the width of the island regions originating from descending step edges depends on annealing time (or quenching rate) under NH_3, while the remainder of the surface remained unchanged. This last surface could equivalently be obtained by galliding the surface of Figure 40a. In short, the initial surface of Figure 39a corresponds to Figure 40c and that of Figure 39b corresponds to Figure 40a. Guided by these results, as well as the measurements presented in the preceding paragraph, the islands on the nitrided surface are interpreted as an initial coverage of strongly bound Ga, $q_{s,o}$.

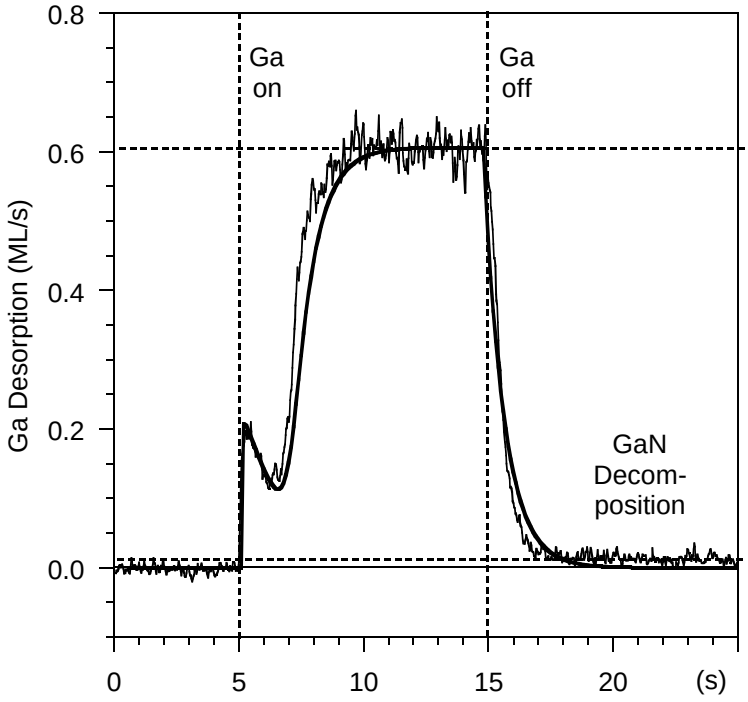

Figure 41: Average of 10 uptake curves from a nitrided surface at 756°C in the absence of NH_3, and a fit using Eq. 5-1 to 5-3 with $q_{s,o}$=0.23, a=0.45, and k=35 ML/s.

For some of the curves similar to Figure 39b, the initial knee showed a slight decrease between the first signal rise and the final rise to steady state. However, the decrease was comparable to the noise in the data. In order to increase the signal to noise ratio, the experiment of Figure 39b was repeated ten times, and those curves were then averaged. Figure 41 shows this average, obtained under similar conditions in the absence of NH_3. After each measurement, the surface was annealed in NH_3 for 1 min at 1×10^{-4} Torr. As before, a nearly instantaneous increase in the desorbing Ga flux is observed upon opening the Ga shutter. After this initial rise, a decrease in the desorbing Ga flux is clearly seen. This is followed by the increase to steady state, where the desorbing flux equals the incident flux. As for the data presented in Figure 39a, data averaged on the gallided

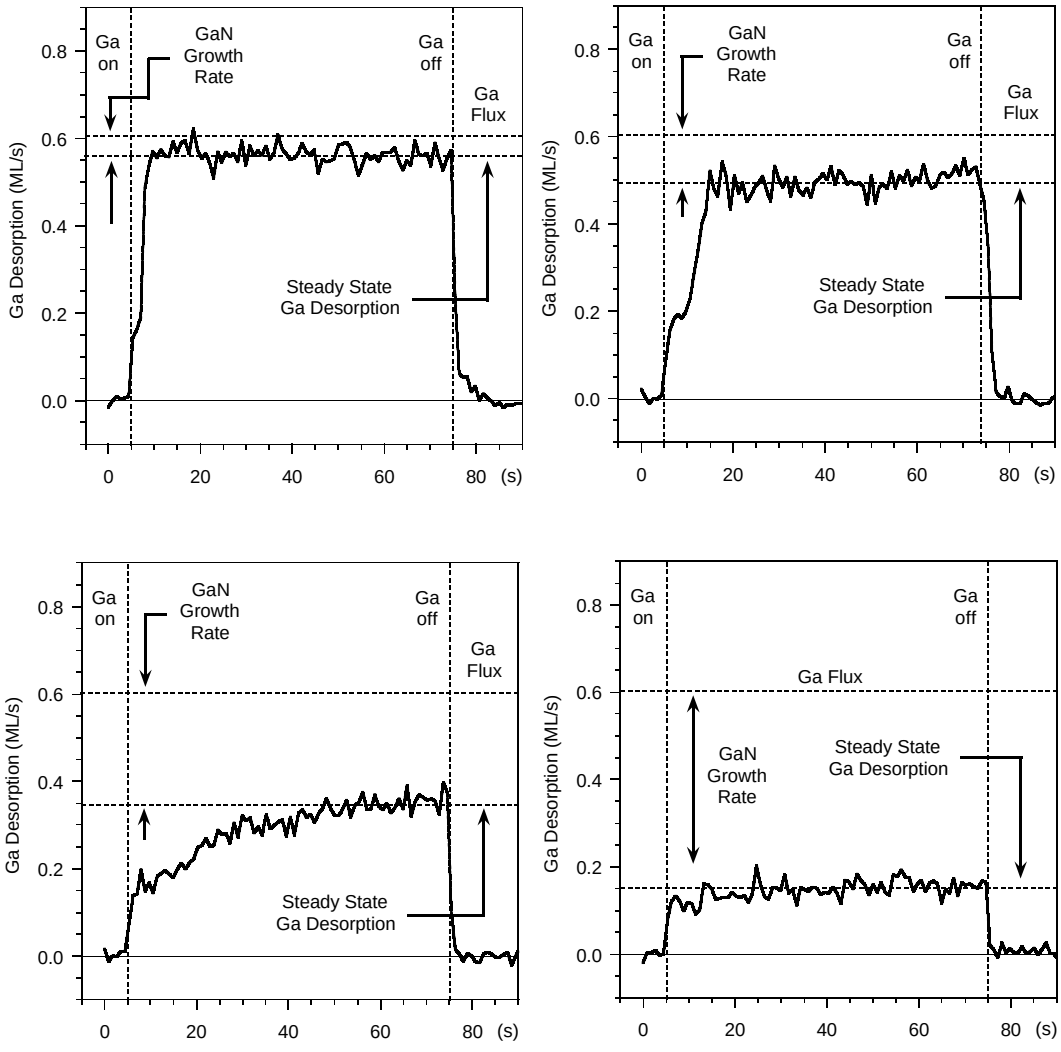

Figure 42: Measured Ga desorption vs time during growth (filtered). The incident Ga flux was 0.6 ML/s, the incident NH_3 flux was (a) 0.5, (b) 2.5, (c) 3.0, (d) 4.0×10^{-6} Torr, and the substrate temperature was 765°C.

surface does not show the knee after opening the Ga shutter. Though averaging significantly increased the signal to noise ratio, this technique was not employed for the rest of the uptake curves due to the long time required to acquire each data set.

The initial rise in the transient signal of Figure 39b is fast, within the resolution of the DMS, which was limited by the 100 ms time constant of the signal pre-amplifier. This rise is fast enough to ask whether the incident Ga is reflected or just quickly desorbed. Atoms trapped in an adsorption state, even briefly, are expected to lose all information associated with their angle of incidence. In order to resolve this issue the angle between the sample and the incident beam was varied by 30^{o}, leaving the detector fixed. No angular dependence was found in the shape of the transient uptake data, indicating that this initial rise in the data of Figure 41 is not due to a reflected signal, instead suggesting desorption from a weakly bound state. More information about the nature of this state is revealed by noting that H_2 desorbed from the surface during the duration of the knee (see chapter 3).[11] Consequently, the knee is associated with Ga adsorption onto a hydrogen covered, nitrided surface.

When there were both Ga and NH_3 incident on the sample surface, growth occurred. Depending on the NH_3/Ga flux ratio, different curves were obtained. A sequence of desorption curves for increasing NH_3/Ga flux ratios are shown in Figure 42, starting with Figure 42a obtained at a low NH_3/Ga flux ratio. The desorption behavior is similar to that of Figure 39b, but in this case the desorbing steady state Ga flux is reduced, corresponding to the growth rate. In Figure 42b and c, the NH_3 flux is successively increased. Again, the curves show the same general features. In these two, the steady state Ga flux was reduced as well due to growth, and the height of the knee remained approximately at the same level. The main difference is the duration of the knee, which increases with NH_3 flux. Finally, in Figure 42d, at an NH_3 BEP of 4×10^{-6} Torr, the second rise in Ga desorption is

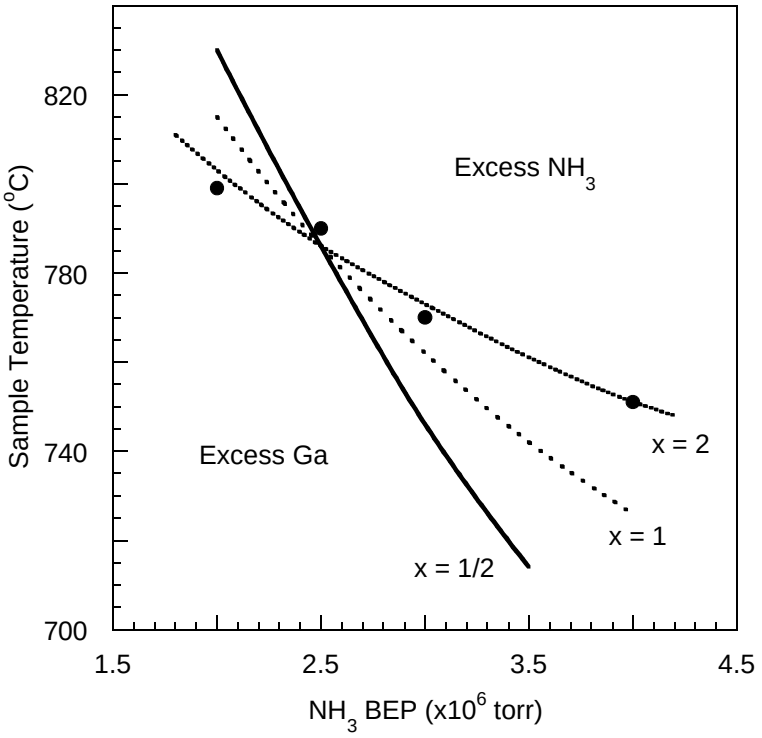

Figure 43: Crossover between excess Ga and excess NH_3 growth as a function of NH_3 flux and substrate temperature for a fixed Ga flux of 0.6 ML/s.

completely absent. This last curve shows that there is a maximum in the growth rate, with some Ga desorbing even under excess NH_3 conditions.

When increasing the NH_3/Ga flux ratio, the duration of the knee increases at an increasingly faster rate. The increase is not linear in NH_3 flux, featuring an abrupt change. Past this point, as in Figure 42d, the desorbed Ga flux remains at the first, intermediate value. This abrupt crossover suggests that two distinctly growth modes are observed, and that this feature can be used to determine whether the growth is excess Ga or excess NH_3. Using datasets as in Figure 42, this crossover was measured as a function of ammonia flux. Figure 43 shows that both increasing the NH_3 flux as well as the substrate temperature led to a change in growth mode.

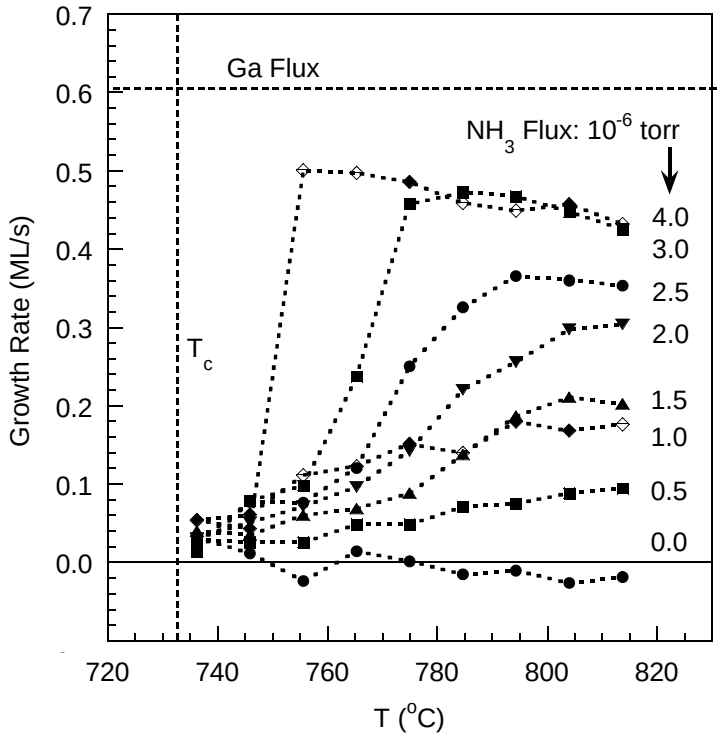

Figure 44: Steady state growth rate as a function of temperature for several NH_3 fluxes, at a constant Ga flux of 0.6 ML/s.

The abrupt change in uptake behavior is also seen in measurements of the steady state growth rate. Note that since there is no Ga accumulation at these temperatures and Ga flux, the instantaneous growth rate is given by the incident Ga flux minus the desorbing Ga flux (see chapter 3 and appendix 9.1).[17] Figure 44 shows the steady state growth rates measured as a function of temperature for several NH_3 fluxes at a fixed Ga flux. The most noteworthy feature is that the growth rate abruptly increases at about the same temperature as the crossover between growth regimes in Figure 43. For low NH_3/Ga flux ratios, as in Figure 42a-c, the steady state growth rate is only a small fraction of the incident Ga flux. This relatively unreactive steady state surface, as well as the shape of the transient desorption signal, remind us of the transition from a nitrided to a gallided surface in vacuum (Figure 39a). On the other hand, for high NH_3/Ga flux ratios as in Figure 42d, a second rise in Ga desorption is never observed. The absence of the second

rise in Ga adsorption and the abrupt increase in growth rate suggest that the surface is being continuously nitrided, never reaching the completely gallided state.

5.4 Discussion

In order to develop a kinetic growth model, the dramatically different transient Ga desorption curves shown in Figure 39 are examined first. Ga adsorbed onto the gallided surface is seen to be only weakly adsorbed (physisorbed). It completely leaves the surface after the Ga shutter is closed. It was shown previously that this process is well described by the equilibrium between liquid Ga and its vapor; hence the desorption rate can be described as q_w/t where t is obtained from tabulated equilibrium vapor pressure data.[27] Note that for the Ga fluxes used in these experiments, the substrate temperatures were always higher than the temperature at which liquid Ga would condense on the sample surface.

To account for the initial knee in the data of Figure 41, it is suggested that some fraction of the incoming Ga flux is returned from nitrided parts of the surface, via a very weak adsorption site, while the remainder chemisorbs. Such state is best described as an intrinsic physisorption precursor state, defined as an intermediate step necessary for chemisorption.[45] This is a reasonable suggestion since hydrogen desorbs from the nitrided surface during Ga exposure, which could passivate the surface to inhibit chemisorption. Part of this physisorbed Ga desorbs again, and the other part is chemisorbed while releasing hydrogen. Finally, extrinsic physisorbed Ga is allowed on gallided parts of the surface to diffuse to chemisorption sites on nitrided parts of the surface. Together, these simple assumptions are used to describe the data.

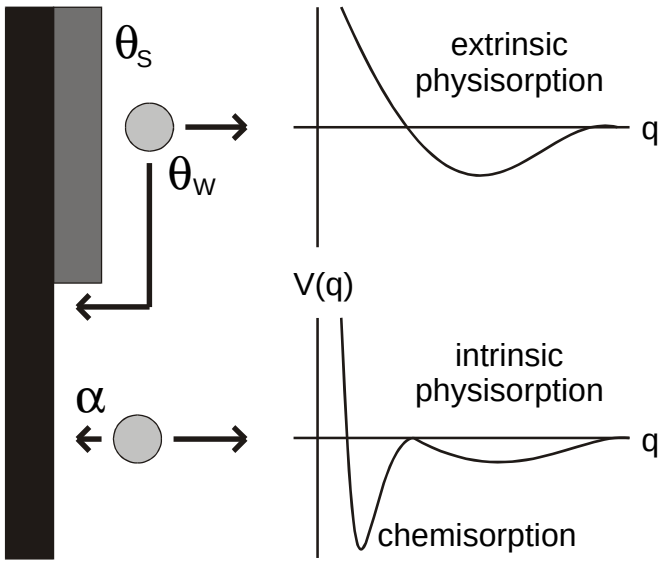

Figure 45: Illustration of the different statess on gallided and nitrided parts of the surface. On the left a 'vertical' film is shown, with the top being gallided and the bottom being nitrided. The gallided surface has only one extrinsic physisorption state, while the nitrided surface has an intrinsic physisorption and a chemisorption state.

This model is described more explicitly by the following rate equations:

$$\frac{\mathrm{d}q_{\mathrm{s}}}{\mathrm{d}t} = (1-q_{\mathrm{s}})aF_{\mathrm{Ga}} + q_{\mathrm{w}}(1-q_{\mathrm{s}})k \qquad (5\text{-}1)$$

$$\frac{\mathrm{d}q_{\mathrm{w}}}{\mathrm{d}t} q_{\mathrm{s}}F_{\mathrm{Ga}} - q_{\mathrm{w}}/t - q_{\mathrm{w}}(1-q_{\mathrm{s}})k \qquad (5\text{-}2)$$

$$F_{\mathrm{d}} = (1-a)F_{\mathrm{Ga}}(1-q_{\mathrm{s}}) + q_{\mathrm{w}}/t \qquad (5\text{-}3)$$

where q_{s} is the coverage of chemisorbed Ga, and q_{w} is the coverage of physisorbed Ga in extrinsic physisorption states on top of chemisorbed Ga, with a residence time of t. The fraction of incident Ga that adsorbs into chemisorption sites via intrinsic physisorption states is described by a, which implies that 1-a is the fraction of Ga desorbed from those states. The diffusion of Ga into chemisorbing sites on nitrided parts of the surface, via

extrinsic precursor states on gallided parts of the surface, is described by k. The first two equations describe the relative rates at which the chemisorbing and extrinsic precursor states are filled. No equation is given for the population of the intrinsic precursor states, which are sufficiently described by a due to their short residence time. The third equation is the desorption Ga flux as measured by DMS, F_d, which is the sum of Ga desorbed both from intrinsic and extrinsic physisorption states.

Eq. 5-1 contains the strongest assumptions, which are illustrated by Figure 45. Two states are shown on the nitrided surface, plotted vs some very general reaction trajectory. Since the surface is passivated with hydrogen, incident Ga first physisorbs into the fast intrinsic physisorption state. Part of the Ga then desorbs, and the remaining fraction, a, then chemisorbs into the deep well while releasing H_2. The number of precursor sites is assumed to equal the number of empty chemisorption sites, $1-q_s$, where q_s is the fraction of filled chemisorption sites. The first term in Eq. 5-1 covers this chemisorption process, which is proportional to the incident Ga flux, the number of unfilled chemisorption sites, and the fraction of Ga atoms chemisorbing from the fast intrinsic precursor state. The second term describes the filling of empty chemisorption sites from physisorbed Ga in the extrinsic precursor state on gallided parts of the surface (filled chemisorption sites).

The second equation, Eq. 5-2, contains three terms describing the rate at which the population of physisorbed Ga in extrinsic precursor states changes. The first term states that incident Ga physisorbs on top of filled chemisorption site. No physisorbed intermediary is required for this process and we do not consider multilayer physisorption since $q_w<1$. The second term states that physisorbed Ga desorbs at a rate proportional to its coverage. The last term describes the depletion of physisorbed Ga due to diffusion to chemisorption sites, which is the balance to the last term in Eq. 5-1. There is no transfer from chemisorbed Ga to physisorbed Ga in the extrinsic precursor state. This second equation, with $q_s=1$, fits the data in Figure 39a. For the residence time, $t=t_0e^{-Eo/kT}$ is used

where t_o=4.88×10^{14} s and E_o=2.70 eV.[27] This equation is mainly a statement that the extrinsic physisorption state obeys first order desorption and zeroth order adsorption kinetics.

Eq. 5-3 is only necessary to compute the desorbing flux to compare to the measured data. The first term covers physisorbed Ga desorbed from the fast intrinsic precursor state, proportional to the sites available for chemisorption. The second term accounts for the physisorbed Ga that desorbs from the extrinsic precursor state.

To test this model a fit to the averaged uptake curve of Figure 41 was performed. Both the original data and the computed curve are shown. This particular curve was measured at a substrate temperature of 756^{o}C and a Ga flux of 0.606 ML/s. For this curve, following the procedure described in chapter 5.3, a net adsorption of 0.77 ML was measured; hence to integrate Eq. 5-1 and Eq. 5-2, the initial conditions $q'_{s,o}$=0.23 ML and $q_{w,o}$=0 are used. The best fit was achieved with a=0.45 and a surface diffusion flux, k, of 35 ML/s. As can be seen, all of the details of the measured data are reproduced by the model.

The requirements on the fitting parameters are strict. The total Ga uptake fixes the fraction of initially filled chemisorption sites. Given $q_{s,o}$, a is determined by the initial signal rise just after opening the Ga shutter, since from Eq. 5-3, $F_{d,o}$=(1-a)F_{Ga}(1-$q_{s,o}$). The only fitting parameter is the temperature dependent surface diffusion parameter, k, which mainly determines the magnitude of the drop in the Ga desorption signal between the first and second rise. The higher this diffusion flux, the deeper the drop. Ga atoms will tend to diffuse to nitrided parts of the surface before a significant coverage of physisorbed Ga can build up on gallided parts of the surface, which is the cause of the second rise in the desorption signal.

Next all three fitting parameters ($q'_{s,o}$, a, k) were extracted as a function of temperature, from data as of Figure 39, by visually fitting the best possible curve. A similar procedure as for the averaged curve of Figure 41 was followed, and the results are shown in appendix 9.5. For a, a value close to ½ was extracted without a definite temperature dependence. This result indicates that physisorbed Ga in this state is ejected in roughly equal proportions onto the surface (chemisorbed) and off the film (desorbed), independent of temperature. For k, on the other hand, an activation energy for surface diffusion of roughly 1.2 eV with a pre-exponential of 1.2×10^7 ML/s was obtained.

As mentioned earlier, an initially nitrided surface anneals in vacuum to the gallided surface, i.e. q_s goes from $q_s=q_{s,o}$ over $q_s=q'_{s,o}$ to eventually $q_s=1$ in a roughly linear manner. It is apparent that during the time required to remove the NH_3 from the chamber and the start of the adsorption experiments, q_s changes from $q_s=q_{s,o}$ to $q_s=q'_{s,o}$. The progress of this annealing process can be monitored by RHEED, and the initial steady state coverage of chemisorbed Ga, $q_s=q_{s,o}$, can be extracted from the measured $q'_{s,o}$ and the change in RHEED intensity, as covered in appendix 9.3. After correcting for this annealing process, it was found that $q_{s,o}$ is slightly temperature dependent and approximately given by $q_{s,o} = 2.62 - 0.00235\ T$, with T in K.

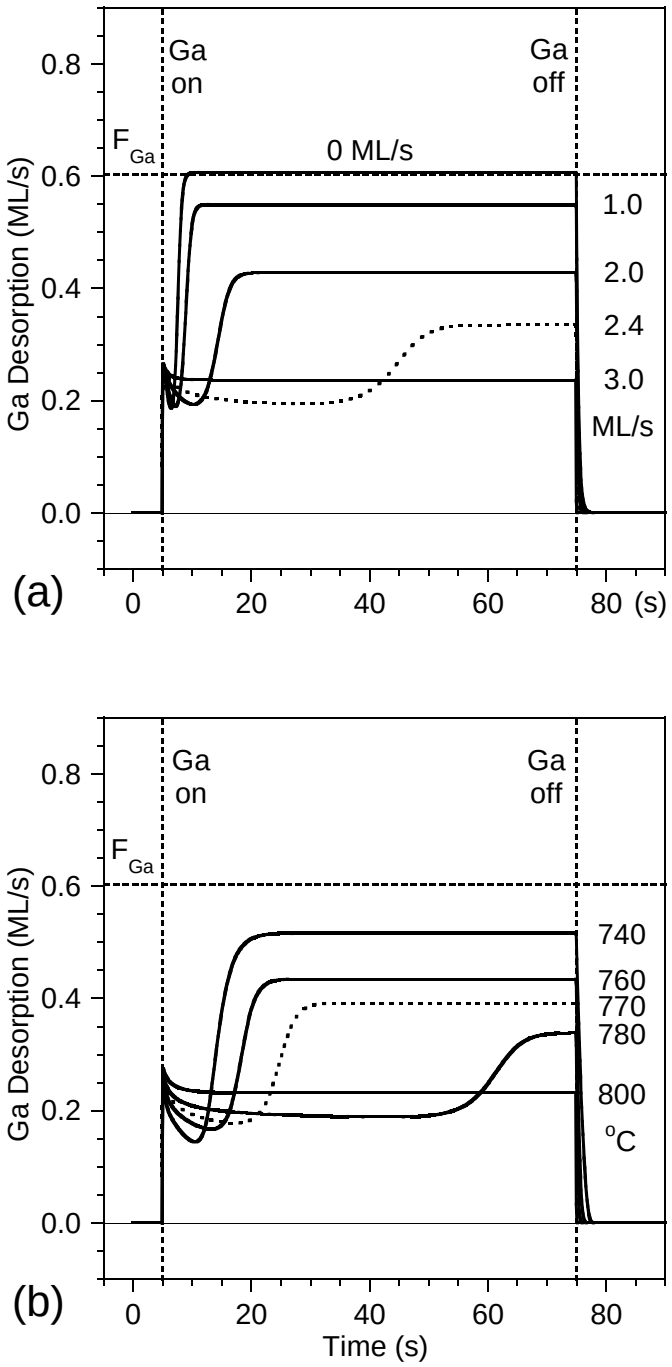

Figure 46: Calculation of uptake curves vs NH_3 flux and temperature; a) F_{Ga}=0.6 ML/s, T=786°C; b) F_{Ga}=0.6 ML/s, NH_3 BEP = 2.5´10^{-6} Torr;

Using the parameters determined by fitting to the data obtained without NH_3, the model is now expanded to include a simultaneous NH_3 flux. When opening the Ga shutter in the presence of NH_3, it can be easily argued that filling chemisorption sites (galliding the surface as in Figure 38c) competes against re-nitridation. Assuming that nitridation only occurs at step edges of gallided parts of the surface (islands seen by AFM), the equation has to be modified only for the time behavior of the chemisorbing Ga:

$$\frac{\mathrm{d}q_\mathrm{s}}{\mathrm{d}t} = (1-q_\mathrm{s})aF_\mathrm{Ga} + q_\mathrm{w}(1-q_\mathrm{s})k - (q_\mathrm{s}-q_\mathrm{s,o})^x(1-q_\mathrm{s})^x F_\mathrm{N} - f(q_\mathrm{s}-q_\mathrm{s,o})kF_\mathrm{N} \qquad (5\text{-}4)$$

where F_N is proportional to the flux as measured by the ion gauge. In the third term, it is assumed that nitridation occurs only at the island step edges, with x=1/2 to account for the available step perimeter. The fourth term corresponds to growth at step edges under excess Ga conditions, including the result that physisorbed Ga inhibits growth (see chapter 3) [11,17] expressed as $\kappa=(1-q_\mathrm{w})$. Note that the inhibitation term is neglectible for predicting the crossover between growth regimes. Results of these calculations are shown in Figure 46 vs NH_3 flux and vs substrate temperature. Note that the approximate temperature dependence of $q_{\mathrm{s,o}}$ was used as described earlier. The main result is that this model qualitatively fits the data and that there is a very sharp crossover as a function of both temperature and NH_3 flux. For the calculation of Figure 46 a relatively high step edge related growth efficiency of f=0.1 was used, shifting the crossover only slightly. This illustrates that the crossover is relatively independent on the density of step edges on the gallided surface.

As a measure of how well the experimental data fit the model, the crossover from step flow to island nucleation as a function of temperature and NH_3 was calculated and

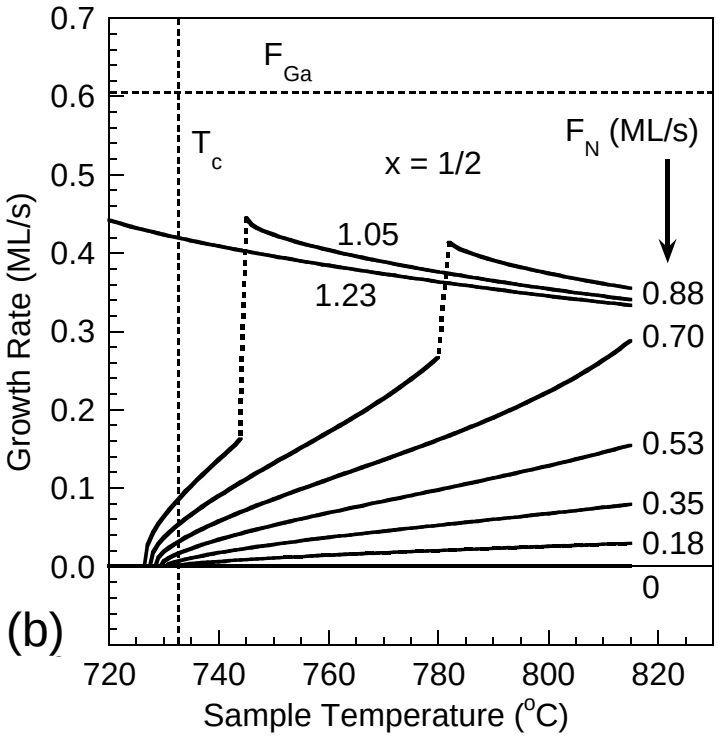

Figure 47: Steady state growth rates simulated using the model.

compared to Figure 43. The model equations 5-1 and 5-4 were then used to fit the experimental data for several values of x: 1/2, 1, and 2. For all three x parameters, F_N was adjusted to fit the experimental data for an NH_3 flux of 2.5×10^{-6} Torr. For x=1/2, assuming renitridation to be proportional to the island perimeter, gives the worst fit. A better fit is obtained by using the first order approximation, x=1, to account for zero renitridation on a steady state nitrided and a completely gallided surface. Using x=2 gives the best fit, although no satisfying explanation can be offered from the data available. One should consider that x is not only determined by the available island perimeter, but also by the details of the bonding arrangements and related availability of reaction sites.

Next, the measured growth rates of Figure 44 were compared to the model, and the results are plotted in Figure 47. As seen, the simulated curves qualitatively track the measurements in support of the model. The abrupt crossover is indicated by the dotted

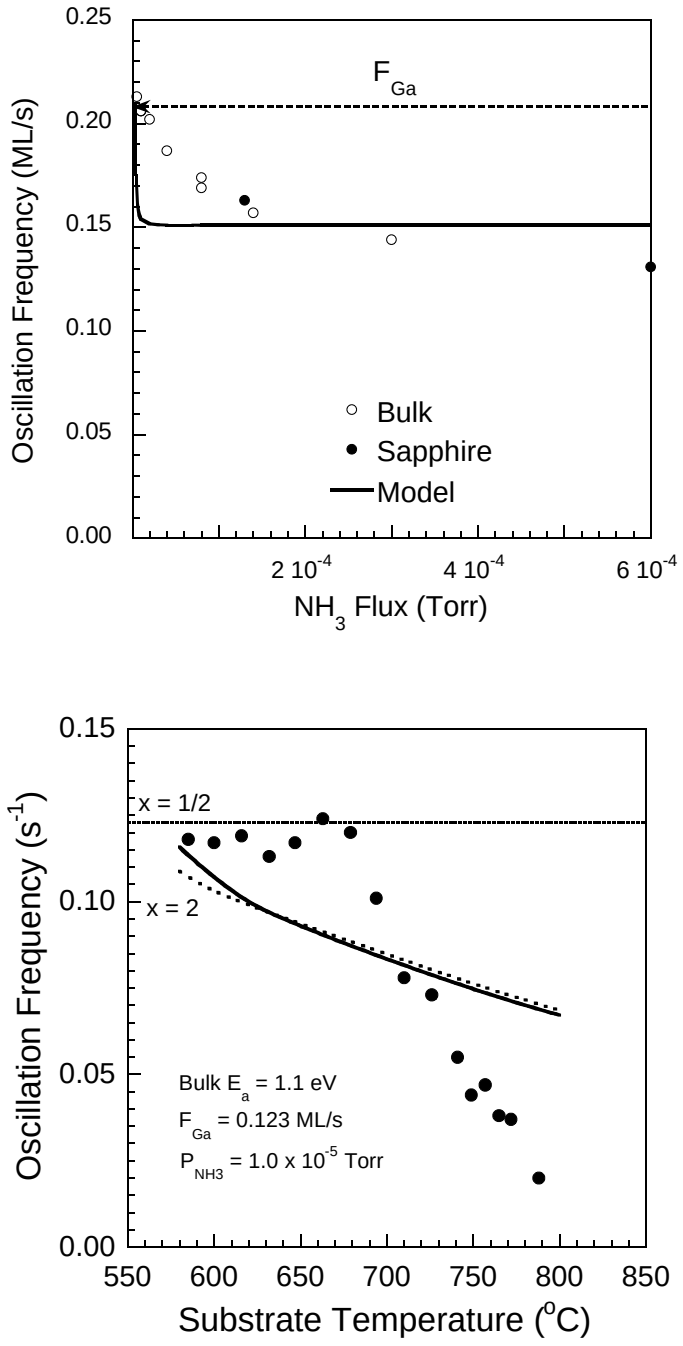

Figure 48: Measured RHEED intensity oscillations compared to growth rate as predicted by the model; a) versus NH_3 flux; b) versus T_s.

lines. Again, using x=2 instead of ½ gives a better fit. Further, for the excess Ga regime, the growth rate increases with temperature, and abruptly rises at crossover into the excess NH_3 regime. In the excess NH_3 regime, the growth rate slightly decreases with temperature due to a decreasing coverage of chemisorbed Ga which increases the desorbing Ga from the fast physisorption state. Last, for the excess Ga regime, the growth rate goes to zero at or slightly below the Ga condensation temperature. This feature is experimentally observed as well, in support of the inhibitation term of $\kappa=(1-q_w)$ in the model.

Finally, the results of the model are compared to RHEED intensity oscillations as shown in Figure 48. Figure 48a compares the model predictions versus ammonia flux. The ammonia flux was related to the ion gauge reading by adjusting the growth regime crossover of the model to the disappearance of the RHEED intensity oscillations at an NH_3 BEP of 5×10^{-6} Torr. As seen, the model predicts that the period of the RHEED intensity oscillations decreases with ammonia flux. Although the measured decrease is not as fast as predicted by the model, the model correctly predicts the endpoints. Close to the regime crossover the oscillation frequency agrees with the model giving unity Ga incorporations. At high NH_3 fluxes the model predicts that the oscillation frequency stabilizes at a value dictated by $q_{s,o}$, which is also observed by experiment. Figure 48b compares RHEED intensity oscillations versus substrate temperature. A decrease in the period of the oscillations is observed, with an activation energy of 1.1eV. This decrease is predicted by the model qualitatively, but is quite a bit off quantitatively. These results show that there are quantitative limitations to the model. For example, diffusion of chemisorbed Ga on nitrided portions of the surface are completely ignored.

Note that the model developed in this chapter is fundamentally different from the much more simplistic model of chapter 3. In chapter 3 it was assumed that growth occurs on the whole surface ignoring step edges, and that the rate equations were only valid in the

excess Ga regime. The crossover between regimes was a result of a competition between Ga and NH_3 flux, modified by a term that allowed for weakly adsorbed Ga to inhibit growth at strongly bound Ga. In this chapter it is assumed that growth can only occur at nitrided portions of the surface as well as step edges of chemisorbed Ga. A completely gallided surface is assumed to be unreactive to Ga, regardless of the coverage of weakly adsorbed Ga, except for the step edges. Only at these step edges growth is inhibited proportional to the coverage of weakly adsorbed Ga. As mentioned in the previous paragraph, this term is essential in letting the growth rate go to zero in the excess Ga regime at or slightly below the Ga condensation temperature.

5.5 Conclusion

In conclusion, a quantitative model for the GaN-B surface was developed which explains the transitional Ga uptake, steady state growth, as well as the abrupt transition between growth modes. This transition, between island nucleation and step flow, occurs as a function of growth parameters, which determine the steady state coverage of chemisorbed Ga. Ga is chemisorbed via two types of physisorption sites, one of which is an extrinsic precursor state, while the other corresponds to an intrinsic precursor state with a very short residence time. A gallided surface is obtained by filling all chemisorption sites, which is completely unreactive to additional Ga, even in the presence of NH_3, permitting growth only at step edges. This step flow growth mode is obtained at high Ga to NH_3 flux ratios, and the window widens at lower substrate temperatures permitting lower Ga fluxes. For conditions used in chapter 4 on bulk GaN, this window lies below about 750^oC. These gallided surfaces in the presence of NH_3 could only be obtained by quenching. In support of this growth model, AFM and vacuum STM measurements showed no islands on the terraces between steps, but a few monatomic steps appear to propagate from the base of an ascending step edge to the next descending step edge. These results suggest a mechanism for lateral epitaxial overgrowth (LEO) in the excess Ga regime.

6. SURFACE MORPHOLOGY OF BULK GaN-B

6.1 Introduction

Among the multiple challenges in growing high quality GaN material by molecular beam epitaxy (MBE) is the control of surface morphology. GaN has to be grown by heteroepitaxy since bulk GaN is still not available commercially. The most commonly used substrates, sapphire and SiC, are poorly lattice matched to GaN. This poor lattice match gives rise to a large defect density at the interface, which is believed to be the ultimate cause for the poor surface morphologies observed.

In this chapter the evolution of the surface morphology from initially very flat bulk GaN-B crystals is investigated. These flat surfaces have a defect density at least 2 orders of magnitude lower than GaN grown on sapphire or SiC, which reduces the effect of defects on surface morphology. Different surface morphologies as a function of growth parameters will be shown, as well as the effects of annealing in vacuum and NH_3.

6.2 Experimental

Single-crystal bulk GaN platelets were used for the experiments in this chapter, with the opposing c-plane faces corresponding to the two possible polarities. These roughly hexagonal shaped substrates, approximately 5×5 mm in size, were grown in Ga solution at high nitrogen pressures.[46] The GaN-B polar face can be chemo-mechanically polished [47] utilizing KOH, resulting in an atomically smooth surface with an RMS roughness on the order of half a lattice constant, where c=5.2 Å. Figure 49 shows such surface.

Polishing could produce a slight misorientation from the c-plane. These bulk samples were cleaned by heating them at 65^{o}C in acetone followed by methanol, before mounting them on a Mo sample holder. Two mounting methods were used: The samples were either coated on their back side with 2000 Å of Ti and mounted without stress by mechanical means (see chapter 2.1), or by bonding to a Al_2O_3 wafer using a GaSn eutectic.

Prior to the experiments the samples were outgassed for several hours at 300^{o}C and 1 hour at 500^{o}C in the Varian Gen II molecular beam epitaxy (MBE) chamber. The base pressure of the growth chamber, with cryoshrouds cold, was $<3\times10^{-9}$ Torr.

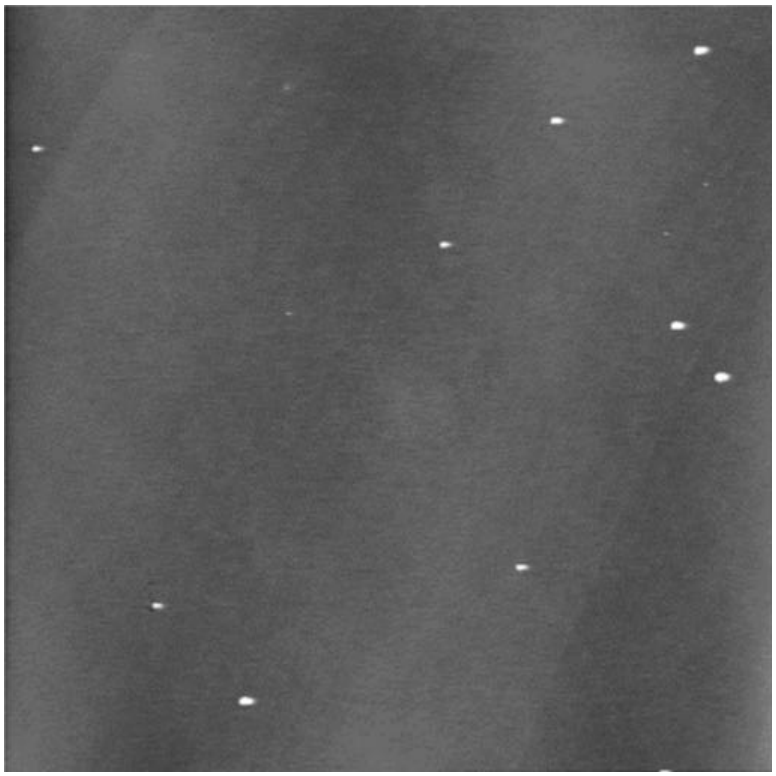

Figure 49: 15 micron AFM scan after chemo-mechanical polishing using KOH. The RMS roughness is on the order of half a lattice constant, c/2 2.6 Å

6.3 Results

For initial comparison, three films were grown using a fixed substrate temperature and NH_3 flux, but varying the Ga flux. One film was grown under excess Ga conditions by using a high Ga flux. Another film was grown under excess NH_3 condition. The third film was grown approximately between those two growth regimes (see chapter 3). The resulting surface morphologies are shown in Figure 50. The excess Ga film shows flat topped posts several microns in diameter. The flat tops have a RMS surface roughness on the order of $c/2$. The excess NH_3 film shows a high hillock density with macrosteps in between. The sample grown in between showed regions of both flat topped posts as well as macrosteps.

Next the effect of temperature on surface morphology was investigated. Films were grown at the same conditions as the excess NH_3 film of Figure 50, but at varying substrate temperatures. A significant reduction in hillock density is observed when lowering the substrate temperature, shown in Figure 51. The macrosteps become clearer as the hillock density reduces due to the AFM tip being able to reach between them. The height of the macrosteps is approximately 25 Å. No quantitative statements can be made on the hillock density versus temperature since only a limited number of samples were grown.

It was further observed that the macrosteps appear faceted at higher temperatures, while at lower temperatures they are more rounded. Three sample films are shown in Figure 52, grown at various temperatures around 700^{o}C under the same fluxes as of Figure 51. This result is not unexpected since at high temperature detachment kinetics are fast, preferentially maintaining the most stable facet. At low temperatures though, growth rates exceed detachment kinetics, permitting growth to occur on less stable facets as well at a comparable rate.

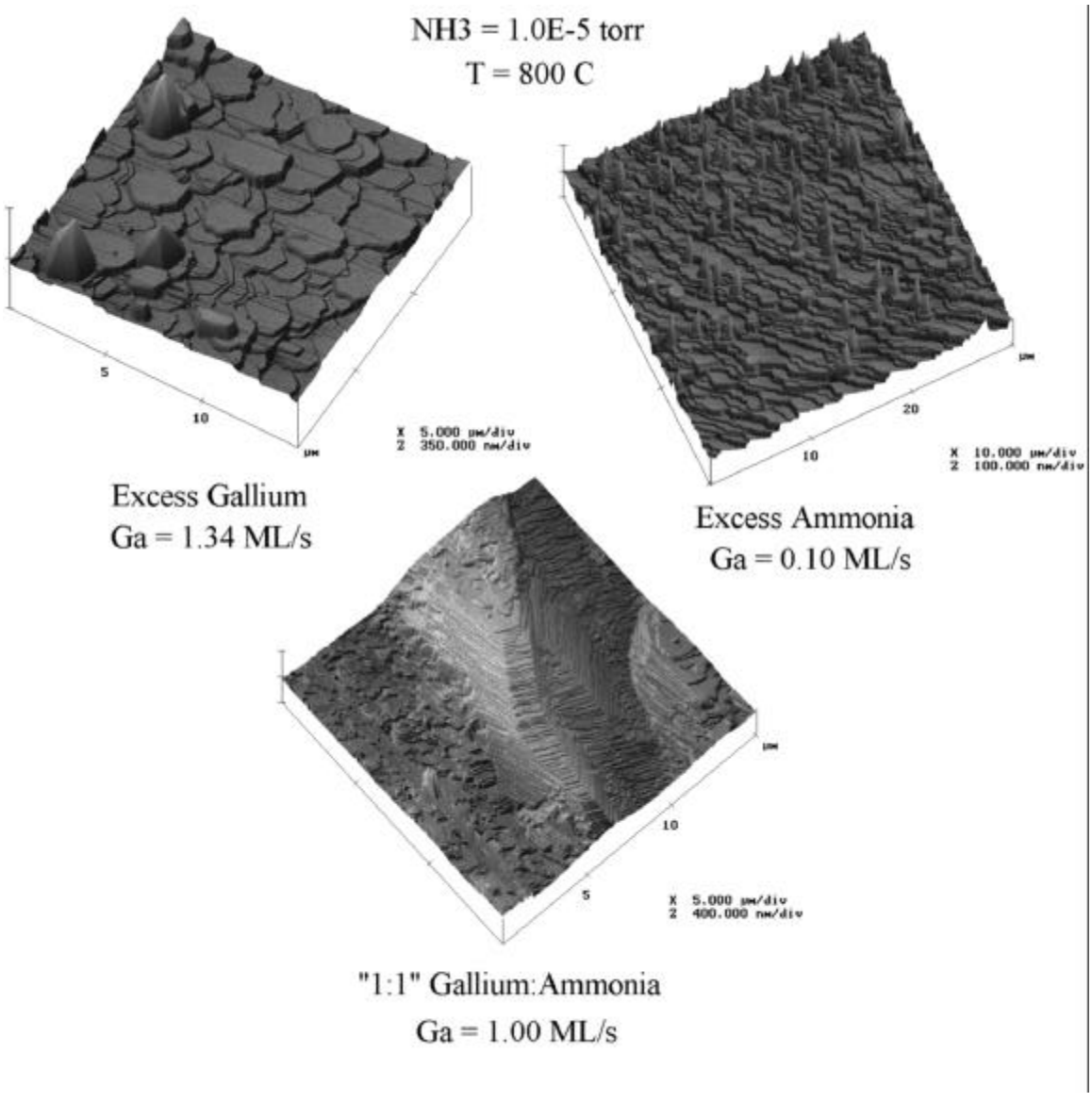

Figure 50: Surface morphology of films after 3 hours of growth at 800^{o}C and 1.0×10^{-5} torr ammonia: a) at a Ga flux of 1.34 ML/s; b) 1.0 ML/s; c) 0.10 ML/s;

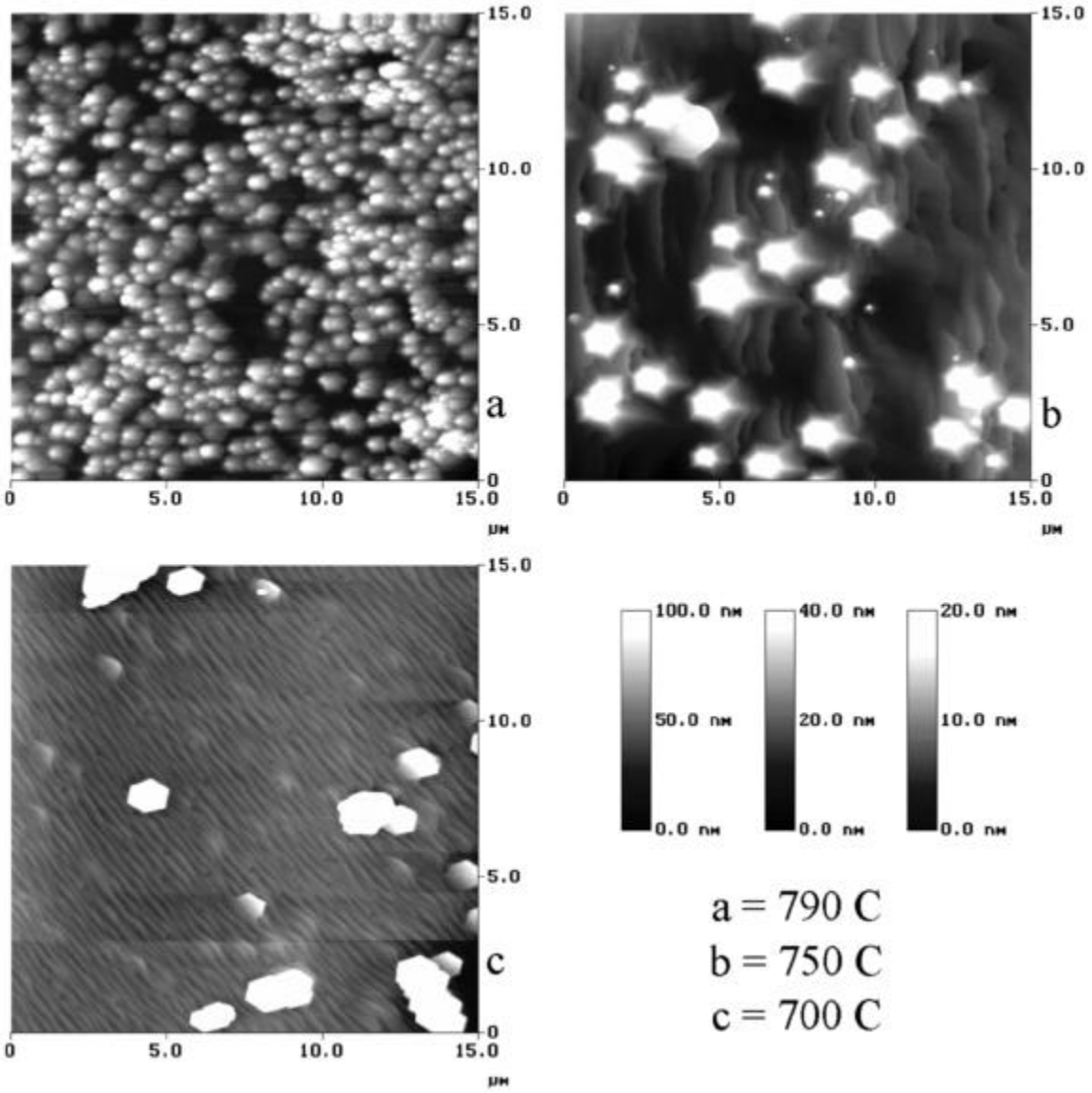

Figure 51: Hillock density on films after 3 hours of growth at a Ga flux of 0.10 ML/s and 1.0×10^{-5} torr ammonia: a) at a temperature of 790°C; b)750°C; c) 700°C; (15 mm scans)

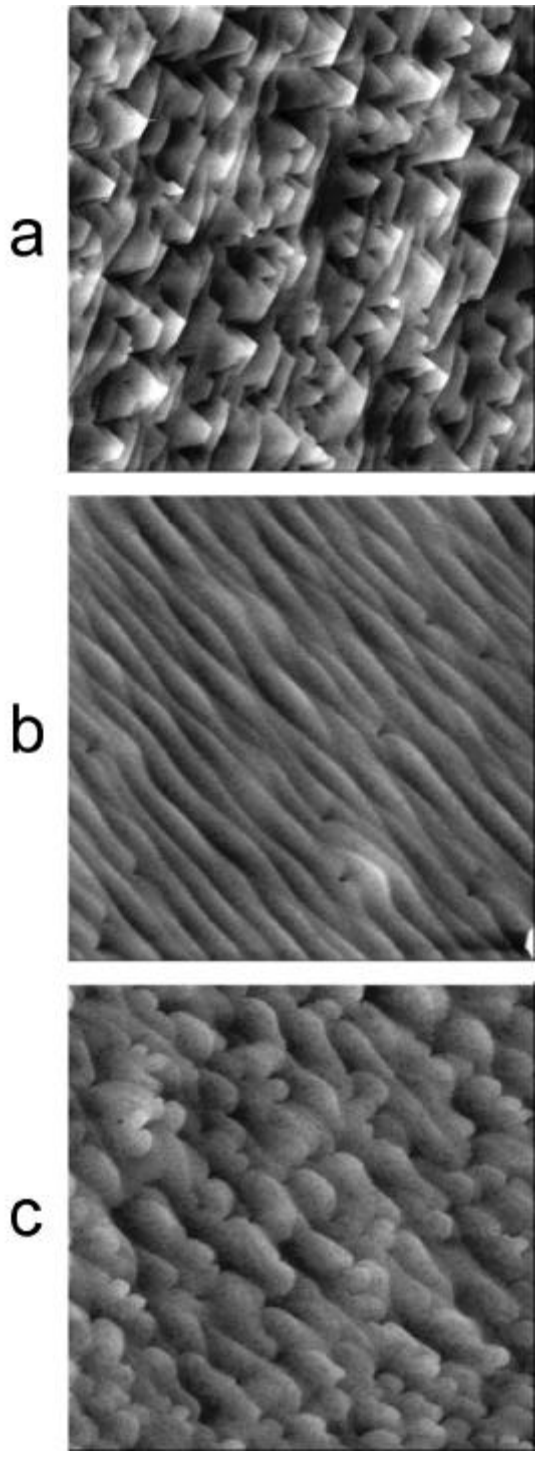

Figure 52: Macrosteps on films after 3 hours of growth at a Ga flux of 0.10 ML/s and 1.0×10^{-5} torr ammonia: a) at a temperature of 725°C; b)700°C; c) 675°C; (5 mm scans)

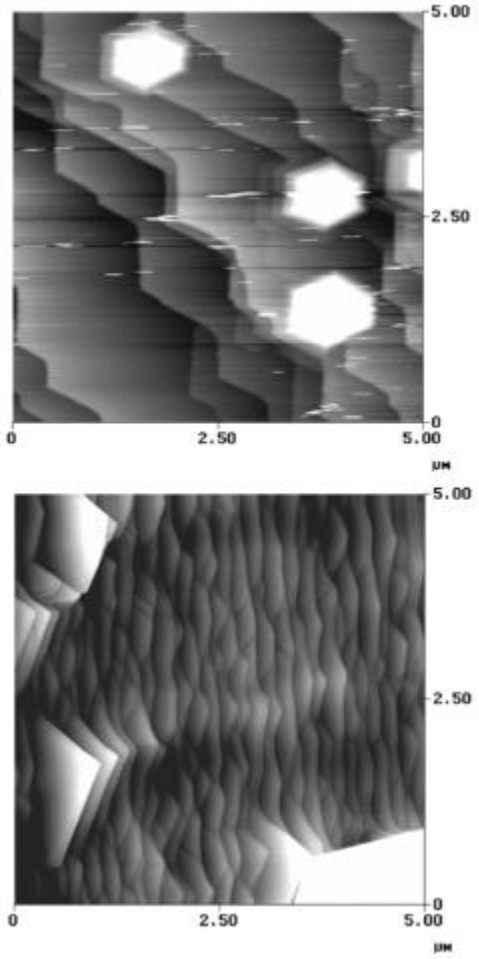

Figure 53: 5 mm scans of films with both macrosteps and hillocks. The facets of the macrosteps are lined up with the facets of the hillocks. The hexagonal hillocks line up with the hexagonal shape of the crystal. Therefore the facet direction could be determined from X-ray analysis of the crystal to be {1$\underline{1}$00}.

The direction of the facets on the macrostep edges was determined Figure 53 to be <1$\underline{1}$00>. Figure 53 shows macrosteps with hexagonal hillocks. The facets of the macrosteps are lined up with the facets of the hillocks. The hillocks have much larger facets, which could easily be correlated to the sides of the hexagonal shaped platelet. The crystallographic direction of the platelet is known from X-ray analysis.

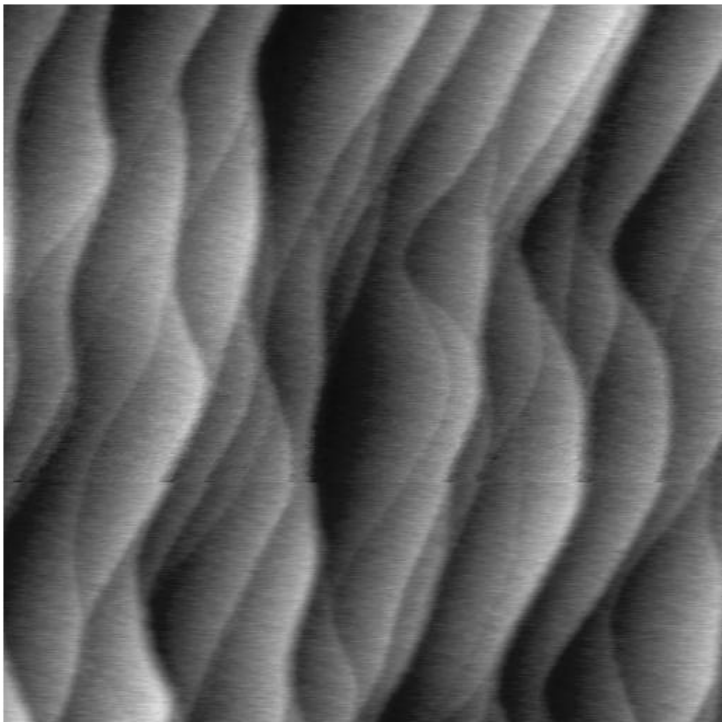

Figure 54: 1 mm scan of a gallided surface. This surface was obtained after Ga only exposure. The macrosteps are approximately 25 Å in height.

Guided by results shown in section 4, the terraces between macrosteps were investigated in more detail. It was shown in chapter 3.4.1 and 4 that two surface terminations can be prepared on GaN-B, after either Ga or NH_3 only exposure. In order to perform AFM on a surface after Ga only exposure, the NH_3 flux was switched off after growth. Then the film was exposed to Ga only for a long time, above Ga condensation. The resulting gallided surface, Figure 54, shows no resolvable features on the terraces between macrosteps. This results was confirmed by vacuum STM measurements[48].

In order to investigate the nitridation process, we first grew films under excess Ga conditions. Then the Ga flux was interrupted and the film exposed to NH_3 at growth temperature for different lengths of time, after which the films were cooled to room temperature. The NH_3 flux was held fixed since it could not be interrupted easily.

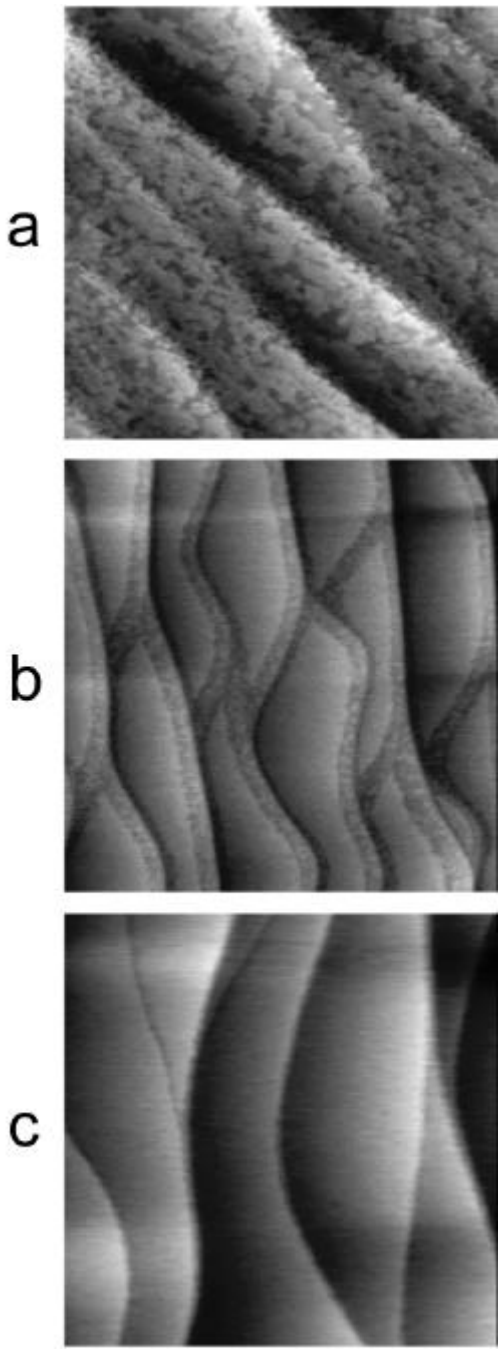

Figure 55: Three 1 mm AFM scans of the GaN-B surface with macrosteps cooled at different rates under NH_3 after growth was interrupted at 725^{o}C. a) annealed, then cooled; b) slowly cooled; c) quenched. Note that the same featureless surface as in c) is obtained after Ga only exposure in the absence of NH_3 .

Specifically, Figure 55a shows a sample that was annealed after growth for several minutes under NH_3 before cooling, which resulted in terraces covered with irregularly shaped islands on the order of 500 Å across and 2-5 Å in height. Figure 55b shows a sample that was cooled down slowly, at a rate of roughly 100^o per min. Areas with similar islands are observed, but only in regions starting at a descending step edge. Apart from this island region, the rest of the surface appears to be featureless. The width of these regions was approximately equal, each roughly 350 Å. Finally, the sample shown in Figure 55c, was quenched rapidly after the Ga shutter was closed. These last data were obtained in a different MBE apparatus, with a base pressure of 1×10^{-10} Torr, but using otherwise similar growth conditions. In this last case, all terraces appear to be featureless, except for a few small steps between the macrosteps. The height of these steps was approximately half a lattice constant *c*/2. The width of the island regions originating from descending step edges depends on annealing time (or quenching rate) under NH_3, while the remainder of the surface is unchanged.

It was shown in chapter 5 that the gallided surface is terminated by a layer of strongly adsorbed Ga, while the nitrided surface incorporates a fraction of a layer of strongly adsorbed Ga in form of the observed islands. When the gallided surface is exposed to a large burst of NH_3, a small amount of Ga is detected by Desorption Mass Spectroscopy (DMS). This suggests that the strongly bound Ga layer is breaking up during nitridation, instead of just adsorbing NH_3 to form islands. Note that this desorbed Ga accounts only for a small fraction of the broken up layer, leading to the conclusion that most of the Ga finds new attachment sites, perhaps step edges.

Further, gallided films were annealed in NH_3 while monitoring the RHEED intensity recovery, as shown in chapter 5. In this experiment, the sample was quenched in an early stage of this recovery. The result is shown in Figure 56, which is similar to Figure 55b, showing partial nitridation originating from descending step edges. These results clearly

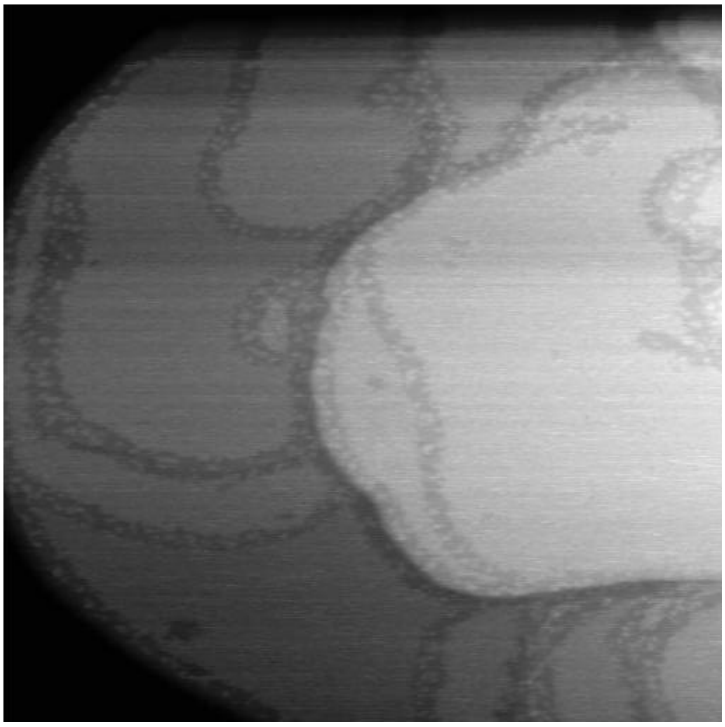

Figure 56: 1 mm AFM scan of a partially annealed surface, quenched after the initial stages of recovery as judged from RHEED.

showed that the change in RHEED intensity during annealing in NH_3 originates from the development of the island zones on the sample surface.

These island zones on partially annealed surfaces could sometimes also be observed on flat posts, often giving rise to flower like structures, as shown in Figure 57. Assuming that the nitridation process can only originate from decending step edges, this suggests that this particular post had a large island on top of the post. Smaller circular nitrided regions suggest a surface defect as its origin, since completely gallided posts usually did not show any islands or dislocations.

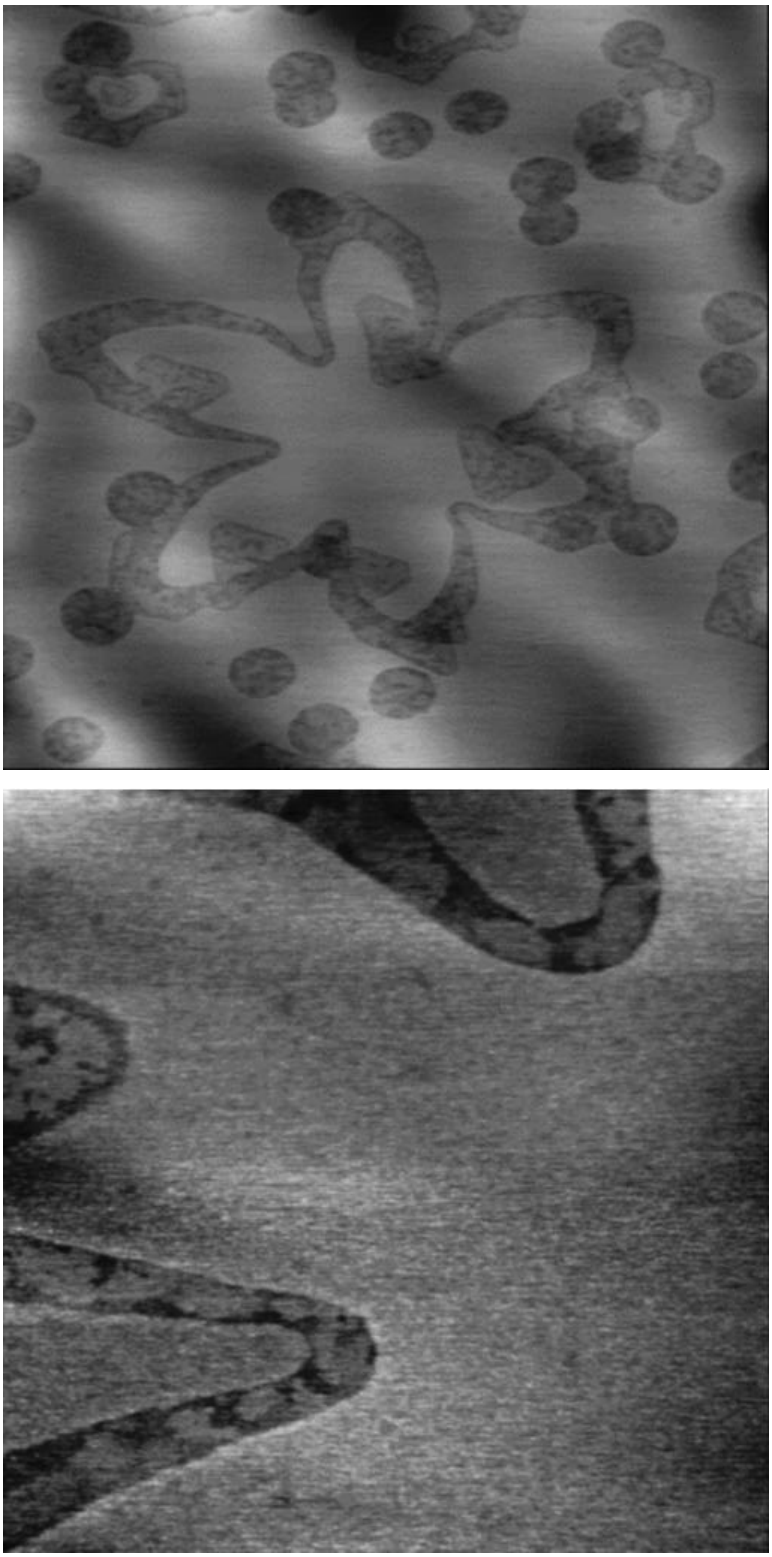

Figure 57: Partially nitrided flat post. Scan sizes are 5 and 1 mm, respectively.

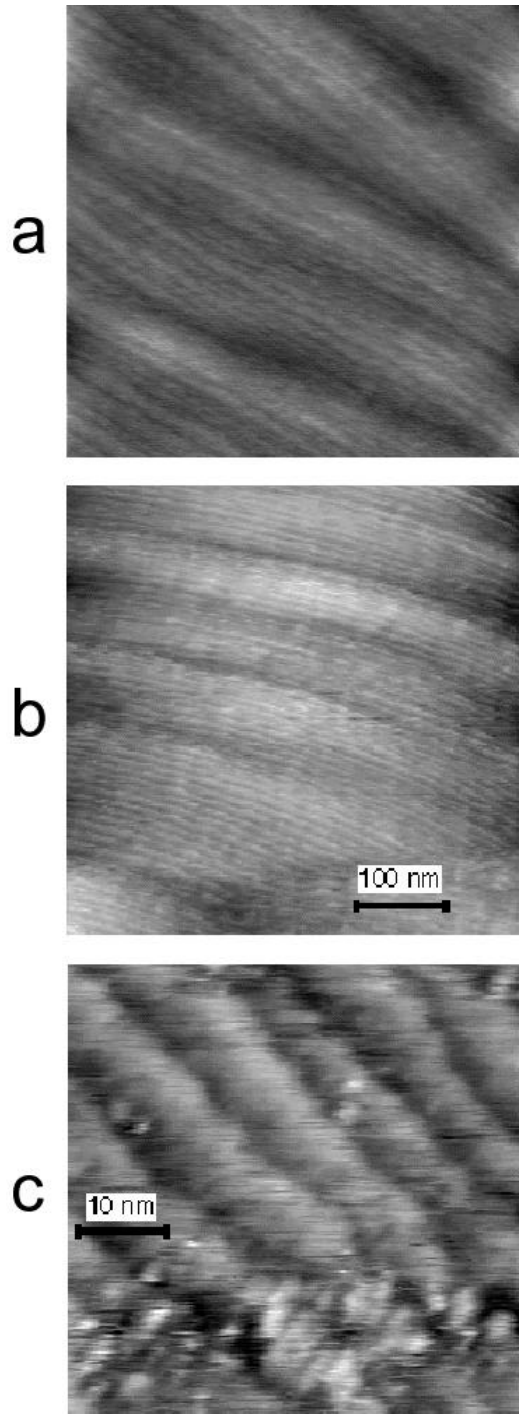

Figure 58: Monatomic Steps on a GaN-B surface. a) 500´500 nm STM scan; b) 50´50 nm STM scan.

Monatomic steps, instead of the macrosteps of Figure 55, could sometimes be observed as shown in Figure 58. Figure 58a shows a 500×500 nm STM scan, and *c*/2 steps on the order of 200 Å. These were only barely resolvable in AFM. A zoom is shown in Figure 58b. This film was annealed in ammonia and then cooled to room temperature before STM. Steps are observed, measured to be half a lattice constant (*c*/2) in height, and separated by approximately 100 Å. At the higher magnification in Figure 58b one can see line defects perpendicular to the step edges.

Last the annealing behavior of the bulk GaN surface was studied. This was done with the hope of finding a procedure to smoothen rough surfaces. Figure 59 shows a film that was roughened by first depositing GaN at a low temperature. Then the same film was annealed under NH_3 for 5 min at different temperatures. Between each annealing step the surface was exposed to air for AFM. No changes are seen up to about 800^{o}C. Above 800^{o}C groves are starting to appear, and above 900^{o}C pitting occurs. Therefore it was not possible to smoothen the film by annealing in NH_3, but it should be noted that exposure to air between annealing steps could have altered the surface.

Samples annealed in vacuum were always found to become rough, samples of which are shown in Figure 60. Surfaces looked very different between samples, and no particular preferential facets could be resolved or identified. Therefore annealing in vacuum is not a suitable method for smoothening films.

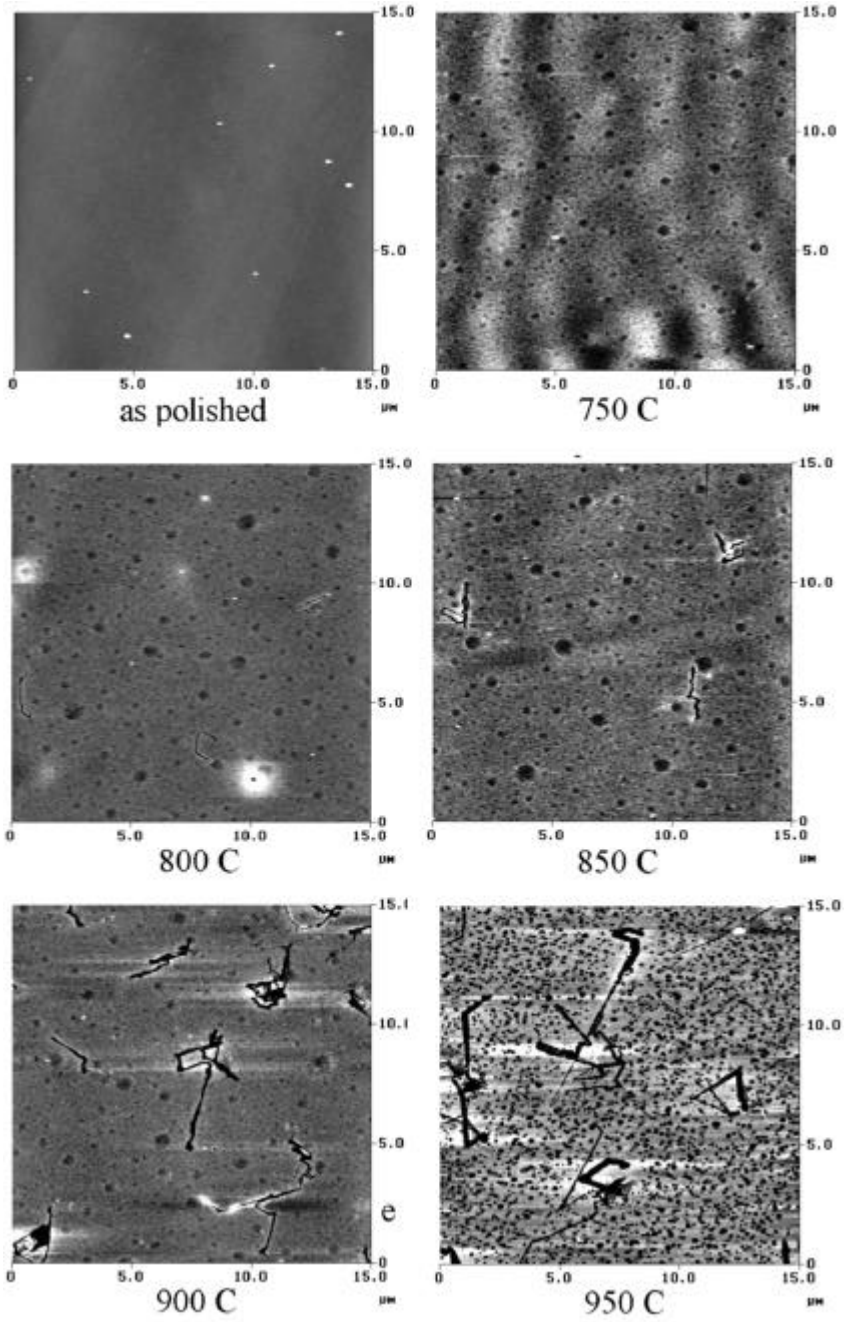

Figure 59: 15 mm scans after annealing in NH_3 at $1.0 \acute{} 10^{-5}$ torr for 5 minutes. a) surface as polished; b) 750°C; c) 800°C; d) 850°C; e) 900°C; groves occur above 800°C, pits above 900°C.

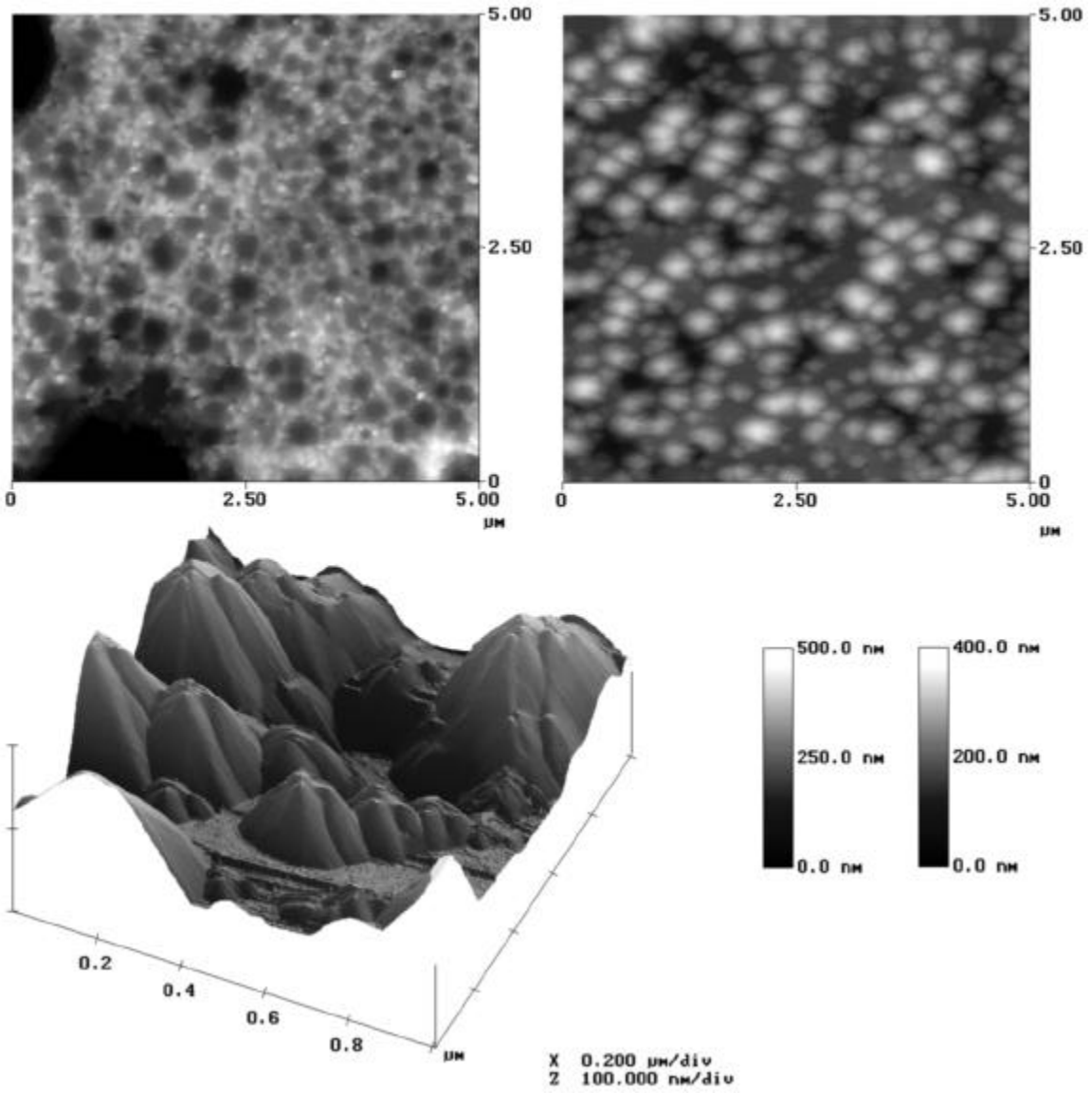

Figure 60: Samples annealed in vacuum around 900°C.

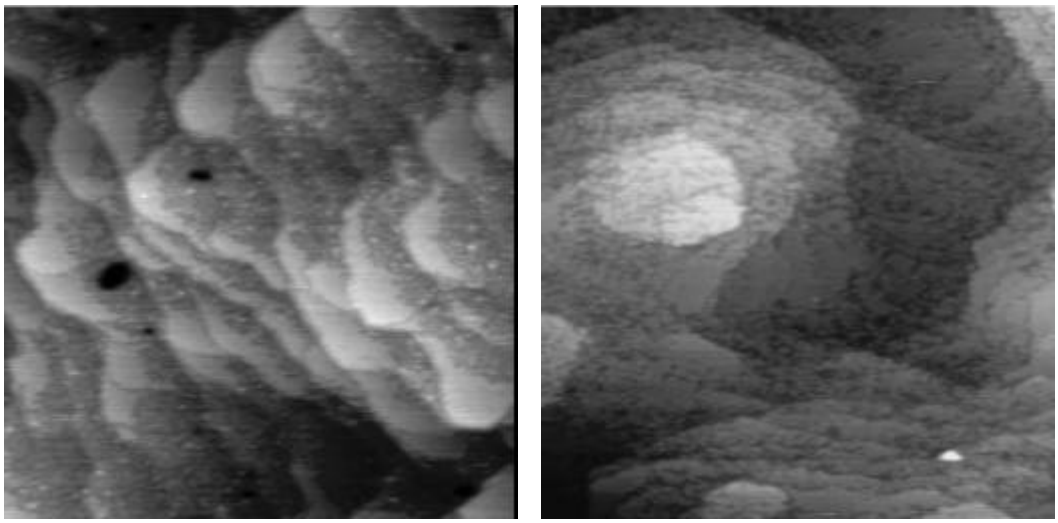

Figure 61: 1 mm scans of the initial stages of sample decomposition. a) gallided surface after 1 min in vacuum at about 750°C; b) decomposed surface after exposure to Ga;

This result lead to a preliminary study of the early stages of decomposition. Figure 61a shows such film after 1 min at about 750°C in vacuum. Surface roughening can be seen to occur preferentially at ascending step edges. This roughening looks similar to films annealed in NH_3, as in Figure 55b. In fact, this structure is very different. Figure 61b shows a slighly decomposed surface after exposure to Ga only, and the surface did not return to the featureless surface as expected for an initially nitrided surface. Further, the uptake behavior of such films correspond to a gallided surface, as shown in chapters 4 and 5.

6.4 Summary

The evolution of the GaN-B surface morphology was investigated as a function of growth parameters by ex situ Atomic Force Microscopy (AFM) in air. Under excess Ga, very smooth surface were obtained, consisting of atomically flat posts several microns in diameter. Under excess NH_3, macrosteps and hexagonal hillocks are observed. The hillock density can be reduced by decreasing the substrate temperature. The macrosteps have facets at high temperatures, and become more rounded at low temperatures. The surface structure on the macrostep terraces is nearly featureless after Ga only exposure, and has an irregular island structure after NH_3 only exposure. During NH_3 exposure, a featureless surface converts to the island structure starting from decending step edges by breaking up strongly bound (chemisorbed) Ga. Monoatomic ($c/2$) steps have also been observed on this surface, but their origin is unclear. Attempting to smoothen the surface by annealing in NH_3 results in the formation of pits and groves. Annealing under vacuum results in surface roughening as well, preferentially starting from ascending step edges.

7. DECOMPOSITION

7.1 Experimental

The decomposition experiments described in this chapter were both performed on bulk GaN-B crystals as well as GaN-B grown on 1 inch sapphire substrates. Approximately 1μm of GaN-B on sapphire was prepared using a GaN initiation layer (see chapter 4.2). Bulk GaN-B films were prepared by chemo-mechanical polishing them to an atomically smooth finish[49]. The films grown on 1 inch sapphire were mounted mechanically into a moly block for such sized substrates, while the bulk GaN crystals were mounted into a moly block that accepts samples of varying size via interleaving sliders with notches (see chapter 2.1).

Decomposition experiments were carried out by heating the GaN samples in vacuum. The decomposition rate of the samples was measured by Desorption Mass Spectroscopy (DMS). The core of the DMS is a quadrupole-masspectrometer with a cryo-shrouded ionizer in order to reduce the background signal due to NH_3, which effects the signal to noise ratio of the Ga signal measured. A collimator in front of the ionizer limits the field of view to about 6 mm in diameter on the sample surface. This collimator size was chosen in order to limit the sample area to the smallest possible amount that still permits a large enough signal to be measured.

The monitoring area was limited for several reasons. For the GaN on sapphire samples, which were 25 mm in diameter, limiting the area reduced any temperature gradient across the sample surface as much as possible. The remaining gradient was estimated to be on the order of only $1^{o}C$ using RHEED (see chapter 9.2), permitting temperature dependent

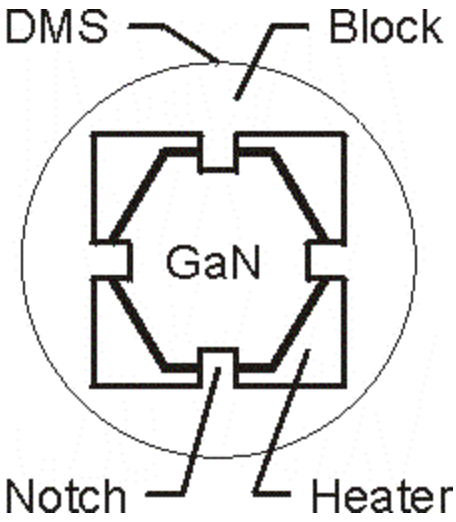

Figure 62: Diagram for mounting bulk GaN crystals. Note that the DMS not only sees the GaN surface, but also the hotter substrate heater as well as surrounding colder parts of the moly sample block.

measurements, like decomposition, to be carried out with high precision. More complicated issues arose for the smaller bulk GaN samples, which will be addressed after covering how the DMS was calibrated .

In order to quantify any desorbing GaN flux due to decomposition from the GaN surface, the DMS current was first calibrated to a known Ga flux. This was achieved by heating the GaN sample to a high enough temperature, above the condensation temperature (see chapter 3.5.1) for a known Ga flux, but low enough so that GaN decomposition can be neglected. A typical temperature was 750^{o}C and a known Ga flux of 0.6 ML/s, for which condensation occurs below 735^{o}C only. Therefore, once steady state is reached after opening the Ga shutter, the desorbing Ga flux equals the known incident Ga flux. The incident Ga flux was calibrated using GaAs RHEED intensity oscillations. This flux was checked before and after the series of experiments to be presented, and had changed by less than 1 percent. Once the DMS current was calibrated, GaN decomposition could be measured in terms of absolute fluxes by monitoring the Ga atoms released from the GaN surface, under the assumption that no Ga condenses on the surface.

The above described calibration of the Ga flux worked well for the 1 inch GaN on sapphire samples, but a set of problems were encountered in case of the much smaller bulk GaN, typically only about 4 mm across and irregulary shaped. An illustration of the mounting arrangement is shown in Figure 62. We notice that the irregulary shaped bulk GaN crystal is confined roughly in a square hole of the size of the largest dimensions of the crystal. The area around the square is the molybdenum sample block, which is significantly lower in temperature than the sample itself. The heater is located behind the sample block, and only covered by the sample block as well as the sample, keeping some heater area around the sample exposed. The DMS, which monitors an area of about 6 mm in diameter, therefore not only measured Ga desorbing from the sample surface, but also Ga from the heater as well as the molybdenum block. This caused some problems with the DMS calibration described, which were not encountered for GaN on sapphire.

As covered before, the DMS was calibrated by exposing the GaN sample to a known Ga flux at a temperature high enough to desorb all incident Ga. But in case of the small bulk GaN crystals we only want to measure the desorbing Ga flux from the sample surface. It is clear that other desorbing surfaces lead to a calibration error. The exposed parts of the hotter sample heater is one source of error, while the colder molybdenum block around the sample is another source. It was found that the colder molybdenum block could be completely neglected when keeping the sample just above condensation temperature. The molybdenum block was found to be at least 100^{o} colder than the sample, therefore most Ga just accumulates on the holder surface without significantly contributing to the calibration signal. Of bigger concern was the exposed heater area, from which all incident Ga is returned. The only way to minimize this error is to mount the sample in such a way as to cover most of the square hole, or by using samples which resemble a square as close as possible. Another source of error is the temperature gradient across the sample, especially colder surface areas around the clips. To minimize such error the sample temperature was chosen hot enough to keep most of the sample above the Ga

condensation temperature, but low enough in order to avoid significant signal contributions from the colder molybdenum block.

Another set of problems were encountered during the actual decomposition experiments, from residue Ga that had accumulated during the calibration on the colder Mo block and around the clips. Again, the signal contribution from colder areas around the clips was minimized by choosing a temperature somewhat above that for Ga condensation. For most experiments, the flux was calibrated after the decomposition experiment in order to completely avoid this accumulation problem. Last, in order to avoid any signal contributions from GaN encrusted on the GaN holder, the holder was sandblasted and cleaned before the experiment. This was followed by a high temperature outgas at 1300^{o}C for 1 h in vacuum before sample mounting. The holder was monitored by DMS during the heating to ensure complete outgasing, and this high temperature outgasing hat the additional benefit of removing Ga deposited on the front molybdenum aperture of the DMS located 2½ inches from the sample.

7.2 Results

It was shown elsewhere (chapter 3.4.1, chapter 4) that two main surface terminations can be maintained on GaN-B: A nitrided and a gallided surface. It was also shown that the nitrided surface anneals in vacuum to give the gallided surface (chapter 4, chapter 9.3). The nitrided surface can be distinguished from the gallided surface by measuring the surface reactivity to an incoming Ga flux.

Figure 63 shows such an experiment. Three different GaN-B surfaces were prepared just prior. One surface was exposed for a long time to Ga at a temperature high enough to avoid condensation, resulting in a gallided film. Another surface was exposed to to NH_3 for a long time, resulting in a nitrided film. The last film was prepared by taking a nitrided film and annealing it for a long time in vaccum. All three films were then exposed to a known Ga flux above Ga condensation, in the absence of NH_3. The desorbing Ga flux from the surface was measured by DMS, and most attention was paid to the transient behavior of this signal.

Figure 63 shows that for the gallided surface, as well as the annealed nitrided surface, the DMS signal quickly rises to a steady state value. This steady state value is equal to the incoming Ga flux since all incoming Ga is now desorbed, i.e. there is no Ga condensation on the surface. In contrast, the nitrided surface shows a two step signal rise with a plateau between rises. It was shown elsewhere that this plateau is due a physisorption site associated with nitrided parts of the surface, with a very small residence time (chapter 5). After capturing incoming Ga atoms for a very short time, these atoms are again ejected, part of which chemisorb on the surface, while the remainder desorbs.

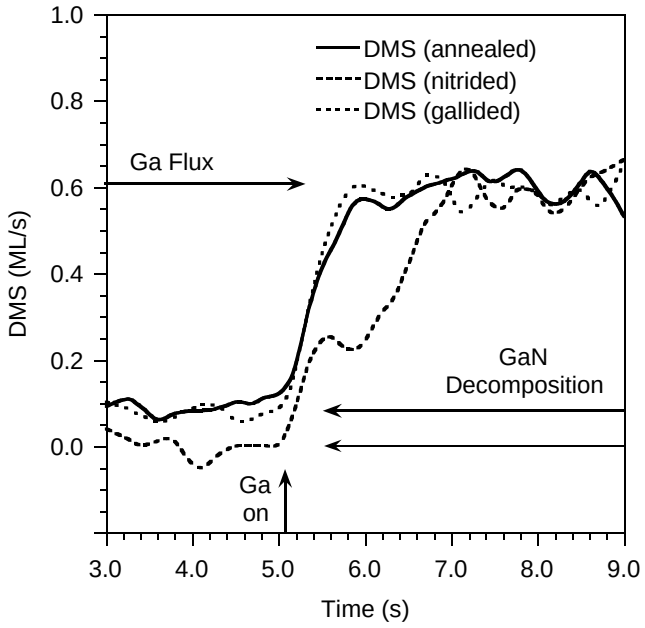

Figure 63: Uptake curve from a gallided, nitrided, and vacuum annealed nitrided surface. T = 813°C, Ga = 0.61 ML/s.

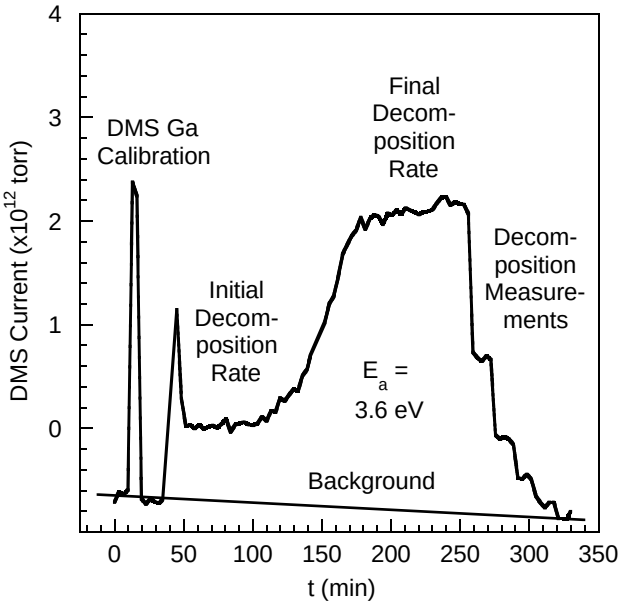

Figure 64: Decomposition Experiment.

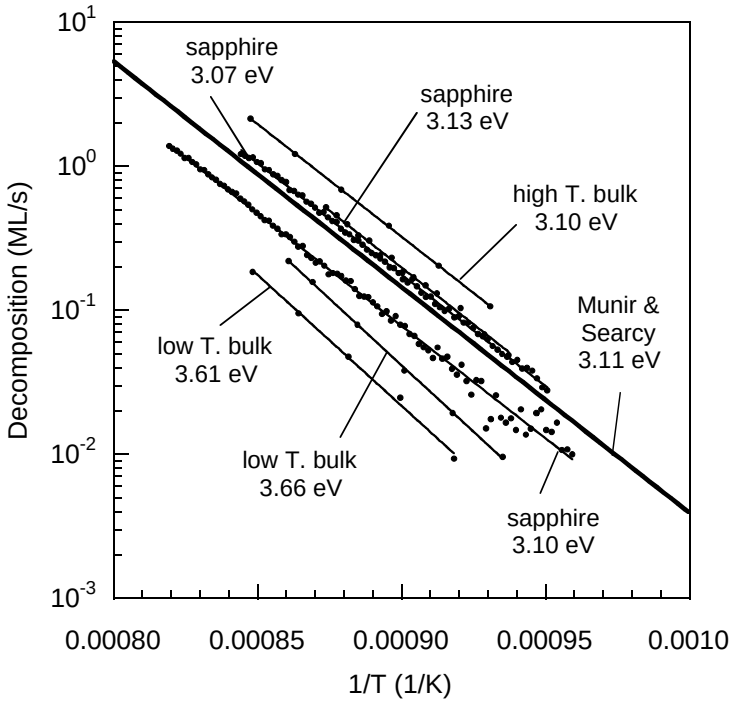

Figure 65: Activation energies depending on sample history.

Since the nitrided surface anneals to the gallided surface during annealing in vacuum, and no additional sites are detected on the gallided surface, it is assumed that GaN decomposition is measured from gallided surfaces only, which does not have any additional sites except for the weakly adsorbing Ga site.

A typical decomposition experiment is shown in Figure 64, where the desorbing Ga flux is plotted as a function of time. Initially the film is kept at temperatures below which significant decomposition occurs, but above the temperature for Ga condensation. A known incident Ga flux is then permitted to hit the GaN surface. Since in steady state the known incoming Ga flux equals the desorbing Ga flux, we can calibrate our DMS. The Ga flux is then removed and the film heated to a temperature at which measurable GaN decomposition occurs. After an initial spike in the signal, first a fairly steady GaN

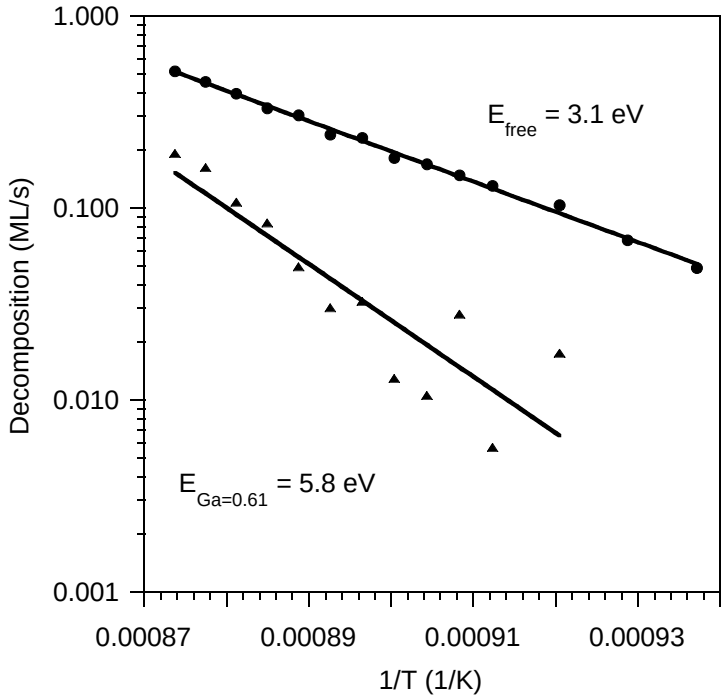

Figure 66: Decomposition of a bulk sample in vacuum and under a Ga flux.. This sample had previously been kept at 900^{o}C for several minutes to attain steady state decomposition.

decomposition signal is observed, which then rises progressively faster. At some point there is a definite break in the rise of the signal, and steady state is reached. After reaching this steady state the sample temperature was reduced in small amounts with enough time in between changes to permit the signal to stabilize. These steady state values as a function of temperature can then be plotted to give the activation energies.

Several of these measurements are shown in Figure 65, for both GaN on sapphire and GaN on bulk. Bulk samples that were initially atomically flat and carefully heated to about 800^{o}C, and then permitted to attain stable decomposition as in Figure 64. Subsequent decomposition measurements as a function of temperature resulted in an activation energy of about 3.6 eV. Measurements were also taken from a sample which was not permitted to reach steady state, which decomposed at a noticeably lower rate.

Measuring the activation energy resulted in 3.7 eV, comparable to the steady state sample, which indicates that only the prefactor of the energy equation changed. Last, measurements were taken from samples that were kept above 900^{o}C for a long time. Subsequent decomposition measurements resulted in the highest measured decomposition rate, and a different activation energy of 3.1 eV. Next, the decomposition of the bulk material was compared to GaN on sapphire. Independent of the history of those GaN-B on sapphire films the activation energy was always 3.1 eV, as for the high temperature bulk sample.

A few GaN-A polar films were decomposed as well. GaN-A film grown on sapphire gave an activation energy of 3.6 eV, and no non steady state decomposition behavior as on GaN-B was observed. Reliable values from bulk GaN-A could not be obtained due to the small size of the samples available.

Last, measurements were taken to see how an incident Ga flux effects GaN-B decomposition, on a bulk film that was heated previously to above 900^{o}C. The result is shown in Figure 66. Again, the activation energy for free decomposition is 3.1 eV. In the presence of Ga the decomposition is significantly reduced, resulting in a higher activation energy.

8. CONCLUSION

In this thesis a quantitative model was developed to describe MBE growth of GaN on the GaN-B polarity. Two distinct growth regimes were identified: Growth under excess NH_3 (Ga-limited growth) and growth under excess Ga (NH_3-limited growth). Under conditions of excess NH_3, oscillations in the specular RHEED intensity were observed, suggesting growth by island nucleation. Under conditions of excess Ga, RHEED intensity oscillations were not observed, indicating a step-flow growth mode. Further, it was shown that two surface terminations could be prepared on GaN-B, after Ga and after NH_3 only exposure. From DMS measurements, these surface terminations were found to have very different surface reactivities. Based on those results, a quantitative model for the GaN-B surface was developed which explains the transitional Ga uptake, steady state growth, as well as the abrupt transition between growth modes. This transition, between island nucleation and step flow, is determined by the steady state coverage of chemisorbed Ga. Ga is chemisorbed via two types of physisorption sites, one of which is an extrinsic precursor state, while the other corresponds to an intrinsic precursor state with a very short residence time. The gallided surface is obtained by filling all chemisorption sites, which is then completely unreactive to additional Ga, even in the presence of NH_3, permitting growth only at step edges. This step flow growth mode is obtained at high Ga to NH_3 flux ratios, and the window widens at lower substrate temperatures permitting lower Ga fluxes. In support of this model, bulk samples quenched during excess Ga growth showed no islands on the terraces between steps, but a few monatomic steps appear to propagate from the base of an ascending step edge to the next descending step edge. These results suggest that the excess Ga regime is better suited for lateral epitaxial overgrowth (LEO) than the excess NH_3 regime.

9. APPENDIX

9.1 Growth Rate Measurement

So far most existing growth rate data on GaN were obtained by ex situ thickness measurements, which even when a superlattice is grown require long growth times for each data point. Some in situ methods were reported, for example, using the period of RHEED intensity oscillations [21,20] and IR interference[50], but little growth rate data is published. Under GaN growth conditions of high Ga:NH_3 flux ratios as well as high substrate temperatures RHEED intensity oscillations were not observed so that other in situ growth rate measurements are required.

We consider deposition onto a surface at a temperature above which Ga condenses. A fraction of the incident Ga incorporates as GaN, and the remainder supplies a steady-state Ga surface coverage which desorbs at the same rate at which it is supplied. Without any NH_3 flux all the incident Ga desorbs. We assume that an NH_3 flux does not affect the angular distribution of the desorbed Ga flux. In order to obtain the incorporating flux we measure the difference between these two Ga desorption fluxes.

An examples of the Ga desorption signal with and without NH_3 is shown in Figure 12a taken without collimation to improve the signal to noise ratio. Here we measure the change in the desorbed Ga signal when the Ga flux is interrupted since it is somewhat easier to be certain that steady state signals are measured. With NH_3 impinging on the surface GaN is grown until steady state conditions are obtained. The Ga flux is then interrupted and the DMS signal quickly decreases to a constant background level. We take the drop in the measured mass spectrometer current, ΔI_{growth}, to be proportional to the Ga flux leaving the sample surface. Similarly, without NH_3, there is a drop in the Ga

reference signal, ΔI_{ref}, that is proportional to the incident Ga flux. The growth rate is then computed from

$$G = \frac{\Delta I_{\text{ref}} - \Delta I_{\text{growth}}}{\Delta I_{\text{ref}}} \cdot F_{\text{Ga}} \qquad (9\text{-}1)$$

using F_{Ga} as measured by GaAs RHEED intensity oscillations and implicitly taking into account the proportionality factor between the measured mass spectrometer current and the desorption flux. Note that at substrate temperatures greater than about 800^{o}C the decomposition of GaN, not included in Eq. A1, must also be considered.

9.2 Temperature Measurement

The implications of the observations described in the body of this thesis are that the Ga condensation temperature on GaN is a function of the incident Ga flux and that this condensation temperature is determined by the detailed balance of the incident Ga flux and the flux evaporating from liquid Ga. Therefore to calibrate the substrate thermocouple, we only need to know this incident flux, which can be measured using GaAs RHEED intensity oscillations. Using either DMS (Figure 25) or RHEED (Figure 11) observations, at a given incident Ga flux we find the lowest temperature at which the incident flux equals the desorbing flux, i.e., the onset of Ga condensation. We then determine the temperature offset of the thermocouple reading by setting the known incident flux equal to the flux corresponding to the equilibrium vapor as follows:

$$F_{\mathrm{Ga}} = \frac{p_{\mathrm{eq}}}{\sqrt{2pmkT_{\mathrm{c}}}} \qquad (9\text{-}2)$$

where peq is usually tabulated as[27]:

$$\log\left(p_{\mathrm{eq}}\right) = A + BT^{-1} + C\log T \qquad (9\text{-}3)$$

with p given in units of atm., A = 6.754, B = -13984, and C = -0.3413. Here F_{Ga} is the incident Ga flux and $T = T_{\mathrm{c}}$.

Alternatively, both the incident and desorbing fluxes can be expressed more symmetrically by measuring the incident flux in GaN monolayers per second, $1/t_{\mathrm{i}}$, and by

fitting the flux desorbing from the surface in the right side of Eq. B1 to an exponential over a range between 500 - 1000^{o}C (also in GaN ML/s). Then Eq. B1 becomes:

$$\frac{1}{t_{\mathrm{i}}} = \frac{1}{t_{\mathrm{o}}} \exp\left(-\Delta H / k_{\mathrm{B}} T_{\mathrm{c}}\right) \qquad (9\text{-}4)$$

where ΔH is the enthalpy of vaporization of Ga and $1/\tau_{o}$ is an attempt frequency. Hence at a given incoming Ga flux, the lowest possible surface temperature to avoid Ga condensation is given by:

$$T_{\mathrm{c}} = \frac{\Delta H}{k_{\mathrm{B}} \ln\left(t_{\mathrm{i}} / t_{\mathrm{o}}\right)} \qquad (9\text{-}5)$$

here ΔH is 2.71 eV, $\tau_{o} = 4.43\times10^{-14}$ s/ML, and t_{i} is the time it would take to form one ML of GaN on a {0001} plane assuming complete Ga incorporation. Thus once the Ga source is calibrated, the surface temperature can be determined by finding the temperature at which Ga condenses, using either RHEED or DMS.

9.3 Annealing Correction

A significant experimental problem is encountered for uptake data obtained from a nitrided surface in vacuum. While the gallided surface is stable in vacuum, it was found that the nitrided surface converts to a gallided surface, with a time constant on the order of a few minutes at temperature above 800^{o}C (see chapter 4.3). When a previously nitrided surface is completely annealed, uptake curves are obtained that are identical to the gallided surface Figure 39a. Therefore, when taking uptake curves similar to Figure 39b in the absence of ammonia, partial anneal has to be accounted for between shutting off the NH_3 flux and opening the Ga shutter. This annealing behavior can also be seen in the specular RHEED intensity, shown in Figure 67, which decreases approximately linear in time. In order to account for partially annealed surfaces, the decrease in RHEED intensity is used to approximate the fractional conversion from a nitrided surface to a gallided surface. As
indicated in Figure 68b, it will be assumed that there is a linear relationship between the decrease in RHEED intensity and the conversion process. Therefore, with reference to Figure 68b, the fraction of conversion can be written as:

$$c = \frac{a}{a+b} \qquad (8\text{-}1)$$

The initial fraction of gallided surface in steady state can therefore be written as

$$q_{s,o} = q'_{s,o} - c\left(1 - q_{s,o}\right) \qquad (8\text{-}2)$$

Solving for $q_{s,o}$:

$$q_{s,o} = \frac{q'_{s,o} - c}{1 - c} \qquad (8\text{-}3)$$

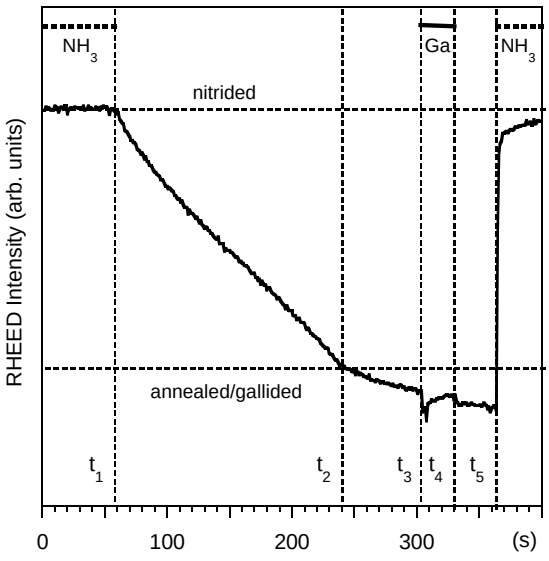

Figure 67: RHEED behavior during annealing in vacuum from a nitrided to a gallided surface, at T=823°C. This figure is repeated here, and explained in detail in chapter 4.3.

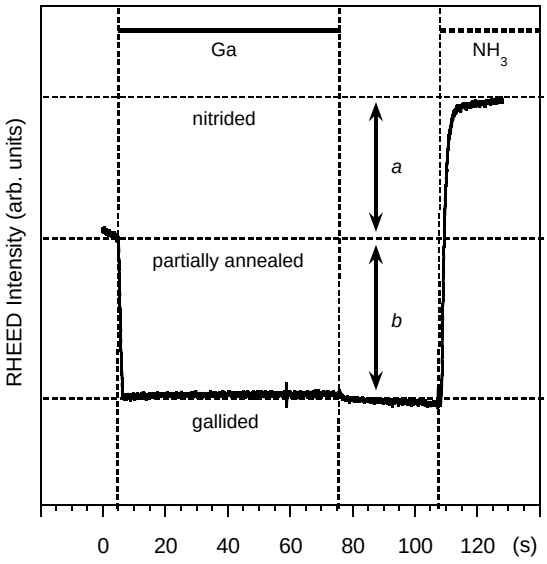

Figure 68: Annealing correction using RHEED

9.4 MATLAB Code for Growth Model

This section contains the MATLAB code used to simulate the growth model:

```
% Parameters

F_N_para = 0.35;     % flux - BEP relationship
step_edge_density = 0.1;     % step edge nitridation
efficiency
order = 1/2;     % order of excess N growth
%theta_so_para = .24
%F_l_para = 40
%F_d_para = .303
%T_para = 775

% nitrogen loop parameters

F_N_i_start = 0;
F_N_i_end = 10;
answer = 0;
limit = 20;
divide = 2;

% temperature loop parameters

T_p_i_start = 700;
T_p_i_end = 820;
T_p_i_step = 1;
T_i_start = 1;
T_i_end = (T_p_i_end - T_p_i_start) / T_p_i_step + 1;
```

```
% define output

uptake = zeros(F_N_i_end+2,T_i_end+1);
growth = zeros(F_N_i_end+2,T_i_end+1);

% nitrogen loop

for F_N_i = F_N_i_start:F_N_i_end

   F_N = F_N_i / divide;

% temperature loop

for T_i = T_i_start:T_i_end
   F_N
   T_C = T_p_i_start + (T_i - 1) * T_p_i_step

   uptake(1,T_i+1) = T_C;
   uptake(F_N_i+2,1) = F_N;

   if answer < limit

% parameters

F_Ga = 0.606;   % ML/s
growth_desorb = F_Ga;

% initial conditions

%theta_so = 1;
theta_so = 1.9774 - 0.0023471 * T_C;
```

```
if theta_so < 0
   theta_so = 0;
end
theta_wo = 0;

% constants

k = 1.38062E-23;   % J/K
e = 1.60219E-19;   % J/eV
temp_K = 273.15;   % C <--> K

% convert to K

T = T_C + temp_K;   % Kelvin

% nitrogen incorporation

F_p_N = F_N_para;   % ML/(s Torr) fitted
E_N = 0;   % eV fitted
F_p_p_N = F_N * F_p_N * exp(-E_N * e / (k * T))   % ML/s

% desorption

F_p_o = 2.0511E13;   % ML/s CRC
E_o = 2.70;   % eV CRC
F_o = F_p_o * exp(-E_o * e / (k * T));   % ML/s

% surface Diffusion

F_p_l = 1.2058E7;   % ML/s fitted
E_l = 1.182521939;   % eV fitted
F_l = F_p_l * exp(-E_l * e / (k * T));   % ML/s
```

```
%F_l = F_l_para;

% returned Ga flux

F_d = F_Ga / 2;

% effective Ga flux

F_p_Ga = F_Ga - F_d;

% derivative time parameters

time_step = .001;
time_total = 100;

% define size of output arrays (time)

if time_total/time_step <= 1000
   reduce = 1;
else
   reduce = (time_total/time_step)/1000;
end

time_size = time_total / (time_step*reduce);

% define output arrays (time)

time = linspace(0,0,time_size);
desorb = linspace(0,0,time_size);
theta_s = linspace(0,0,time_size);
theta_w = linspace(0,0,time_size);
```

```
% set initial coverage

theta_s_old = theta_so;
theta_w_old = theta_wo;
theta_s_new = theta_so;
theta_w_new = theta_wo;

% compute uptake model

for x = 1:(time_size * reduce)

   % fix time

   i = fix(x/reduce + 1 - 2/reduce) + 1;
   time(i) = x * time_step;

   % Ga on/off

   if time(i) < 5
      F_p_Ga_now = 0;
      F_d_now = 0;
      F_Ga_now = 0;
   elseif time(i) < 75
      F_p_Ga_now = F_p_Ga;
      F_Ga_now = F_Ga;
      F_d_now = F_d;   % test function
      growth(F_N_i+2,T_i+1) = F_Ga - growth_desorb;   %
growth rate
      else
      F_p_Ga_now = 0;
      F_d_now = 0;
      F_Ga_now = 0;
```

```
   end

   % write output array

   desorb(i) = F_d_now * (1 - theta_s_old) + theta_w_old *
F_o;
   growth_desorb = desorb(i);
   theta_s(i) = theta_s_old;
   theta_w(i) = theta_w_old;
   %if theta_s_old < .9
      if time(i) >= 5
         if time(i) <= 75
            uptake(F_N_i+2,T_i+1) = uptake(F_N_i+2,T_i+1) +
(F_Ga - desorb(i))*time_step;
         else
            uptake(F_N_i+2,T_i+1) = uptake(F_N_i+2,T_i+1) -
desorb(i)*time_step;
         end
      end
   %end

   % compute new values

   growth_1 = theta_s_old - theta_so;
   if growth_1 < 0
      growth_1 = 0;
   end

   growth_2 = 1 - theta_s_old;
   if growth_2 < 0
      growth_2 = 0;
   end
```

```
   theta_s_new = theta_s_old + ( (1 - theta_s_old) *
F_p_Ga_now + theta_w_old * (1 - theta_s_old) * F_l -
(growth_1^order) * (growth_2^order) * F_p_p_N - growth_1 *
(1 - theta_w_old) * step_edge_density * F_p_p_N) *
time_step;
   theta_w_new = theta_w_old + ( theta_s_old * F_Ga_now -
theta_w_old * F_o - theta_w_old * (1 - theta_s_old) * F_l) *
time_step;
   theta_s_old = theta_s_new;
   theta_w_old = theta_w_new;

end

uptake(F_N_i+2,T_i+1)

% interrupt

if uptake(F_N_i+2,T_i+1)>=limit
   answer = limit
end

end   % interrupt loop

end   % temperature loop

answer = 0;

end   % nitrogen loop

% output results
```

```
F_d

plot(time,desorb,time,theta_s,time,theta_w)

fid = fopen('desorb.txt','w');

for x = 1:i

fprintf(fid,'%f\t%f\t%f\t%f\r',time(x),desorb(x),theta_s(x),
theta_w(x));
end

status = fclose(fid);

uptake

fid = fopen('data.txt','w');
fprintf(fid,'%f\t%f\t%f\t%f\t%f\t%f\t%f\t%f\t%f\t%f\t%f\t%f\
r', uptake);
status = fclose(fid);

growth
```

9.5 Extracting Fitting Parameters

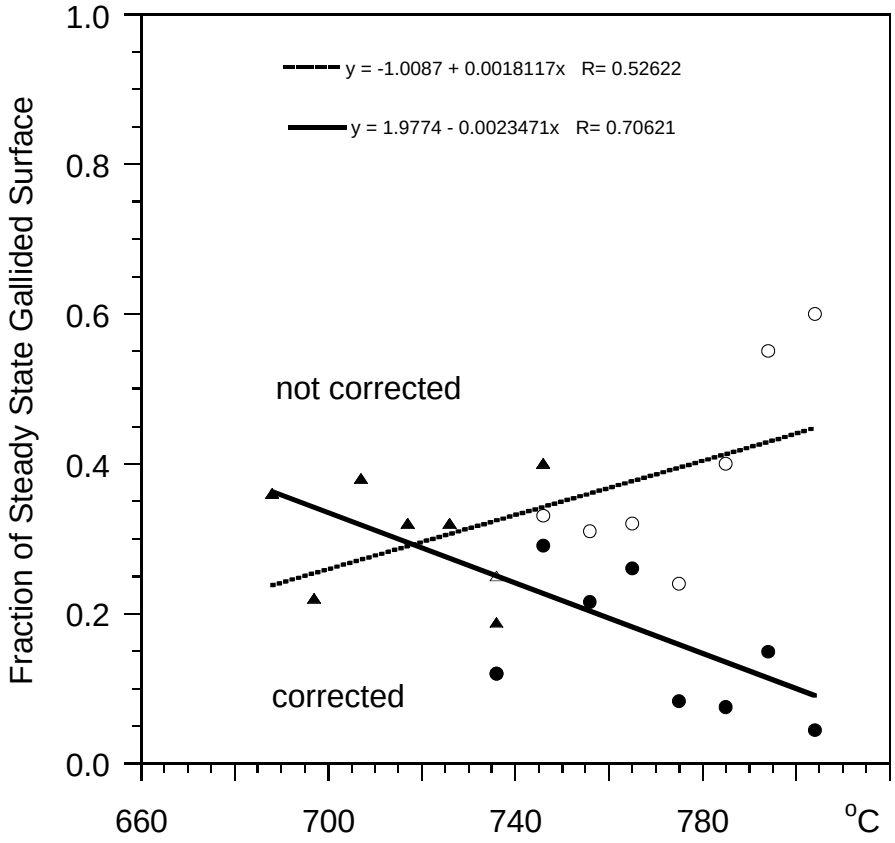

Figure 69: The 'not corrected' curve is the measured fraction of initially chemisorbed Ga, $q'_{s,o}$, just before the uptake experiment. The 'corrected' curve is the initial steady state fraction of chemisorbed Ga, $q_{s,o}$, before vacuum annealing. $q_{s,o}$ was extracted from $q'_{s,o}$ and RHEED data as covered in appendix 9.3.

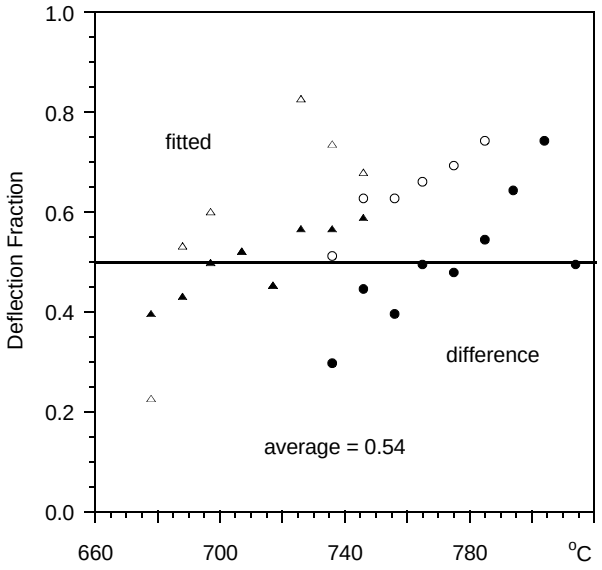

Figure 70: Extracting fraction of returned Ga from intrinsic physisorption state, a.

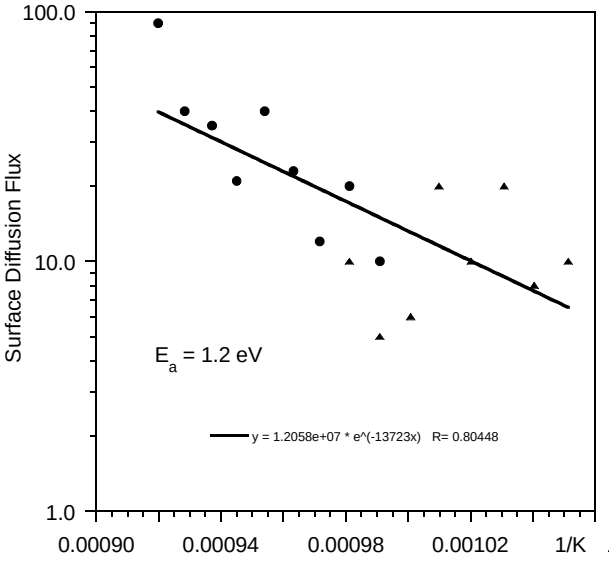

Figure 71: Extraction of surface diffusion parameter, k.

9.6 Sensitivity to Fitting Parameters

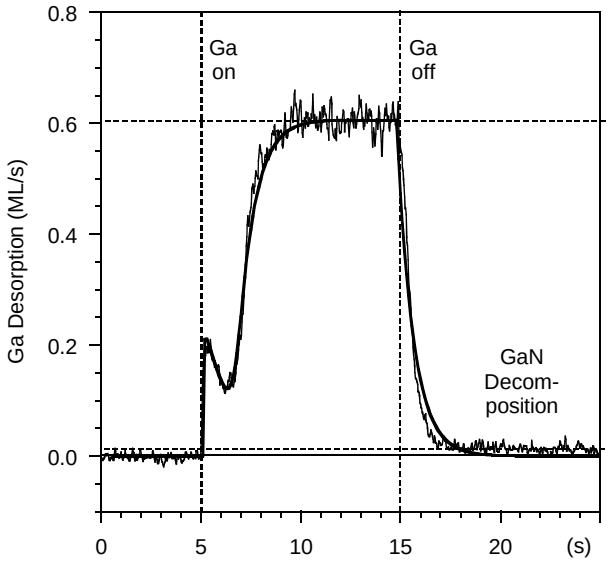

Figure 72: 'Perfect' Fit with q_{so} = 0.40,a = .42 F_{Ga}, k = 40 ML/s

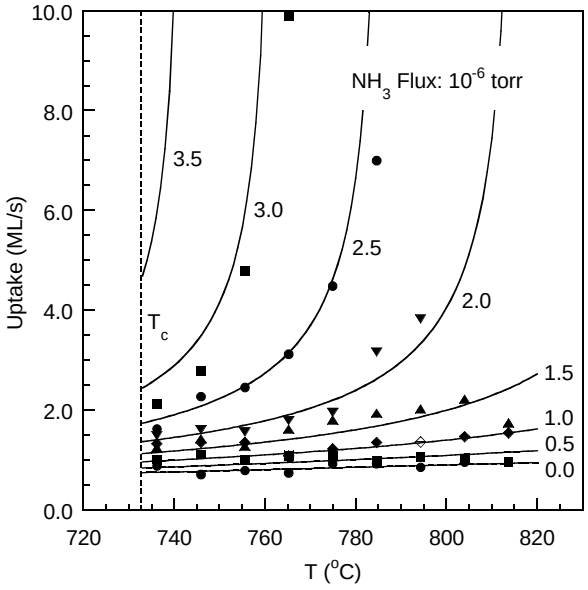

Figure 73: Uptake Fit for x=1, f=0, g=0.87

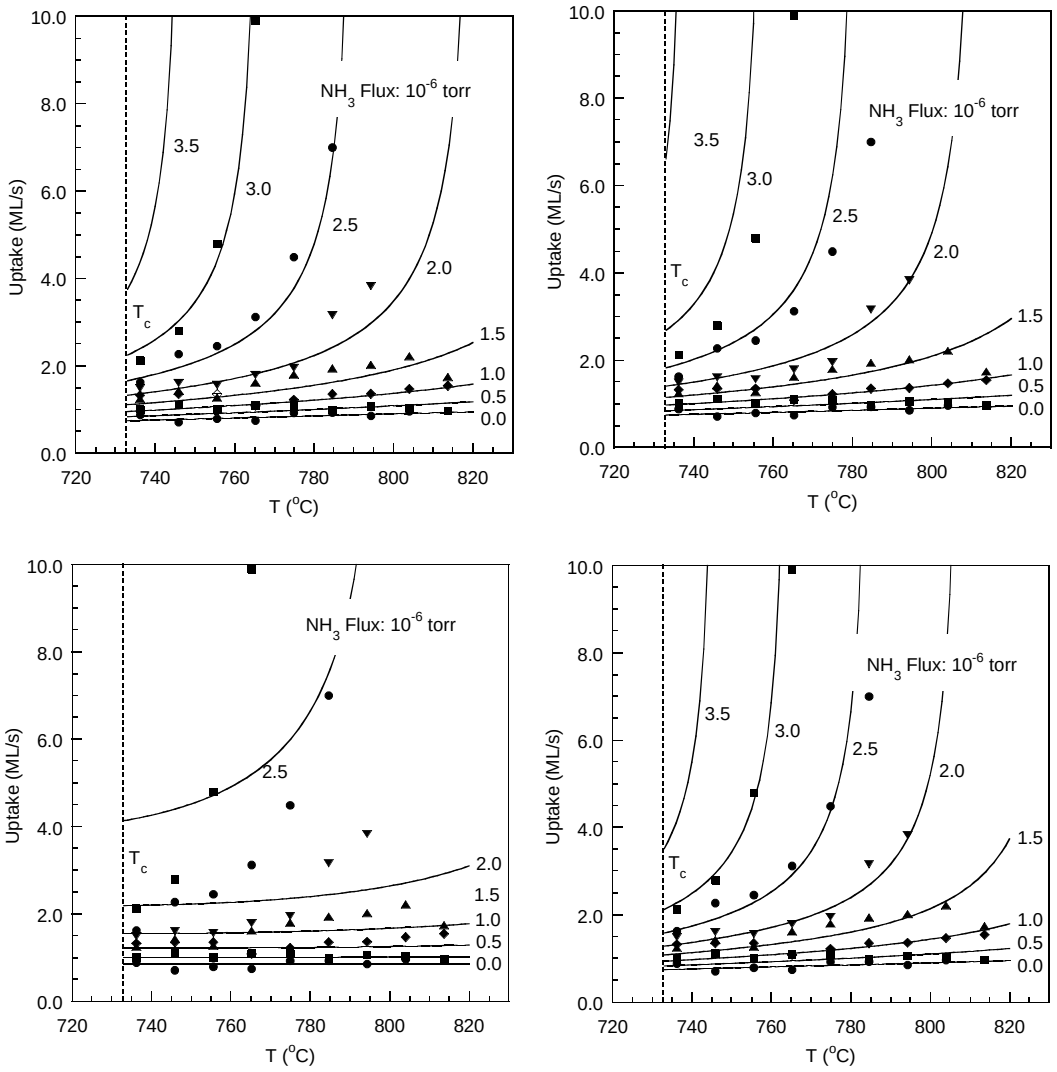

Figure 74: Sensitivity to fitting parameters with x=1, f=0, g=0.87: a) g = 0.84; b) g = 0.90; c) $q_{so} = q_{so}(T = 780^oC)$; d) k = k(T = 780°C)

9.7 Additional Uptake Simulations

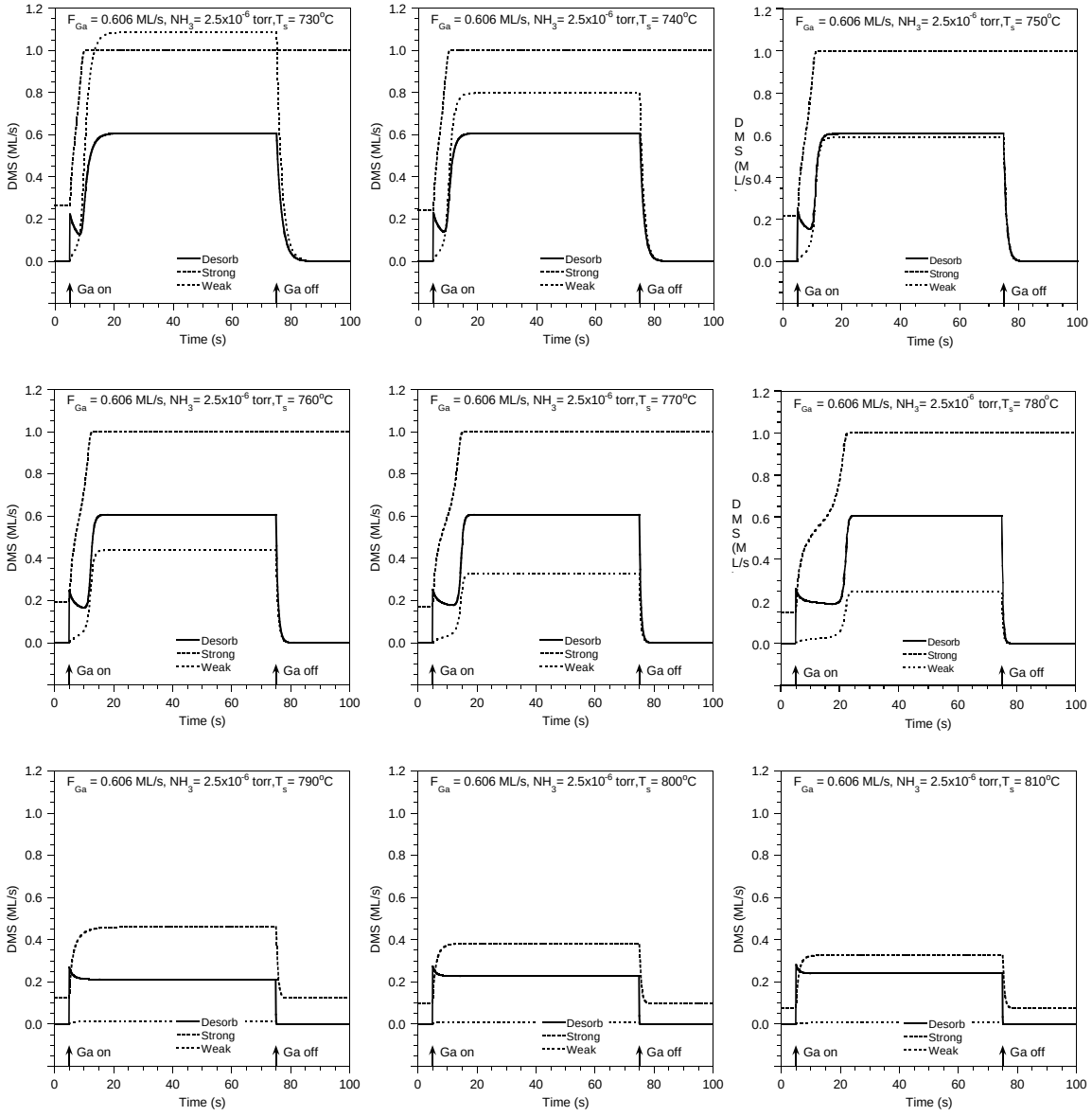

Figure 75: Uptale curves forx=1, f=0, g=0.87, F_{Ga} = 0.606 ML/s and NH_3 = 2.5´10^{-6} torr, from 730^{o}C to 810^{o}C in 10^o steps. All curves show the desorbing Ga flux, coverage of strongly bound Ga, and coverage of weakly bound Ga. Excess Ga conditions below 785^{o}C, excess NH_3 above. Note that the condensation temperature is 733^{o}C, therefore the >1 coverage of weakly adsorbed Ga at 730^{o}C means that Ga accumulates on the surface.

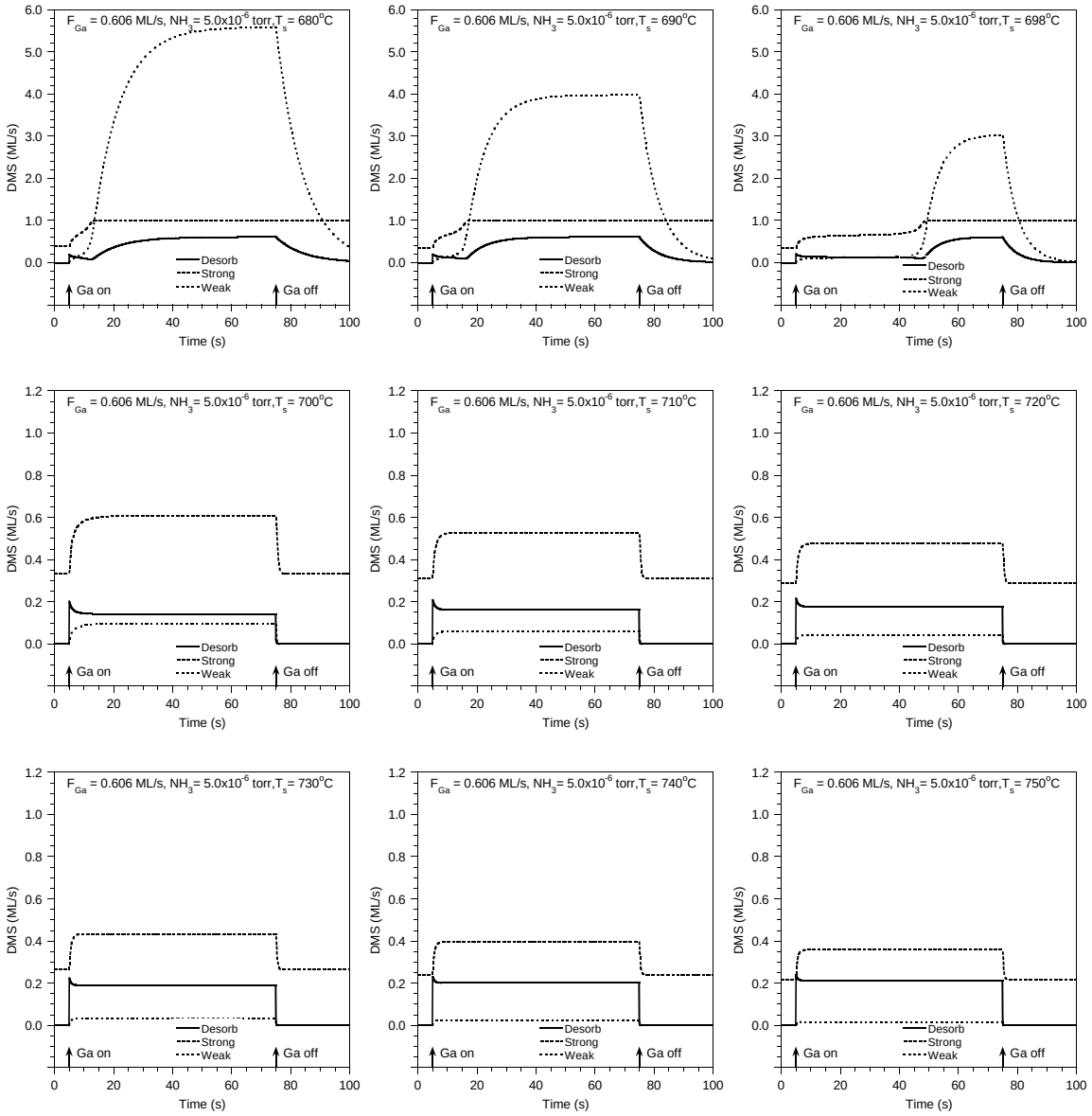

Figure 76: Uptale curves forx=1, f=0, g=0.87, F_{Ga} = 0.606 ML/s and NH_3 = 5.0´10^{-6} torr, from 680^{o}C to 750^{o}C in 10^o steps. All curves show the desorbing Ga flux, coverage of strongly bound Ga, and coverage of weakly bound Ga. Note that the condensation temperature would be at 733^{o}C with no NH_3 or at excess Ga consitions. Therefore growth is possible below 733^{o}C as long as excess NH_3 consitions are maintained. In this case contiuous growth occurs above 698^{o}C. Note the scale change for the y-axis between 698^{o}C and 700^{o}C.

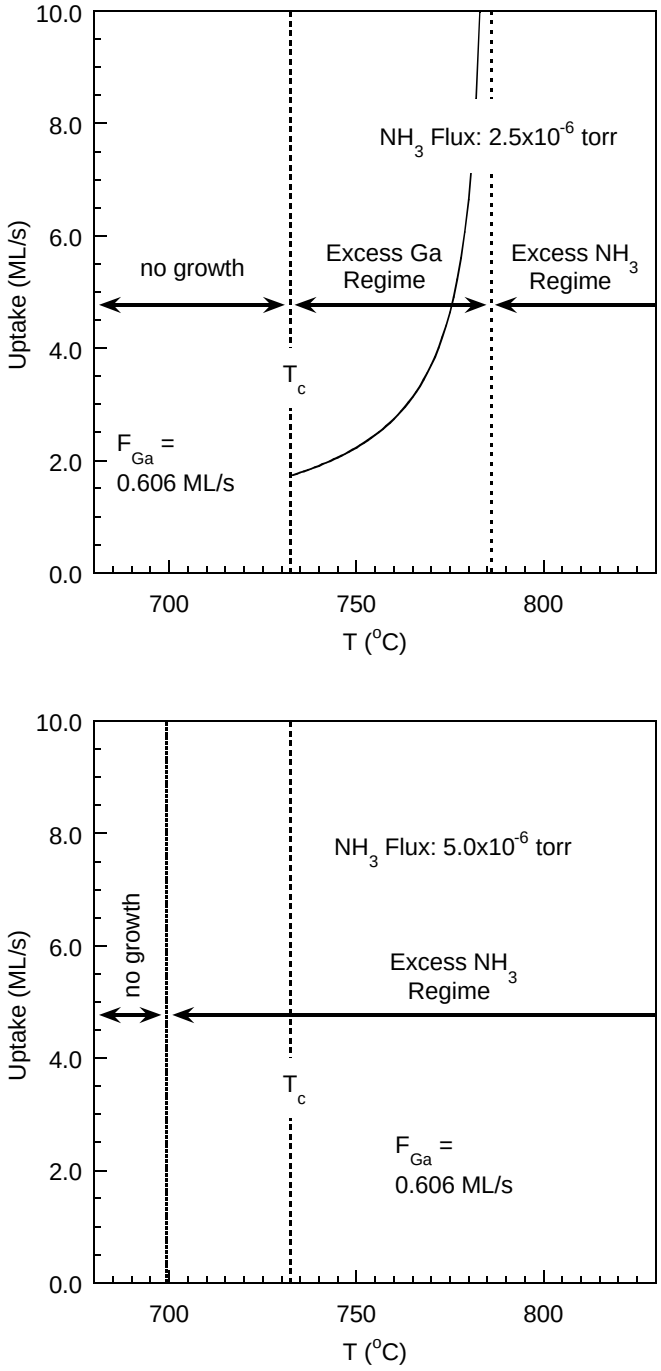

Figure 77: Growth regime deduction from previous 2 figures. Next figure shows composite for the whole range of conditions used.

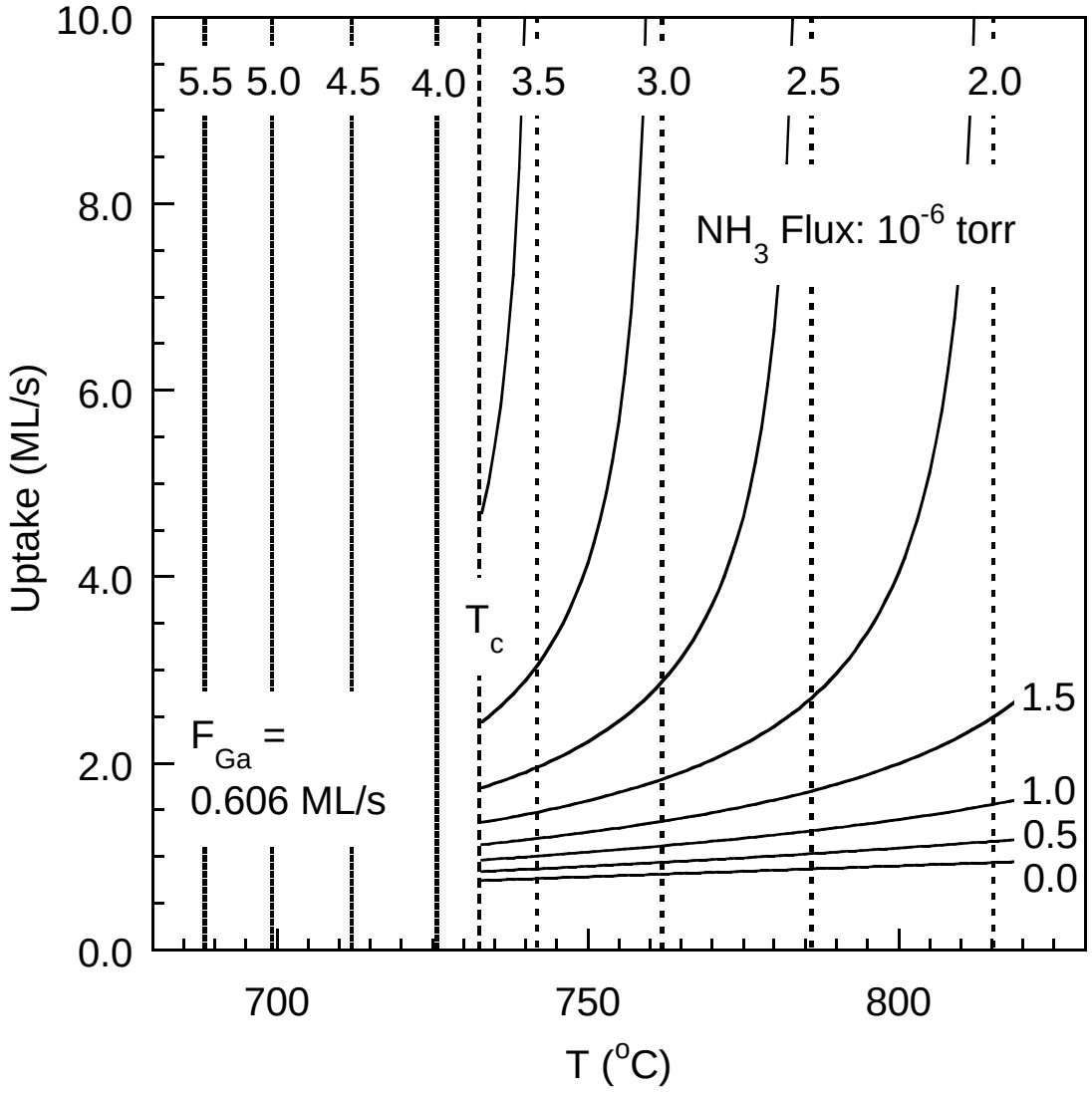

Figure 78: Growth regimes and low temperature growth limits (x=1, f=0, g=0.87). For NH_3 fluxes indicated at temperatures above T_c, growth is excess Ga between T_c and the dotted line. Beyond this line, growth is excess NH_3. Below T_c, no growth takes place due to Ga accumulation. For NH_3 fluxes indicated at temperatures below T_c, growth can only proceed above the dotted line and is always excess NH_3. Below the dotted line, no growth takes place due to Ga accumulation.

10. BIBLIOGRAPHY

[1] S. N. Mohammad, A. A. Salvador, and H. D. Morkoc, *Proceedings of the IEEE*, **83**, 1306 (1995)

[2] S. Strite, M.E. Lin, and H. Morkoc, *Thin Solid Films*, **231**, 197 (1993)

[3] R. F. Davis, *Journal of Crystal Growth*, **137**, 161 (1994)

[4] S. Strite, H. Morkoc, *J. Vac. Sci. Technol.*, **B 10**, 1237 (1992)

[5] N.-E. Lee, R. C. Powell, Y.-W. Kim, J. E. Greene , *J. Vac. Sci. Technol.*, **A 13**, 2293 (1995)

[6] C.R. Jones, T. Lei, R. Kaspi, and K.R. Evans, *Mat. Res. Symp. Proc.*, **395**, 141 (1996)

[7] N. Newman, J. Ross, M. Rubin, *Appl. Phys. Lett.*, **62**, 1242-1244 (1993)

[8] I. Grzegory, J. Jun, M. Bockowski, St. Krukowski, M. Wroblewski, B. Lucznik and S. Porowski, *J. Phys. Chem. Solids*, **56**, 639 (1995)

[9] J. Weyher, S. Muller, I. Grzegory, S. Porowski, *J. Cryst. Growth*, **182**, 17 (1997)

[10] J.Y. Tsao, T.M. Brennan, and B.E. Hammons, *Appl. Phys. Lett.*, **53**, 288 (1988)

[11] D.E. Crawford, R. Held, A.M. Johnston, A.M. Dabiran, and P.I. Cohen, *MRS Internet Journal of Nitride Semiconductor Research*, **1**, 12 (1996)

[12] W. T. Taferner, A. Bensaoula, E. Kim, and A. Bousetta, *J. Vac. Sci. Technol.* **B 14**, 2357 (1996)

[13] S. Guha, N. A. Bojarczuk, and D. W. Kisler, *Appl. Phys. Lett.*, **69**, 2879 (1996)

[14] Charles Kittel, *Introduction to Solid State Physics*, (Wiley, New York, 1986)

[15] *Reflection High-Energy Electron Diffraction and Reflection Electron Imaging of Surfaces*, edited by P. K. Larsen and P. J. Dobson, (Plenum, New York, 1988)

[16] Drawing: Amir Dabiran

[17] R. Held, D.E. Crawford, A.M. Johnston, A.M. Dabiran, and P.I. Cohen, *presented at the MRS Fall Meeting*, Boston (1996)

[18] H. Reichert, R. Averbeck, A. Graber, M. Schienle, U. Strauss, H. Thews, *Mater. Res. Soc. Symp. Proc.*, **449**, 149 (1997)

[19] Z. Yu, S. L. Buczkowski, N. C. Giles, T. H. Myers, M. R. Richards-Babb, *Appl. Phys. Lett.*, **69**, 2731 (1996)

[20] L.K. Li, Z. Yang, W.I. Wang, *Electron. Lett.*, **31**, 2127 (1995)

[21] Y. Moriyasu, H. Goto, N. Kuze, M. Matsui, *J. Cryst. Growth*, **150**, 916 (1995)

[22] A. R. Smith, R. M. Feenstra, D. W. Greve, J. Neugebauer, and J. E. Northrup, *Phys. Rev. Lett.*, **79**, 3934 (1997)

[23] For these data the Ga desorption measurements above condensation were done quickly, without waiting for the smoothest morphology before the measurements were made. Hence just above condensation the actual difference in Ga desorption with and without NH_3 should not be used to extract growth rates.

[24] Z. A. Munir and A. W. Searcy, *J. Chem. Phys.*, **42**, 4223 (1965)

[25] R. C. Powell, N.-E. Lee, Y.-W. Kim, J. E. Greene, *J. Appl. Phys.*, **73**, 189 (1993).

[26] S. S. Liu, D. A. Stevenson, *J. Electrochem. Soc.*, **125**, 1161 (1978)

[27] *CRC Handbook of Chemistry and Physics*, 71st Edition, Editor-in-Chief David R. Lide, CRC Press, Boca Raton, p. 5-70 (1990)

[28] L. T. Romano and T. H. Myers, *Appl. Phys. Lett.*, **71**, 3486 (1997)

[29] E. Hellman, *MRS Internet J. of Nitride Semicond. Res.*, **3**, 11 (1998)

[30] A.R. Smith, R.M. Feenstra, D.W. Greve, M.-S. Shin, M. Skowronski, J. Neugebauer, J.E. Northrup, *Appl. Phys. Lett.*, **72**, 2114 (1998)

[31] Ruediger Held, Sean M. Seutter, Brian E. Ishaug, Alexander Parkhomovsky, Amir M. Dabiran, Philip I. Cohen, Grzegorz Nowak, Izabella Grzegory, and Sylwester Porowski, *MRS Fall Meeting* (1997)

[32] A.R. Smith, R.M. Feenstra, D.W. Greve, J. Neugebauer, and J.E. Northrup, *Phys. Rev. Lett.*, **79**, 3934 (1997)

[33] Z. Liliental-Weber, C. Kisielowski, S. Ruvimov, Y. Chen, J. Washburn, I. Grzegory, M. Bockowski, J. Jun, and S. Porowski, *J. Elect. Mater.*, **25**, 1545 (1996)

[34] M. Seelmann-Eggebert, J.L. Weyher, H. Obloh, H. Zimmermann, A. Rar, S. Porowski, *Appl. Phys. Lett.*, **71**, 2635 (1997)

[35] Ruediger Held, Sean M. Seutter, Brian E. Ishaug, Alexander Parkhomovsky, Amir M. Dabiran, Philip I. Cohen, Grzegorz Nowak, Izabella Grzegory, and Sylwester Porowski, *EGW3* (1998)

[36] M. Kasu, N. Kobayashi, *Journal of Crystal Growth*, **174**, 513 (1997)

[37] P. Hacke, G. Feuillet, H. Okumura, and S. Yoshida, *Appl. Phys. Lett.*, **69**, 2507 (1996)

[38] M.-H. Xie, S.M. Seutter, W.K. Zhu, L.X. Zheng, H.S. Wu, and S.Y. Tong, *Phys. Rev. Lett.*, submitted.

[39] W.E. Packard, J.D. Dow, R. Nicolaides, K. Doverspike, R. Kaplan, *Superlattices and Microstructures*, **20**, 145 (1996)

[40] S.Y. Karpov, M.A. Maiorov, *Surface Science*, **393**, 108 (1997)

[41] K.R. Evans, T. Lei, and C.R. Jones, *Solid-State Electronics*, **41**, 339 (1997)

[42] J.R. Arthur, *Surface Science*, **43**, 449 (1974)

[43] STM measurements indicate that the island size can vary. S.M. Seutter and A. Parkhomovsky, private communication.

[44] STM measurements in vacuum, to be published elsewhere, show that the gallided surface is featureless with a RMS roughness of less than 0.5 Å.

[45] G. Attard and C. Barnes, *Surfaces*, Oxford University Press, p. 11 (1998)

[46] I. Grzegory, J. Jun, M. Bockowski, St. Krukowski, M. Wroblewski, B. Lucznik and S. Porowski, *J. Phys. Chem. Solids*, **56**, 639 (1995)

[47] J. Weyher, S. Muller, I. Grzegory, S. Porowski, *J. Cryst. Growth*, **182**, 17 (1997)

[48] STM performed by Sean Seutter

[49] J. Weyher, S. Muller, I. Grzegory, S. Porowski, *J. Cryst. Growth*, **182**, 17 (1997)

[50] S. Nakamura, *Jpn. J. Appl. Phys.*, Part 1, **30**, 1620 (1991)